12-2017

Blast-Induced Traumatic Brain Injury and Subsequent Susceptibility to Parkinson's Disease

Glen G. Acosta
Purdue University

BLAST-INDUCED TRAUMATIC BRAIN INJURY AND SUBSEQUENT SUSCEPTIBILITY TO PARKINSON'S DISEASE

by

Glen Howel Galicia Acosta

A Dissertation

Submitted to the Faculty of Purdue University

In Partial Fulfillment of the Requirements for the degree of

Doctor of Philosophy

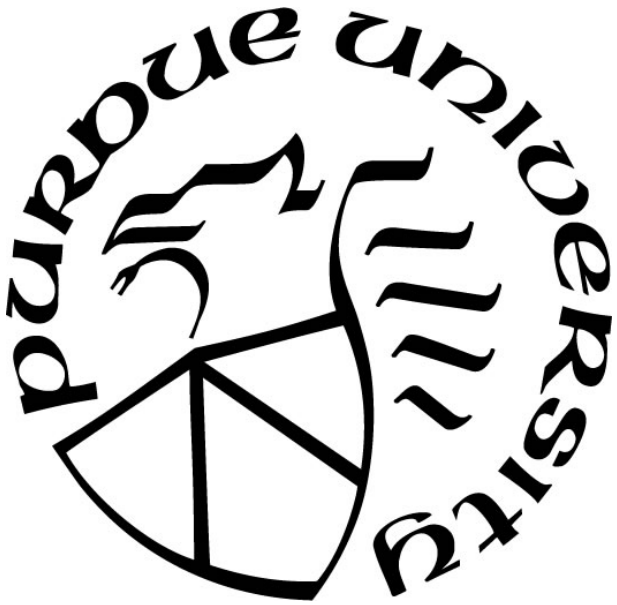

Basic Medical Sciences

West Lafayette, Indiana

December 2017

THE PURDUE UNIVERSITY GRADUATE SCHOOL
STATEMENT OF COMMITTEE APPROVAL

Dr. Riyi Shi, M.D., Ph.D., Chair
Department of Basic Medical Sciences
Weldon School of Biomedical Engineering

Dr. Brad Duerstock, Ph.D.
Weldon School of Biomedical Engineering
School of Industrial Engineering, Center for Paralysis Research

Dr. Kevin Hannon, Ph.D.
Department of Basic Medical Sciences

Dr. Eric Nauman, Ph.D.
Weldon School of Biomedical Engineering
Department of Mechanical Engineering
Department of Basic Medical Sciences

Dr. James Walker, Ph.D.
Department of Basic Medical Sciences
Indiana University School of Medicine-Lafayette

Approved by:

Dr. Laurie Jaeger, D.V.M., Ph.D.
Head of the Graduate Program

To my Family, especially Mom, Dad and Ryan.
Thank you for your endless love and support. You are my inspiration.
To the loving memory of Inang, you left fingerprints of grace on our lives.
This is for you.

ACKNOWLEDGMENTS

I was very fortunate throughout the duration of this challenging journey to have the constant support of my family, friends, colleagues and faculty advisors. First and foremost, I must acknowledge my advisor, Dr. Riyi Shi for your guidance, support, and advice. His genuine passion for science made this journey an enjoyable experience. Thank you for believing in me when no one else did!

Thank you to my committee: Drs. Brad Duerstock, Kevin Hannon, Eric Nauman and James Walker for your mentorship and encouragement, you have challenged me to become a better scientist. Dr. Colleen Gabauer and Dr. Laurie Jaeger for your endless moral support and positive words.

My time here at Purdue has been enhanced by having motivated, intelligent and wonderful people. To the Shi lab members (old and new): Nick, Park, Gary, Melissa, Bre, Michael, Ling, Ran, Chen, Sasha, Jess, Marcela, Jonathan, Seth, and Joe. Thank you for being my sounding board to all my "lab" and "life" problems. To Mock and Shan, thank you for your help with my behavior data. To the BMS purchasing staff, Karla and Janet, thank you for feeding me and the occasional therapy sessions. To my Filipino family here in Lafayette, especially to Ate Syd and Kuya Scott, Mng. Vilma and Mng. Joe; thank you for making me part of your family and making me feel at home.

Lastly, to everyone not mentioned (you know who you are). I am extremely fortunate to have a strong support system. Thank you all for everything!

TABLE OF CONTENTS

LIST OF FIGURES

ABSTRACT

Author: Acosta, Glen Howel, G. Ph.D.
Institution: Purdue University
Degree Received: December 2017
Title: Blast-Induced Traumatic Brain Injury and Subsequent Susceptibility to Parkinson's Disease
Major Professor: Dr. Riyi Shi, M.D., Ph.D.

The prevalence of blast-induced traumatic brain injury (bTBI) is steadily increasing due to escalated terror activities and constitutes the signature injury associated with the current military conflicts. Specifically, a mild-bTBI is the most common injury encountered by our military personnel. This type of injury presents a problem because the individual is initially asymptomatic and functional. Increasing studies have suggested that this type of injury may produce long-term neurological consequences that affect the resilience and the performance of soldiers both on and off the battlefield. One such example is an increased susceptibility to Parkinson's disease (PD) by as many as three folds post-blast injury when compared to the general population. A critical strategy aiming at curtailing this alarming trend is to further our knowledge of pathogenic mechanisms responsible for the escalation of post trauma neurodegenerative diseases. The specific aim of this investigation was to identify the molecular mechanisms underlying the susceptibility to PD in post-blast rats.

To this end, we have identified acrolein, a highly reactive aldehyde that persists days to weeks following CNS injury and perpetuates oxidative insult, as a point of convergence between bTBI and PD. Specifically, we have found that the elevation of acrolein post-blast is capable of triggering pathological changes in the vicinity of the basal ganglion, a known location of brain damage in PD. In particular, we have found signs of neuroinflammation and protein aggregation in blast animals that resembles the pathology in PD, although to a lesser extent. In addition, although a mild blast injury alone cannot elicit typical motor deficits seen in a PD model, additional application of a subthreshold PD-inducing toxin could lead to such deficits. Taken together, we hypothesize that bTBI triggers neurochemical events, such as neuroinflammation and oxidative stress, galvanized by acrolein, could increase the susceptibility of the blast-injured rats to PD and when other PD-triggering factors are present. As such, we hypothesize that acrolein is a key pathological factor linking bTBI and the development of PD in our rat model.

The results from this project are expected to advance our understanding of the long-term consequences of blast-related injuries leading to the development of PD. These efforts could eventually lead to the establishment of biomarkers for an earlier diagnosis as well as strategies for prevention and treatment to curtail the elevating incidence of post-bTBI PD, and significantly improve the quality of life for our men and women who suffer a great deal to ensure our freedom.

1. INTRODUCTION AND BACKGROUND

1.1. Blast Injury Epidemiology and Research Relevance

Blast-induced traumatic brain injury (bTBI) has been a frequent mode of injury associated with increasing efforts against the global war on terrorism and other war-related conflicts [1-3]. Its prevalence has gradually increased in the past decade and has been deemed the "signature wound of the military" [1, 4-6]. Exposure to the primary pressure wave produced by explosive devices is responsible for many of the war-related pathologies during Operation Iraqi Freedom and the Global War on Terror [1]. Recent data have indicated that sixty-five percent of all combat injuries are from explosive blast events. Sixty percent of warfare casualties sustained during current military endeavors in Iraq can be attributed to improvised explosive devices (IEDs) [1, 5-9]. Accordingly, the U.S. Department of Defense has invested a yearly budget of 3.5 billion dollars to improve prevention and treatment of blast injuries [10-13].

Epidemiological studies have shown that bTBI is associated with subsequent neurological deficiencies including brain trauma and spinal cord injury, which can lead to dysregulation of neuronal processes resulting in decreased function [4, 9, 14-17]. Particularly, 15% of troops serving in Iraq show some level of neurological impairment due to blast exposure, and their symptoms are highly correlated with mild TBI (mTBI) [18]. Majority of the mTBI encountered in the military are from blast related incidence, hence there is an increased prevalence of blast-induced mTBI (referred to here as mbTBI to avoid confusion with conventional impact-acceleration TBI) [2, 19], fostering growing concern that blast-related injury may produce long term consequences and affect the resilience and performance of active duty groups [5]. These consequences include depression [20], memory loss [21], dementia [22, 23], and increased susceptibility to Parkinson's disease (PD) [24-26], among others. The risk underlying this pathology is exacerbated by its subclinical nature that can delay treatment past a prime window for intervention. *A vital goal aimed at curtailing post-deployment long-term consequences of mBINT is to further our knowledge of pathogenic mechanisms responsible for the escalation of post-mBINT consequences.*

1.2. Definition and Pathophysiology of Blast Injury

'Blast injury' refers to the clinical syndrome describing the pathophysiological effects of an organism exposed to a high explosive detonation [27]. The Center for Disease Control and Prevention has divided blast injury into four distinct categories: primary, secondary, tertiary, and quaternary blast injury. Secondary, tertiary and quaternary blast injuries are similar to other forms of trauma and have been extensively studied. However, the etiology and mechanisms of the primary injury are not well characterized, and therefore, the main focus of this research. Primary blast injury is the result of a blast-wave impacting bodily tissue and is considered a unique injury modality separate from the other categories. The exposure of bodily tissue, such as the brain, to a shock wave results in a complex series of events. The impact force caused by the shock wave is particularly detrimental to the central nervous system (CNS).

The pathology of blast injury can be through direct contact of the pressure wave to the cranium and/or indirectly to the thoracic region [28-31]. Tissue disruptions in the brain can damage the walls of blood vessels and glial end-feet, which can lead to the disruption of the blood brain barrier (BBB) resulting in increased vascular permeability and subsequent pro-inflammatory response [32, 33]. It is still unclear whether this inflammatory response is beneficial or deleterious, however the over stimulation of this bio-signaling cascade and pro-inflammatory responses following injury can induce neurodegeneration in the neighboring neurons and can result in scar formation [33, 34]. From these events, it is apparent that BINT compromises the brain's defense systems in the BBB in some manner. Neurons require a stable environment to thrive and signal properly and, as such, the post-BINT brain microenvironment can induce large amounts of stress on neuronal tissue.

Additionally, direct damage to the neuronal membranes can lead to an ionic imbalance, and therefore can cause the influx of calcium in the extracellular space. This can trigger an apoptotic-signaling cascade via calcium dependent kinase and protease activation. Activated calcium-dependent proteases such as calpain have been shown to dismantle proteins that anchor myelin to the axonal membrane [35]. Furthermore, damaged neurons can generate reactive oxygen species (ROS), elevate oxidative stress, and lead to further cellular and mitochondrial membrane damage via lipid peroxidation. These damages can lead to the production of reactive aldehydes such as acrolein, which can generate more ROS. This process of self-propagation can

easily overcome the endogenous antioxidant defense system of the neurons and thus can lead to neurodegeneration.

It is clear that the biochemical events (secondary injury) following a blast-induced neurotrauma play a critical role in the pathological progression of the injury (Fig. 1). Of particular interest is the production of ROS after a blast injury, which can lead to the production of reactive aldehydes such as acrolein, and can perpetuate to generate more ROS. Acrolein, a highly reactive product of lipid peroxidation that produces toxic intermediates, highly reacts with glutathione, the most abundant antioxidant found in cells [36, 37]. A self-propagating cycle, local acrolein-induced depletion of glutathione may play a significant role in the pathogenesis of blast injury and perhaps its long-term consequences. Currently, there is no effective treatment to halt secondary injury processes partly due to the lack of understanding of the pathological pathways of these injuries following a traumatic brain injury [38], particularly, BINT. This study proposes that oxidative stress, particularly that perpetuated by acrolein, plays a major role in the pathology of blast injuries and can contribute to long-term consequences such as Parkinson's disease.

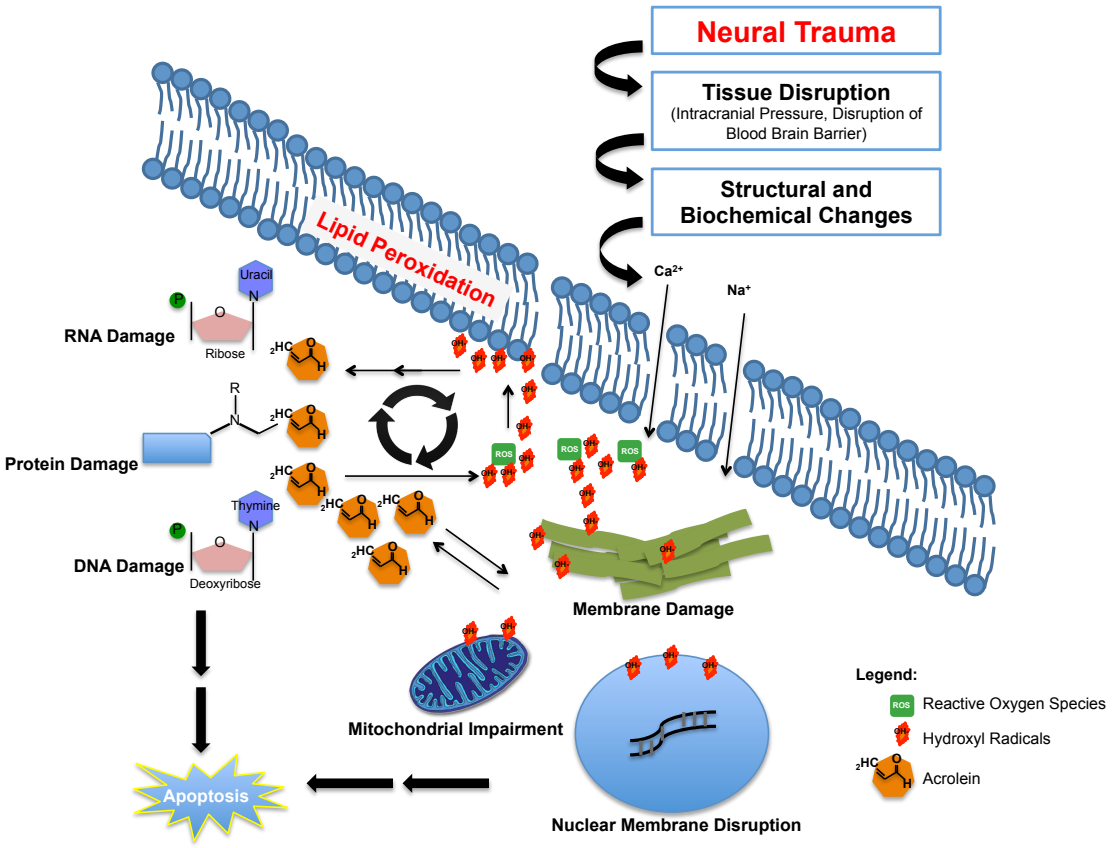

Figure 1: Acrolein Generation Cycle After Neural Trauma. This diagram shows a biochemical cascade of cellular responses after a neural trauma. The tissue disruption and structural damages leads to these biochemical changes. In particular, the ROS (such as H_2O_2) generated by oxidative stress, can readily produce hydroxy radicals (OH*). These radicals induce lipid peroxidation and produces reactive aldehydes such as acrolein, which can directly damage protein, RNA and DNA; and indirectly generate more ROS.

1.3. Oxidative Stress, Lipid Peroxidation, Acrolein Production and Scavengers

Oxidative stress is a collective term used to describe free radical overproduction due to cellular processes. Accumulation of reactive oxidative species (ROS) leads to the activation of several pathways, and is thought to be a major cause of various diseases such as of Alzheimer's disease (AD), amyotrophic lateral sclerosis (ALS), and Parkinson's disease (PD) [39]. The elevation of ROS induces lipid peroxidation, an oxidative degradation of lipids [40]. In the central nervous system, the majority of oxidative stress is manifested by lipid peroxidation, and this leads to the generation of reactive aldehydes such as acrolein and 4-hydroxy-2-nonenal (4HNE) [41-43]. These aldehydes have been shown to modify amino acids, proteins, and

nucleic acids through covalent interactions to form irreversible adducts, thereby inhibiting their synthesis and interfering with their function [44-47]. Furthermore, these products have been shown to induce cell death in cultured neurons [45, 48].

Acrolein is the most reactive of the α, β-unsaturated aldehydes produced endogenously during lipid peroxidation. Acrolein interacts with the sulfhydryl group of cysteine, the amino group of lysine, and imidazole group of histidine forming covalent adducts [44, 49, 50]. Due to its high reactivity towards biomolecules, the excessive endogenous production of acrolein can inflict significant damage within the CNS. Specifically in spinal cord injury, acrolein can induce chemical or secondary damage following the mechanical trauma and has been shown to be highly elevated [51]. Similarly, microinjection or *in vitro* exposure of acrolein to the spinal cord promotes tissue damages including demyelination and cell death. These damages were associated with the motor and sensory behavioral deficits of spinal cord injury [37, 52-55]. With acrolein's relatively long half-life and its proven neurotoxicity, eliciting damages observed in neuronal trauma and degenerative diseases [56, 57], we speculate similar biochemical changes and damages in the brain neurons as a result of the mechanical stress induced by BINT. Therefore, mechanical trauma resulting from BINT can provide an initial source of acrolein in a lipid-rich environment of the brain, which is highly susceptible to lipid peroxidation due to its high lipid content attributed to abundance of myelin and axonal membrane. Additionally, it has been reported that overproduction of acrolein significantly elevated oxidative stress through depletion of glutathione [54]. This leads to a self-regeneration concept, where oxidative stress via lipid peroxidation leads to the production of acrolein, and acrolein in itself can perpetuate oxidative stress (Figure 1). Therefore, the removal of acrolein stunts this cycle proving beneficial for therapeutic intervention and ideally prevention of disease pathology.

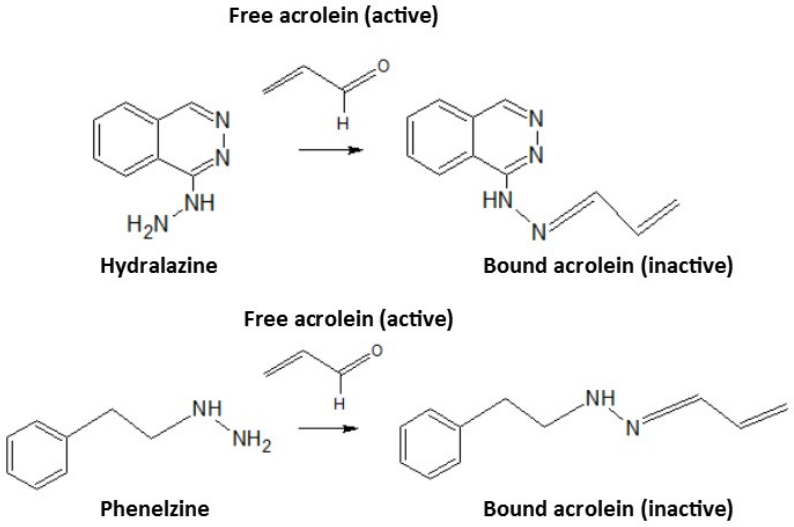

Figure 2: Inactivation of acrolein by acrolein scavengers: hydralazine and phenelzine

Due to the highly reactive properties of acrolein and its ability to modify cell macromolecules underlying its toxicity, a trapping agent would be ideal to prevent such damage. The antihypertensive drug, hydralazine is to date the most studied and well characterized of the acrolein scavengers. It has been demonstrated to bind and neutralize acrolein [58-60] and acrolein-protein adducts [61-63]. Additionally, it has also prevented acrolein-mediated cell death and injuries in vitro [64, 65]. The hydrazine group of hydralazine has been identified to react with acrolein, at a 1:1 ratio [60, 63] (Fig. 2). However, hydralazine's vasodilatory effect is one of the limitations for therapeutic purposes, mainly because it would be undesirable for a patient that suffered from spinal cord injury or blast, as they may be likely suffering from a neurogenic shock. In addition, the half-life of hydralazine does not exceed one hour, which potentially limits its therapeutic efficacy in suppressing acrolein generation and related chronic oxidative stress processes [66].

Phenelzine (PLZ), an irreversible non-selective monoamine oxidase inhibitor (MAOI), has been primarily utilized for the treatment of depression [67-69], but also in other psychiatric disorders such as panic disorders [70, 71], social anxiety disorders and post-traumatic disorders [72-74]. Phenelzine, like hydralazine has a hydrazine group rendering it a potential acrolein

scavenger (Figure 2). PLZ has also been shown to be neuroprotective in a gerbil model of forebrain ischemia by reacting with 3-aminopropanal (3-AP) to form hydrozone, and provides neuroprotection from acrolein induced LDH release *in vitro* [75]. Additionally, PLZ alleviates oxidative stress through acrolein scavenging in a traumatic spinal cord injury rat model [37]. PLZ is not a vasodilator and can be administered safely at higher doses compared to hydralazine. A 15 mg/kg dosage was given subcutaneously to gerbils after ischemia-reperfusion brain injury and effectively neutralized reactive aldehydes such as acrolein, providing neuroprotection [75]. In this study, we used PLZ as an acrolein scavenger following blast injury in efforts to prevent PD-like symptoms in our rat model.

1.4. Parkinson's Disease Neuropathology

Parkinson's disease (PD) is an age-related neurodegenerative disease affecting about 1-3% of the population over 50 years of age [76, 77]. PD is characterized by relatively selective, progressive degeneration of the dopaminergic (DA) neurons in the substantia nigra and the presence of LB inclusions in the affected brain regions. The lack of dopamine supply to the striatum is the major contributing factor to motor dysfunction phenotypes of PD, including shaking tremors, rigidity and gait disturbances. The current therapeutic interventions include drugs such as dopamine agonists and MAO-B inhibitors to increase dopamine levels and at time deep brain stimulation are currently available. However, these treatments only provide relief rather than a cure or preventive measure for combating disease symptoms and the risk-benefit profiles of current treatment options are still inadequate.

This shortage of effective treatments for PD is partially due to our limited understanding of the mechanisms of dopaminergic neuronal death. Therefore, the current treatments only provide symptomatic relief rather than addressing the major cause of the disease. α-Synuclein, the major component of LB inclusions is thought to play an essential role in the pathogenesis of PD [78]. Modified α-synuclein is found within LB inclusions in a PD brain, and mutations in the α-synuclein gene are associated with familial PD [79, 80]. The formation of LBs has been linked with oxidative stress, which is also consequently elevated in PD patients [81-83]. α-Synuclein also has abundant lysine-rich repeats, making it more vulnerable to oxidative stress and the reaction with acrolein [84]. Therefore, we can speculate that α-synuclein aggregation is a major player in DA cell death seen in PD.

It is well established that oxidative stress and lipid peroxidation play important roles in mediating the death of DA neurons [85, 86]. The challenge in the field of PD is to further understand mechanisms of oxidative stress and to identify novel and more effective targets to prevent DA cell death. As mentioned previously, acrolein, produced by lipid peroxidation, can directly damage nerve cells and generate free radicals. Our lab has also shown that in a cell-free system and in vitro studies, acrolein can induce α-synuclein aggregation and leads to neuronal death (data not shown). These findings have led us to postulate that acrolein plays a critical role in neurodegeneration associated with PD. Consequently, it is also important to consider other contributing factors that lead to PD, such as traumatic brain injury (TBI). Epidemiological studies have demonstrated that TBI is a risk factor for PD [87], however the link between the two remains unclear. Previously, our lab has shown the role of acrolein in a PD rat model and in a blunt-force impact TBI model, but not in a BINT model. We further speculate that the acrolein post-blast injury can contribute to the development of a PD-like pathology. This study investigates the susceptibility to PD following a blast injury and we speculate acrolein plays a major role in linking blast injury and PD.

1.5. Research Statement and Aims

Blast induced neurotrauma injuries are usually accompanied by affective disorders and have been linked to an increased risk of developing PD [4, 9, 14-17]. The primary physical trauma sustained from an injury, such as blast injury, is exacerbated by altered physiological conditions including cerebral blood flow, intracranial pressure, inflammatory response activation and phospholipid metabolism, which lead to a delayed phase of chemically-mediated damage termed "secondary injury" [88-93]. Particularly, in human post-mortem brain tissue analysis and animal studies, TBI can induce abnormal α-synuclein accumulations in the axonal swellings, dystrophic neurite formation [94-96], and inflammatory response [97]; similar to what is observed in PD pathology. However, due to inadequate knowledge of underlying mechanisms of both TBI and PD, common pathogenic features remain elusive and therapeutic options are limited. Recently, oxidative stress, the underlying mechanism of secondary injury, has emerged as an important feature of both neural trauma [28, 98] and neurodegenerative diseases, particularly PD [99-102]. However pharmacologically eliminating free radicals offers marginal neuroprotection and has had limited success in attenuating further progression of damage. *Our lab has identified acrolein,*

a highly reactive aldehyde that persists days to weeks following injury and perpetuates oxidative insult, as a potential therapeutic target to curtail chemically-mediated damage, a common feature of TBI and PD.

Despite strong interest, the cellular mechanisms of blast-induced brain injury are essentially unknown due to limitations of human studies and insufficient investigation in animal models, specifically the most common type of blast traumatic brain injury, the mild bTBI. We have recently established a novel rat blast-induced brain injury model that displays significant biochemical and behavioral deficits in the absence of conspicuous acute motor deficits, shown in Fig. 1, [103] a phenotype that closely resembles the mild BINT human condition [104]. The development of such model will allow us to quantify the injury sequelae as well as investigate potential treatments to alleviate potential neurodegeneration. In order to provide a holistic model of injury, as it would progress in clinical cases, we must use an approach that allows us to monitor the injury *in vivo*.

Using the blast-model, we have found that acrolein, a well-known key neural toxin and marker of oxidative stress [44, 91], is significantly elevated in brain tissues (using dot blot) and in urine through the measurements of 3-HPMA, an acrolein metabolite, in days post-injury (data not shown). On the other hand, our lab also investigated that in a 6-OHDA-induced PD animal model, acrolein is elevated. Furthermore, lowering of acrolein using a well-known acrolein scavenger, hydralazine, could lead to alleviation of motor deficits implicating a pathological role of acrolein in PD. Consistent with role of acrolein in PD pathology, our lab in collaboration with Dr. Rochet, has shown that acrolein can promote α-synuclein aggregation, one of the hallmarks of PD *in vitro* and *in vivo*. In addition, acrolein is a known pro-inflammatory aldehyde [105, 106] further suggesting its putative role in inflammation, both in blast injury and PD. In summary, our preliminary data strongly suggest that acrolein plays a critical role in the pathogenesis of PD by directly promoting α-synuclein aggregation, and instigating neuroinflammation, which further exacerbates α-synuclein aggregation. The purpose of this project is to investigate the molecular mechanism underlying the susceptibility of PD in post-blast rats. Our hypothesis is that acrolein is the key, linking blast injury and the development of PD in our rat model. To test this we aim to:

AIM 1. Characterize behavioral deficits and evaluate oxidative stress-related biochemical changes after mild blast-induced traumatic brain injury, and its possible causal effects to enhance susceptibility to PD.

AIM 2. Investigate the behavioral deficits following mild blast-induced traumatic brain injury and sub-threshold 6-OHDA nigral injection.

AIM 3. Investigate the neuroprotective role of acrolein scavengers such as phenelzine, to mitigate PD-like behavioral deficits following blast-induced traumatic brain injury.

2. BEHAVIORAL ASSESSMENT & BIOCHEMICAL CHARACTERIZATION OF MILD-bTBI

2.1. Mild bTBI Behavioral Assessment

2.1.1. Rationale

Despite the aforementioned short and long term consequences of mild blast injuries, the underlying mechanisms governing the associated functional loss are poorly investigated. This lack of understanding is due in part to limitations of human studies and insufficient investigation in animal models. As such, we have successfully established a rodent model of mild bTBI, which resembles the human condition. Our model utilizes a consistent pressure intensity wave to induce mild bTBI (data not shown) and lacks gross hemorrhage and neurocognitive deficits at 24 and 48hrs post-injury that is consistent with the human cases of mild bTBI [107, 108]. Currently, there is a limited set of unproven and under-investigated hypothesis regarding primary bTBI pathophysiological mechanisms. By developing a reproducible model of mild bTBI, we can elucidate underlying pathophysiological cellular responses and better identify targets for therapeutic intervention.

2.1.2. Brief Methods

2.1.2.1. Animal model of primary blast induced neurotrauma

Animals were anesthetized with 80 mg/kg ketamine and 20 mg/kg xylazine cocktail. After verification of absence of toe-withdrawal reflex, they were secured in open-ended shock tube style blast apparatus and a body shield was placed over the animals for protection during injury allowing for the study of mild TBI without systemic confounders. Mild bTBI was produced by a blast wave generator, which delivered a global blast pressure wave in a laboratory setting. Blast generation was achieved when pressure built up in a reservoir until it exceeded the burst strength of the diaphragm. The blast wave was directed downward at a distance of 50 mm from the nozzle of the blast generator to the head of the animal, with a peak pressure of 150 kPa. Sham animals were anesthetized accordingly and place in the same room of the blast set-up but outside the blast wave range.

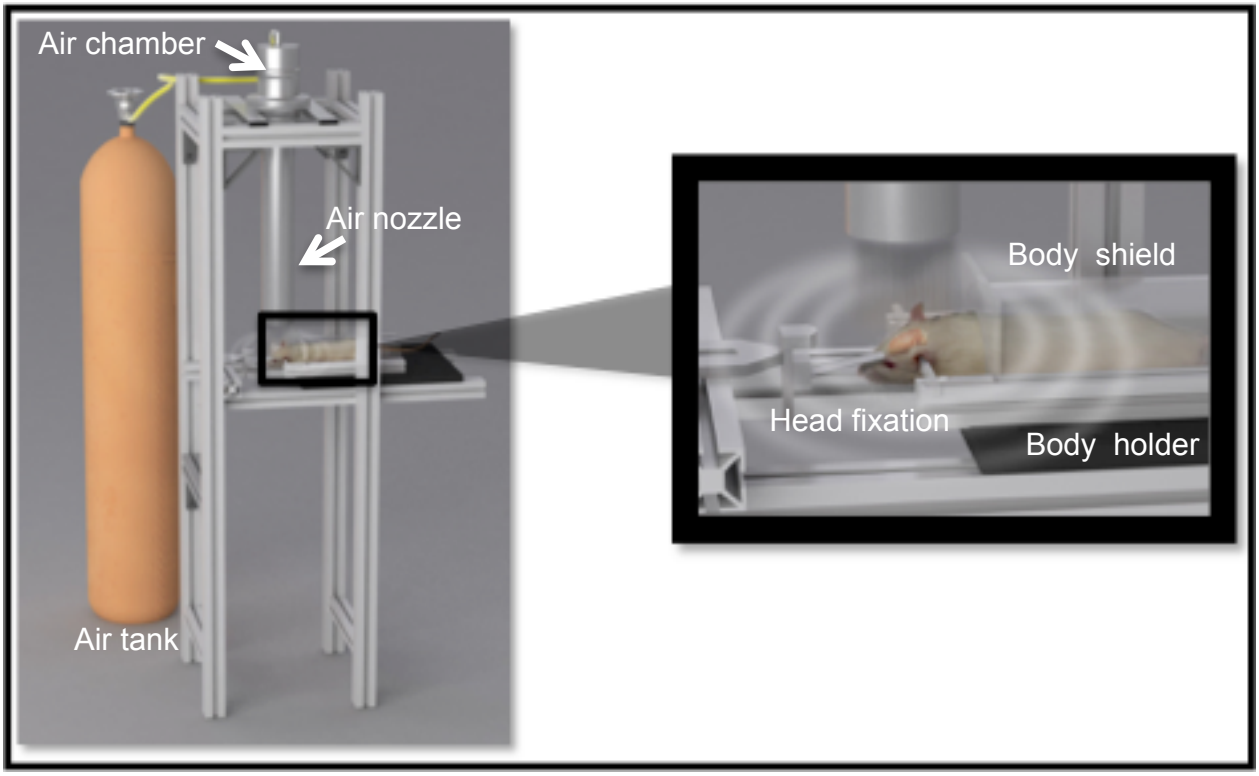

Figure 3: Illustration of rat blast experimental set up. Enlarged area view of the surface of the rat brain where the blast wave was aimed

2.1.2.2. Behavioral assessment methods

Gross motor deficits were examined by 5 minute excursion sessions in an open field activity box as described by Koob et. al.[109] with video feed motor metric analysis conducted using AnyMaze software (Stoelting Co., Wood Dale, IL). Briefly, the activity was evaluated for distance travelled, average speed, and maximum speed. Additionally, rats were evaluated for locomotion on a rotarod. The rotarod speed ramped gradually from 0 to 30 revolutions per minute (rpm) over three minutes and remained at 30 rpm until stopping at the three minute and thirty second mark or earlier if the rat falls. Sham animals (anesthesia and blast noise only without shock wave exposure) were examined in tandem to control for lingering effects of anesthesia in the acute post-injury period.

2.1.3. Results and Discussion

2.1.3.1. Rotarod and open-field behavioral assessment results

The rotarod motor function test revealed no statistically significant difference between blast and sham group. Prior to the injury, animals were trained with a protocol designed to ensure

familiarity and ability to complete the task. Rotarod test was assessed by maximum speed and total run time at 24 and 48 hours post-injury (Fig. 3).

Behavioral analysis of motor function in an open-field activity box at 24 and 48 hours post-blast showed no significant deficits resulting from the blast injury (Fig. 5). Analyses included average speed (A), maximum speed (B), and total distance traveled (C). No statistically significant differences were found before or after blast in any of the three assessments related to open-field activity (n=4/group). This lack of gross motor deficits in rotor rod and open box is consistent with lack of motor deficits in the acute term after a mild blast-induced neurotrauma observed in human cases [107, 108, 110].

Despite the increasing studies that have further our understanding of primary blast injury models and pathophysiology, post-bTBI physiological modifications have yet to be studied in the context of injury which requires the assessment of acute and long term functional neurological outcomes and post -mortem tissue analysis. According to Center for Disease Control (CDC) and Department of Defense (DoD) mild bTBI is characterized with a loss of consciousness (LOC) ≤ 30 minutes, Glasgow Coma Scale (GCS) 13-15 following LOC, post-traumatic amnesia <24hrs, and no evidence of gross intracranial hemorrhage[107, 108]. Due to inter-species variation and differing modes of blast generation between investigators, post-blast outcomes must be used to assess bTBI severity and verify consistency with accepted guidelines within one's own model. Our model is based on prior work [111] and existing literature to mimic a mild-blast traumatic injury as encountered by humans[112-116]. To our understanding, this is the first study to establish a symptom-based validated model of mild bTBI in rodents.

Typical assessments of motor and cognitive function are provided clinically following brain injury, however patients that are exposed to a mild brain injury are often asymptomatic and therefore are mostly undiagnosed. [107, 108]. In this study, we provide a consistent model of mild bTBI that lacks motor and cognitive deficits 24 and 48 hours post injury which is typical of the clinical human mild bTBI [107, 108]. Additionally, we found that the blood-brain barrier is compromised, inflammation, and oxidative stress is increased following acute exposure to mild-bTBI in our rodent model (Walls paper). We hypothesize that these biochemical cascades post-injury plays a critical role in the development of long term consequences such as the development of Parkinson's disease.

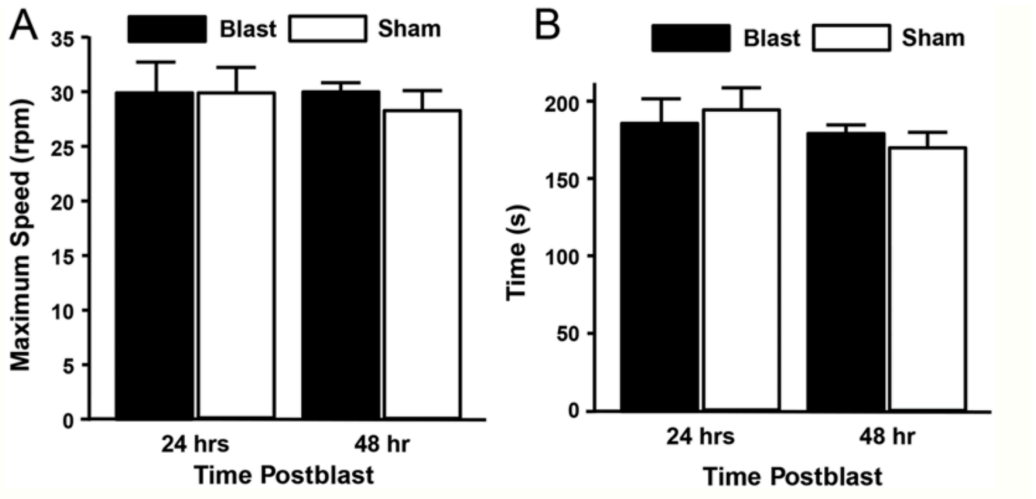

Figure 4: Behavioral analysis of motor function on rotarod indicates no significant effects of injury group or day at 24 or 48 hours post-blast. Criteria were max revolutions per minute (A) and total run time (B). ($p>0.05$, n=4/group, Tukey-Kramer).

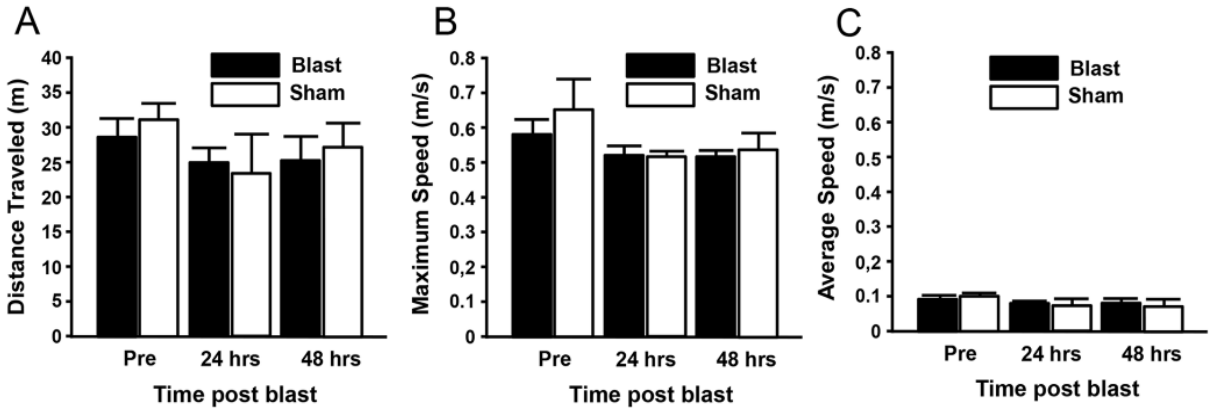

Figure 5: Behavioral analysis of motor function in an open-field activity box indicates no significant effects of injury group or day on gross motor activity at 24 or 48hrs post-blast. Analyses included distance traveled (A) and maximum speed (B) and average speed (C). ($p>0.05$, n=4/group, Tukey-Kramer).

2.2. Short-Term Mild bTBI Biochemical Assessment

2.2.1. Introduction and Rationale

In the general civilian population, traumatic brain injury (TBI) has been independently identified as a risk factor for Parkinson's disease (PD), suggesting TBI increases PD susceptibility [26, 117, 118]. Athletes, boxers, and veterans, all of whom are at-risk sub-populations for traumatic brain injury (TBI), have a higher risk of developing Parkinson's disease (PD) symptoms later in life [119]. Veterans, specifically, have been reported to be three times as likely to develop PD when compared to the general populous [4, 120-124]. The majority of combat-related TBI results from explosive blasts (b-TBI) [2, 125], which are most commonly mild in nature (mb-TBI) [19, 126-131]. Mild brain injuries often go undiagnosed or unreported, fostering growing concern that clinically 'silent' injuries may later precipitate PD, among other consequences [5]. Unfortunately, despite mounting clinical evidence associating TBI and PD, mechanisms by which TBI-related injurious processes increase PD susceptibility are poorly understood.

During TBI, including those from blast exposure, the brain immediately undergoes primary physical damage to neurons, glial cells, and microvasculature. Primary injury induces secondary cellular and biochemical processes including oxidative stress, lipid peroxidation, abnormal protein aggregation, inflammation, and neuronal death [33, 119, 132, 133]. Secondary injuries initiate on the order of minutes after injury and, even after mild injuries, can continue for months [2, 28, 134-137]. In contrast, idiopathic PD pathophysiological processes occur over the course of many years. In humans, the TBI-PD relationship is thus difficult to mechanistically study as a result of the separation between TBI occurrence (usually younger, more active years) and PD onset (average age: 60), which would require involved, expensive longitudinal studies. As such, animal models are not only suitable, but also necessary for such investigation. Despite the temporal disconnect in humans, it has been demonstrated that TBI secondary injury processes overlap with the degenerative processes observed in PD [119, 138, 139], giving invaluable guidance for investigation using animal models.

PD is classified as a synucleinopathy due to its hallmark pathological finding, Lewy body inclusions, which are primarily composed of insoluble, abnormally aggregated α-synuclein (α-syn) protein fibrils [78, 80]. α-syn is thought to play an essential role in PD pathogenesis, with its aggregation leading to dopaminergic cell death in the substantia nigra (SN) and depletion of the

brain's supply of dopamine in the striatum (STR) [78, 80, 81, 140]. In conjunction to dopamine depletion, the overall activity and protein levels of tyrosine hydroxylase, a rate-limiting enzyme for catecholamine synthesis (including dopamine), are decreased in the SN of PD patients [141, 142]. Consequently, due to the critical role of the dopaminergic nigrostriatal pathway in motor coordination, the cardinal clinical signs of PD emerge: tremor, rigidity, slowness of movement, and postural instability [143-145]. Interestingly, α-syn protein is highly vulnerable to attack by reactive oxygen species and reactive aldehydes, which are suspected to promote its oligomerization and further induce oxidative stress [146], perhaps leading to elevated oxidative stress markers in PD patients [81-83]. As mentioned above, oxidative stress is a known consequence of TBI, suggesting a possible link and pathological convergence between TBI and PD.

We have previously documented typical TBI primary and secondary injuries in a mild blast induced-traumatic brain injury (mb-TBI). Specifically, we have noted conspicuous microvascular damage, neuroinflammation, and increased oxidative stress in the hours and days following injury [137]. Furthermore, we have discovered a significant elevation of acrolein, an α,β-unsaturated aldehyde that is both a product and catalyst of lipid peroxidation and stimulator of oxidative stress and inflammation. In the present investigation, we hypothesized that post-TBI oxidative stress, particularly elevation of reactive aldehydes resulting from lipid peroxidation (i.e. acrolein), could lead to aberrant expression of α-syn and dysregulation of dopamine synthesis.

The present study extends our previous findings in the context of PD-relevant mechanisms after mb-TBI, delving deeper into overlapping neurodegenerative processes shared by mb-TBI and PD in the same animal preparation. Specifically, we investigated α-syn aggregation, dysregulation of tyrosine hydroxylase, and lipid peroxidation in the whole brain, striatum and substantia nigra regions post-blast injury. We demonstrate that acrolein can directly modify α-syn and lead to its aberrant expression *in vitro* and likely *in vivo* as well, in addition to the dysregulation of tyrosine hydroxylase. To our knowledge, this is the first direct *in vivo* evidence implicating the post-TBI role of acrolein, or any other TBI secondary injury-related molecule, in promoting PD-like abnormal expression of α-syn and dysregulation of tyrosine hydroxylase in the brains of rats exposed to mild blast-induced traumatic brain injury.

2.2.2. Brief Methods

2.2.2.1. Post-mortem brain tissue preparation and Western blotting

For the whole brain mapping of acrolein-lysine adducts, after transcardial perfusion 24-hr post blast injury, whole brains were quickly removed and frozen with dry ice and stored in the -80 ^{o}C until processing. Microdissected regional lysates were obtained in 6 consecutive coronal sections, starting just rostral to the olfactory bulb. The coronal sections were each subdivided with 2 frontal cuts and 2 sagittal cuts into 9 distinct regions per section. Coronal sections were cut at the following locations with respect to Bregma (mm): +4, +2, 0, -2, -4, -6, and -9 into sections A-F as illustrated in Figs. 6-12 (according to Paxinos and Watson *The Rat Brain Atlas*). Viewed from the anterior of the specimen, segments will numbered viewer left (subject right) to viewer right (subject left), top (dorsal) to bottom (ventral) such that segments 1, 4, and 7 correspond to R hemisphere neocortex; 3, 6, and 9 correspond to L hemisphere neocortex; 2 corresponds to midline dorsal neocortex; 5 and 8 correspond primarily to subcortical regions. Protein lysates and western blot (acrolein-lys-adducts) were done as described below.

Rats were sacrificed for Western blot at 2 days, 7 days post-mild blast TBI and sham group. After deeply anesthetized with 80 mg/kg ketamine and 20 mg/kg xylazine cocktail, animals were transcardially perfused with Krebs solution and decapitated. Whole brains were quickly removed and frozen on dry ice and stored in the -80^{o}C until processed. Tissue from the striatal regions (STR: B5 (anterior), C5 (posterior)) and substantia nigral region (SN: E8) was dissected out according to Paxinos & Watson's The Rat Brain Atlas as a reference guide for the regional assessment (Supplementary Figure 1). Brain tissues were sonicated in 1x RIPA buffer (Sigma, #R0278) with protease inhibitor cocktail at 1:100 final concentration (Sigma, P8340). Samples were centrifuged at 15,000 g for 40 min at 4^{o}C and only the supernatant was used for the Western blot study. Protein concentrations were measured using the Bicinochoninic Acid protein assay kit (Pierce, Rockford, IL, USA) and SPECTRAmax (Molecular Devices, Sunnyvale, CA). Sixty micrograms of protein with 20% SDS, β-mercaptoethanol, and 2x Laemmli buffer were loaded to a 15% Tris-HCL gels and electrophoresed at 80 volts for 2-3 hours. Proteins were then transferred to a nitrocellulose membrane by electro blotting in 70 volts for 1-2 hours depending on the protein size at 4^{o}C in 1x transfer buffer with 20% methanol (Tris-Glycine buffer from BioRad, Hercules). The membrane was blocked in 1x casein (Vector, #SP-5020) at room temperature for 1 hr, and immunolabeled with one of these primary antibodies, anti-ACR

(Abcam, #37110), anti- α-synuclein (α-syn) (BD Transduction, #610786), anti-TH (Cell Signaling, #2792S), anti-THpSer31 (Cell Signaling, #3370S), anti-THpSer40 (Novus, #NB300-173), and anti-actin (Sigma, #A2066) at 4^{o}C overnight. The experiments were run from the same samples, accordingly from the whole brain, STR (B5, C5), and SN (E8) lysates; and the antibodies were run in parallel. The membranes were further incubated with either biotinylated anti-mouse or anti-rabbit secondary antibody (Vector, #BA-2000, #BA-1000) at room temperature for 1 hr. The DuoLux substrate (Vector, #SK-6605) immunodetection kit was used for chemiluminescent signal acquisition and the Azure c300 Western blot imaging system (Azure Biosystems, Dublin, CA) was used to image the membrane. The AlphaView software (Protein Simple, San Jose, CA) was used to quantify the relative signal for each band. Data are normalized with actin, pTH-Ser31 and Ser 40 are normalized with unp-TH, and expressed as percent control.

2.2.2.2. Detection of acrolein (3-HPMA Measurements)

The quantification of acrolein and its metabolites in urine has recently been established using liquid chromatography-mass spectroscopy (LC/MS); providing a non-invasive detection to monitor acrolein and investigate its pathological role in brain injuries and other diseases [45, 58, 147-151]. Specifically, measurement of acrolein metabolites known as mercapturic acids in blood, urine and feces using LC/MS have shown promise as reliable biomarkers to detect acrolein [152, 153]. N-acetyl-S- (3-hydroxypropyl) cysteine (3-HPMA), the most common mercapturic acid derived from reduction of acrolein by aldehyde reductase, is a stable and non-toxic compound with feasibility of detection [154, 155]. Our lab has optimized a consistent method of detecting 3-HPMA through LC/MS/MS providing a systemic measurements on acrolein dynamics as described in Lingxing et al., 2013 [156]. For a thorough assessment of acrolein levels in the urine, samples were collected one, two, five and seven days post-blast injury in both the blast injured and sham/control rats.

2.2.2.3. Detection of α-synuclein protein modifications by acrolein

Purified α-syn protein (2.5 μM in the final concentration) was incubated in the presence of 0.125, 0.25, 0.5, 1, 5, and 10 mM of ACR at 37^{o}C for 20 h. Then equal volume of the loading buffer (Laemmli sample buffer + β-Mercaptoethanol) was added to the reaction mixture and heated at 95^{o}C for 5 min. The samples were subjected to Western blot analysis, by loading on a 15% SDS-page gel, blotted on a nitrocellulose membrane, and probed with either anti- α-syn or

anti-ACR antibody. The sample with only α-syn protein was used as a control and normalization factor for quantification analysis.

2.2.2.4. Immunoprecipitation assay post-mild bTBI

Immunoprecipitation of the whole brain lysates from sham (control), 2-days, and 7-days post-injury was carried out using Pierce Classic IP Kit (ThermoFisher, #26146). In short, 2mg/mL protein lysate from each sample group was pre-cleared using the control agarose resin. The lysate (2 mg protein) was incubated with either 5 µL of anti- α-syn or anti-ACR primary antibody at 4^{o}C overnight to from immune complex. A 20 µL of Pierce A/G Agarose was added into the mixture to capture the immune complex and incubated at 4^{o}C overnight. The elution of the immune complex was carried out using the 2x non-reducing lane marker sample buffer and DTT. The collection tubes were incubated at 100 ^{o}C for 5 min and eluates were applied to 15% SDS-PAGE for immunoblotting with anti- α-syn and ACR was imaged using Azure c300 Western blot imaging system (Azure Biosystems, Dublin, CA).

2.2.2.5. Immunofluorescence staining

Animals were anesthetized and perfused with 4% paraformaldehyde in Krebs solution. Whole brains were extracted and placed in 15% sucrose solution until the tissue sinks followed by 30% solution until the tissue sinks. When ready, tissue was frozen in OCT and sectioned coronally at 25µm in a cryostat (Leica). Sections were mounted on glass slides immediately after cutting and stored at -20°C. Representative sections of the striatum and substantia nigra (Bregmas approximately 0.7mm and -6.04mm) were selected for staining. Sections were first hydrated in 1xPBS then permeabilized with 0.1% Triton X-100 followed by 3% Triton. Blocking was done with 10% immunobuffer and primary antibody against Acrolein-Lysine adducts and α-synuclein were mixed in 10% immunobuffer and left to costain overnight at 4°C. Sections were incubated for 2hours at room temperature in secondary antibodies conjugated to fluorophores (Jackson Immuno, Alexa 488 and 594). Cell nuclei were labeled with 4′, 6-diamidino-2-phenylindole. Imaging was done with an Olympus IX51 fluorescence microscope. Figures were constructed using Image J with the Figure J plugin.

2.2.2.6. Statistical analysis

All data are presented as mean ± standard error of the mean (SEM). One way ANOVA with Tukey or Fisher post hoc and Student's t test were used for statistical assessment. The statistical significance was set at $p < 0.05$.

2.2.3. Results

2.2.3.1. Regional acrolein-lys adducts brain mapping post-mild TBI

Brain concentrations of acrolein peaked at 24 hours post-injury after a single, mild b-TBI. To assess the spatial profile at peak elevation, we subdivided the forebrains of a separate cohort of Sham (n = 5) and Blast (n = 5) animals at 24 hours post-injury (coinciding with peak acrolein elevation) into 53 sub-regions for similar acrolein-lysine adduct immunoblotting analysis. Overall, 8 out of 53 regions demonstrated significant increases in acrolein-lysine adduct immunoreactivity after mild b-TBI when compared to Sham animals (Fig. 13). Areas with significantly higher oxidative stress relative to Sham included those containing the orbitofrontal cortex (OFC) and agranular insular cortex (AIC) bilaterally (A4 + A6), the anterior striatum (B5), bilateral primary somatosensory cortices (C1 + C3), the caudal hypothalamus + rostral midbrain (E8), and areas containing the auditory cortex + temporal association cortex + hippocampal CA2 bilaterally (F4+F6).

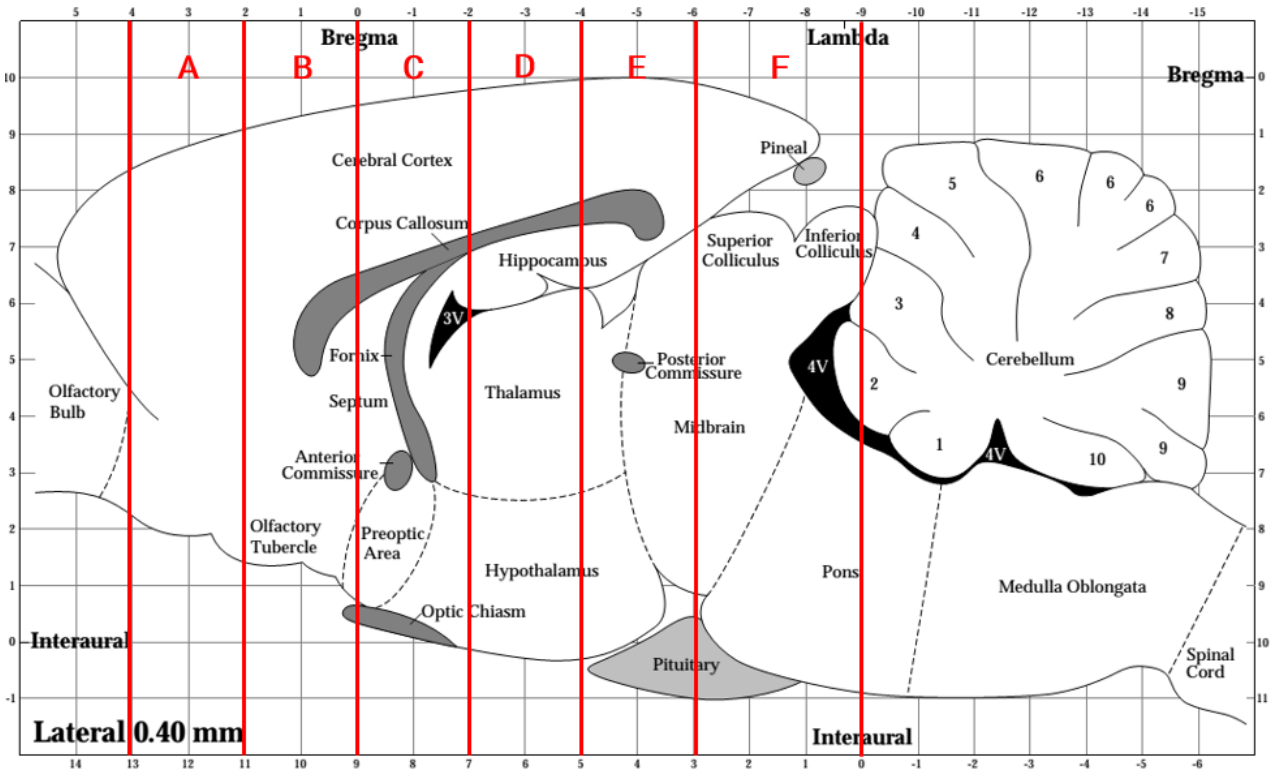

Figure 6: Layout of coronal sections used for Western blotting of acrolein-lys adducts. Adapted from *The Rat Brain Atlas* (Paxinos and Watson).

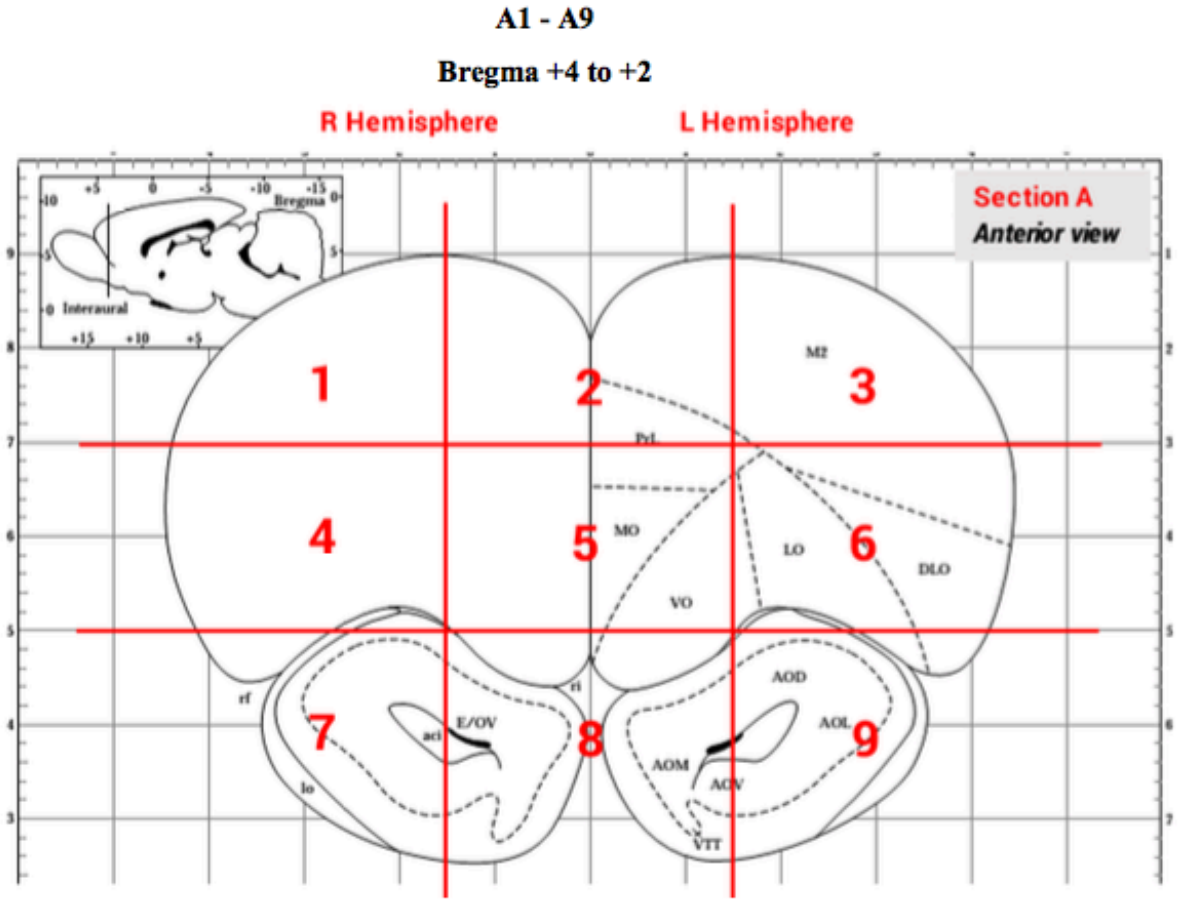

Major Brain Regions

	R Hemisphere	*Middle*	*L Hemisphere*
Dorsal	motor cortex	cingulate cortex	same as R Hemisphere
Middle	orbital cortex, forceps minor of corpus callosum, somatosensory cortex, insular cortex	prelimbic cortex, infralimbic cortex, orbital cortex, dorsal peduncular cortex	"
Ventral	piriform cortex, olfactory tubercle, nucleus accumbens	nucleus accumbens, tenia, tecta, islands of Calleja, anterior olfactory nucleus, olfactory tubercle, ventral pallidum, semilunar nucleus, septal hippocampal nucleus	"

Figure 7: Layout and contents of coronal slice A. Adapted from *The Rat Brain Atlas* (Paxinos and Watson).

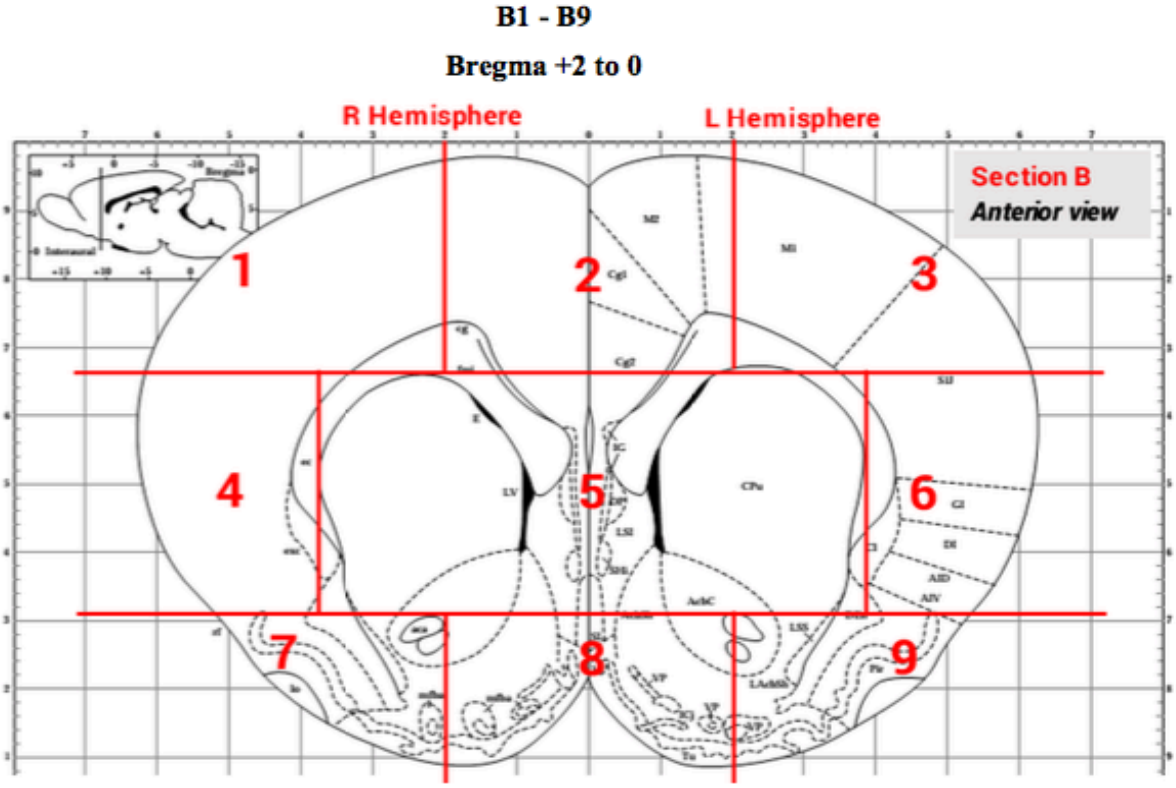

Major Brain Regions

	R Hemisphere	*Middle*	*L Hemisphere*
Dorsal	motor cortex, somatosensory cortex	motor cortex, cingulate cortex, cingulate gyrus	same as R Hemisphere
Middle	somatosensory cortex, insular cortex	striatum, septal nuclei, forceps minor	"
Ventral	nucleus accumbens, ventral pallidum, piriform cortex	islands of Calleja, olfactory tubercle, ventral pallidum, semilunar nucleus, septal hippocampal nucleus	"

Figure 8: Layout and contents of coronal slice B. Adapted from *The Rat Brain Atlas* (Paxinos and Watson).

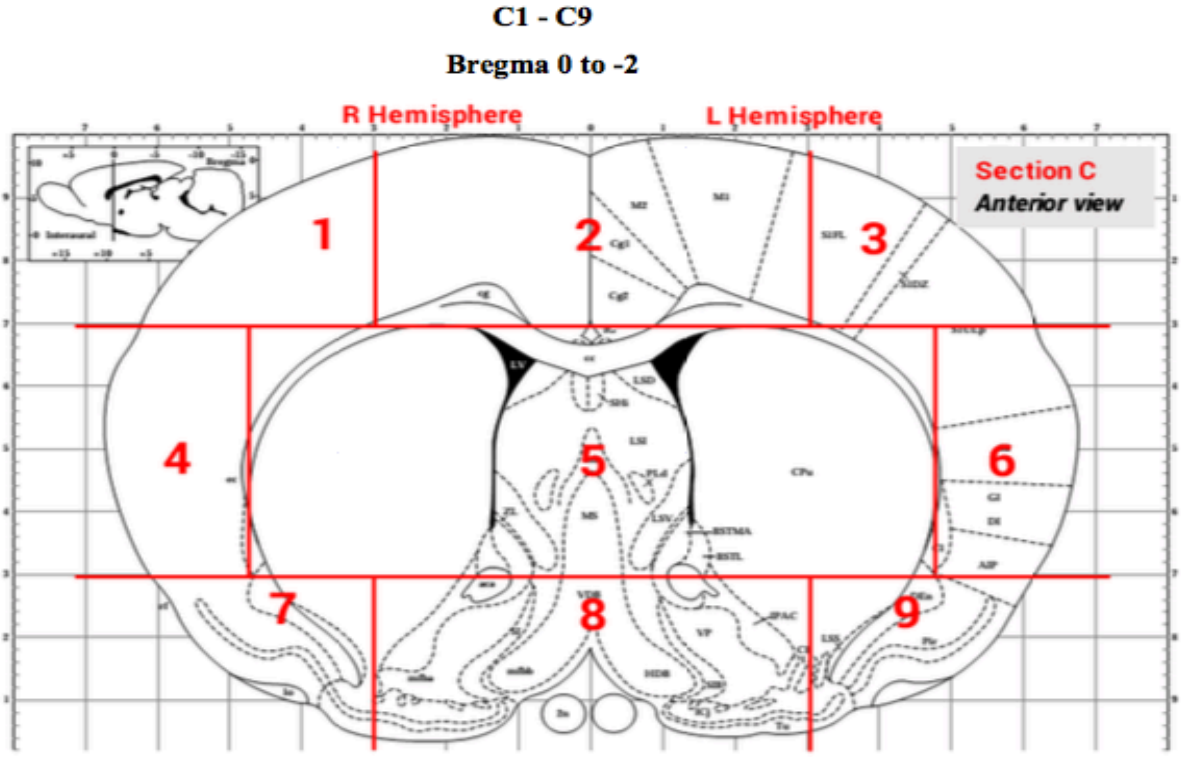

Major Brain Regions

	R Hemisphere	*Middle*	*L Hemisphere*
Dorsal	somatosensory cortex	motor cortex, cingulate cortex, somatosensory cortex, retrosplenial cortex	same as R Hemisphere
Middle	somatosensory cortex, insular cortex	striatum, fornix, anterior commissure, corpus callosum, anterior thalamus, 3rd ventricle, bed nucleus of stria terminalis, septal nuclei	"
Ventral	piriform cortex, anterior tip of amygdala	islands of Calleja, olfactory tubercle, ventral pallidum, preoptic area, optic chiasm	"

Figure 9: Layout and contents of coronal slice C. Adapted from *The Rat Brain Atlas* (Paxinos and Watson).

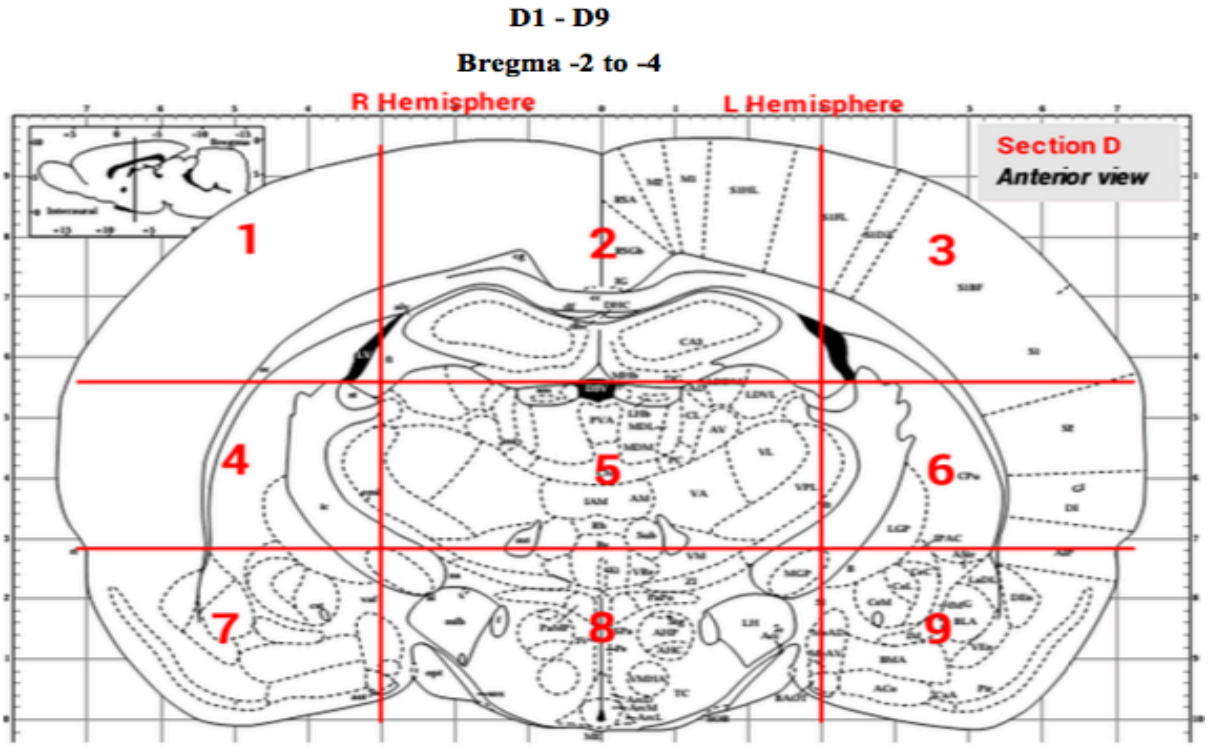

Major Brain Regions

	R Hemisphere	*Middle*	*L Hemisphere*
Dorsal	somatosensory cortex	motor cortex, cingulate cortex, somatosensory cortex, retrosplenial cortex, corpus callosum, anterior hippocampus	same as R Hemisphere
Middle	auditory cortex, somatosensory cortex, insular cortex	thalamus	"
Ventral	most of amygdala (incl. BLA and CeA, piriform cortex, perirhinal cortex, ento/ectorhinal cortex	hypothalamus	"

Figure 10: Layout and contents of coronal slice D. Adapted from *The Rat Brain Atlas* (Paxinos and Watson).

E1 - E9

Bregma -4 to -6

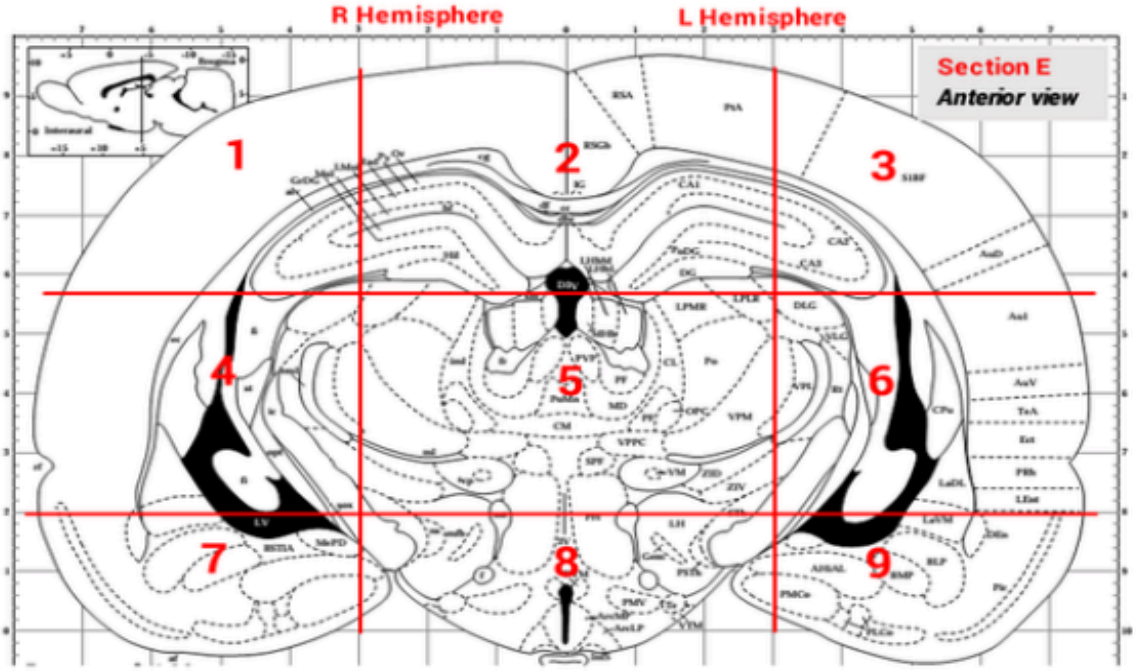

Major Brain Regions

	R Hemisphere	*Middle*	*L Hemisphere*
Dorsal	somatosensory cortex, parietal association cortex,visual cortex	retrosplenial cortex, parietal association cortex, somatosensory cortex, corpus callosum, visual cortex, dorsal hippocampus	same as R Hemisphere
Middle	auditory cortex, temporal association cortex, perirhinal cortex, ento/ectorhinal cortex, lateral hippocampus, MGB	posterior thalamus, posterior commissure	"
Ventral	ventral hippocampus, posterior tip of amygdala, piriform cortex	posterior hypothalamus, substantia nigra, mammillary nuclei, ventral tegmentum, interpeduncular nucleus	"

Figure 11: Layout and contents of coronal slice E. Adapted from *The Rat Brain Atlas* (Paxinos and Watson).

F1 - F9

Bregma -6 to -9

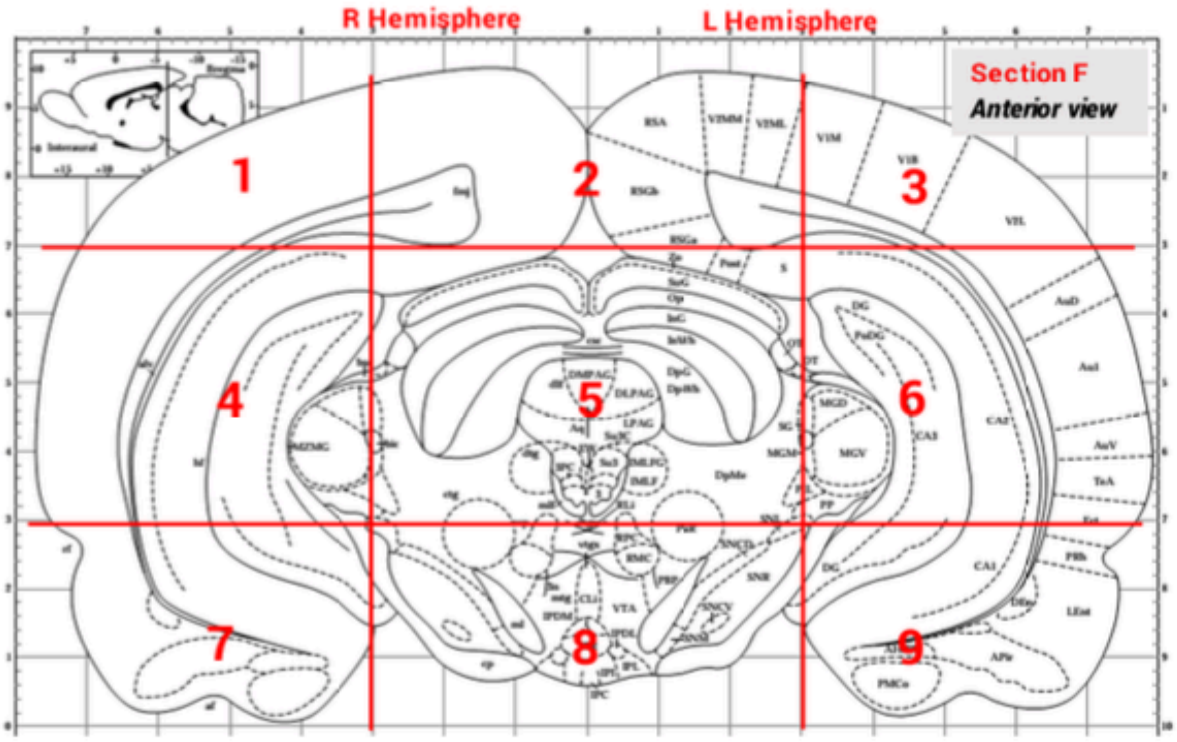

Major Brain Regions

	R Hemisphere	*Middle*	*L Hemisphere*
Dorsal	visual cortex	retrosplenial cortex, visual cortex, forceps major	same as R Hemisphere
Middle	auditory cortex, temporal association cortex, perirhinal cortex, ectorhinal cortex, lateral hippocampus	superior colliculus, inferior colliculus, periaqueductal gray, cerebral aqueduct	"
Ventral	ventral hippocampus, piriform cortex, entorhinal cortex	lateral lemniscus, reticular nucleus, lots of pontine nuclei	"

Figure 12: Layout and contents of coronal slice F. Adapted from *The Rat Brain Atlas* (Paxinos and Watson).

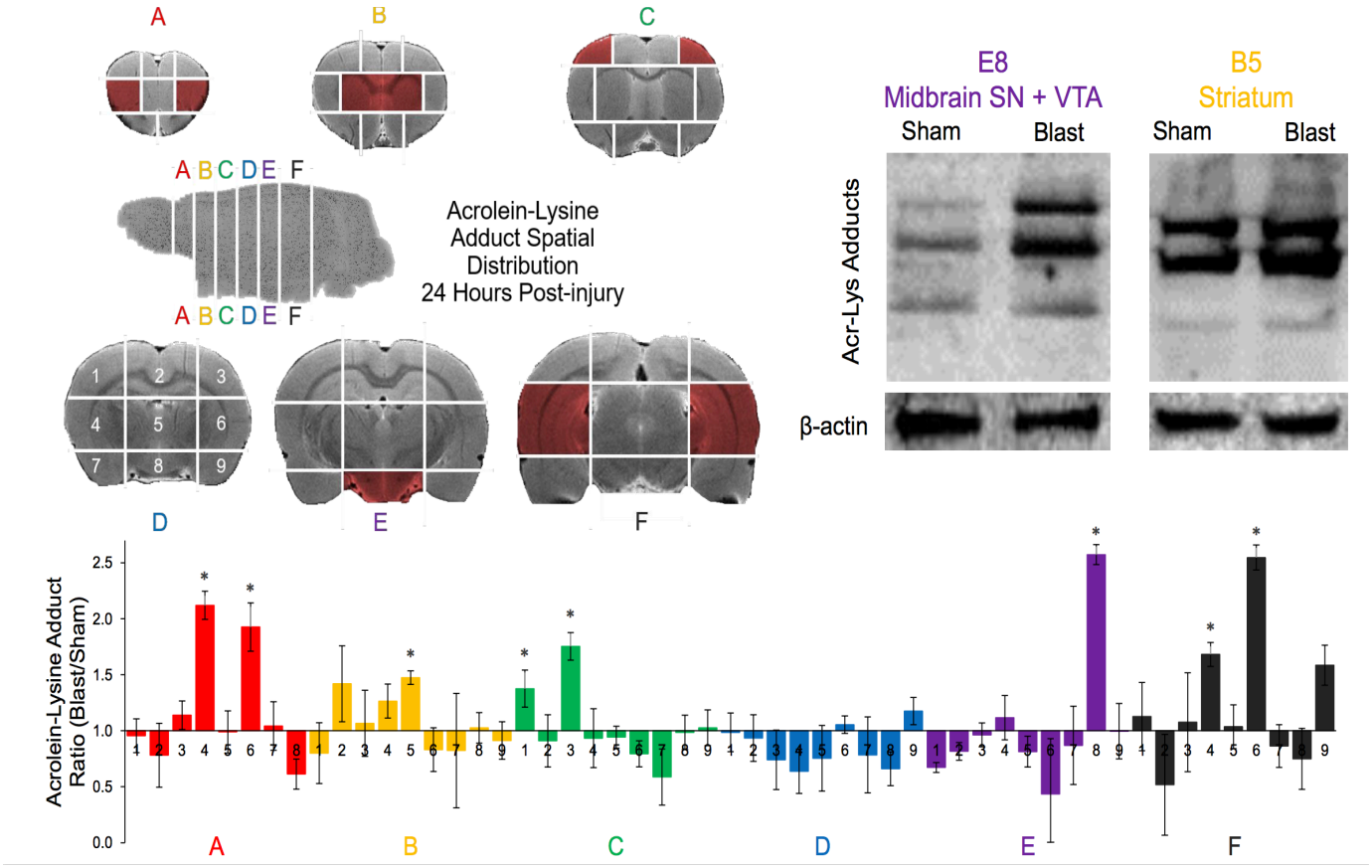

Figure 13: Elevated acrolein-lys protein adducts levels in specific brain regions 24 hrs post-mild blast injury. This figure illustrates specific brain region where oxidative stress is elevated post injury. We dissected specific brain regions from 5 sham (control) and 5 24-hr post-blast injured rats, and isolated protein lysates. Acrolein-lys adduct levels were measured using Western blotting and then normalized to actin. Results displayed as ratio of blast/sham, with only statistically significant results shown in color. We show elevated acrolein levels in the orbital cortex, forceps minor of corpus callosum, somatosensory cortex, and insular cortex (A) both left and right hemisphere. (B) Acrolein is also significantly elevated in the **striatum**, septal nuclei and forceps minor area. (C) Increased acrolein levels in the somatosensory cortex at both hemispheres. (E) Increased levels of acrolein in the ventral mid brain area, including posterior hypothalamus, **substantia nigra**, and ventral tegmentum. (F) Elevated levels of acrolein in the auditory, temporal association cortex, perihinal cortex, ectorhinal cortex and lateral hippocampus.

2.2.3.2. Elevation of acrolein, 3-HPMA measurements, post-mild TBI

The endogenous acrolein metabolite, 3-HPMA (N-acetyl-S-(3hydroxypropyl) cysteine), was measured in the urine post-mild blast TBI utilizing LC-MS-MS method (Fig. 14). Repeated measures ANOVA indicate overall difference [F(4,2.3)=5.20, p=0.005] and pairwise comparison using Fisher's LSD shows significant increased of 3-HPMA levels post-injury as indicated in Fig. 14. In the 1-day (1.93 ± 0.46 μg/mg, n=5), 2- day (2.37 ± 0.40 μg/mg, n=5), 5-days (1.78 ± 0.15 μg/mg, n=4), and 7-day (2.35 ±0.44 μg/mg, n=5) urine collection time points, compared to their baseline (pre) (1.13 ± 0.22 μg/mg, n=5; *p<0.05, **p<0.01)

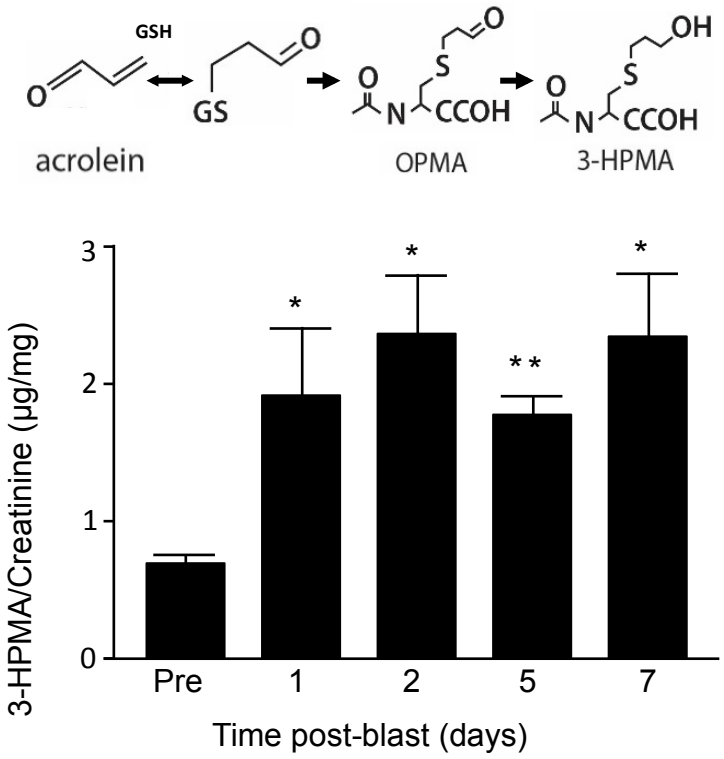

Figure 14. Elevation of 3-HPMA in urine after mild bTBI. Upper panel: schematic of the acrolein reaction with glutathione and production of the metabolites OPMA and 3-HPMA. Lower panel: Urine 3-HPMA detected by LC-MS/MS normalized to urine creatinine content in the blast rats. Urine was collected before injury (baseline), 1, 2, 5 and 7 days post-injury. Repeated measures ANOVA indicate significant effect of day [F(4,2)=5.20, p=0.005]. Pairwise comparisons of post-injury 3-HPMA levels to baseline show significant elevation of 3-HPMA that persists to at least the seventh day post-injury. Data presented as mean ± SEM. Fisher's LSD post-hoc test. *p<0.05, **p<0.01.

2.2.3.3. Increased levels of acrolein-lysine protein adducts in the whole brain, STR and SN regions

Acrolein levels after mild-blast TBI were measured in the whole, STR (B5 (anterior) and C5 posterior) and substantia nigral (E8) brain region by Western blotting (Fig. 15a, 16a,c, 17a). The data shows a significant increase of the acrolein-lysine protein adducts after injury compared to the control (uninjured) group in the whole brain, STR, and SN region lysates. All values were normalized using β-actin and expressed as percent control. Specifically, in the whole brain lysates ANOVA shows a significant group effect [$F(2,22)=5.20$, $p=0.014$] and pairwise comparison shows a significant increase of acrolein-lysine adducts in the 2-day (22.96 ± 4.97 %, n=8), 7-day (22.53 ± 8.01 %, n=8) post-injury groups compared to the control (100 ± 4.28 %, n=9; *$p<0.05$, **$p<0.01$) as shown in Fig 15b. In the striatal B5 (anterior) region ANOVA analysis shows a significant group effect [$F(2,9)=6.58$, $p=0.017$)] and pairwise comparison shows a significant increase of acrolein-lysine adducts in the 2-day (93.18 ± 24.68 %, n=4), 7-day (60.89 ± 10.41 %, n=4) post-injury groups compared to control (100 ± 17.37 %, n=4; *$p<0.05$, **$p<0.01$) as indicated in Fig 16b. Similarly, in C5 striatal region (posterior) ANOVA analysis shows a significant group effect [$F(2,10)=6.22$, $p=0.018$)] and pairwise comparison shows a significant increase of acrolein-lysine adducts in the 2-day (98.44 ± 24.84 %, n=5), 7-day (72.80 ± 20.49 %, n=4) post-injury groups compared to control (100 ± 12.62 %, n=4; *$p<0.05$, **$p<0.01$) as indicated in Fig 16d. In the substantia nigral region (E8) ANOVA analysis shows a significant group effect [$F(2,10)=5.61$, $p=0.023$)] and pairwise comparison shows a significant increase of acrolein-lysine adducts in the 2-day (81.66 ± 23.64 %, n=5), 7-day (117.57 ± 29.07 %, n=5) post-injury groups compared to control (100 ± 19.8 %, n=4; *$p<0.05$, **$p<0.01$) as indicated in Fig 17b.

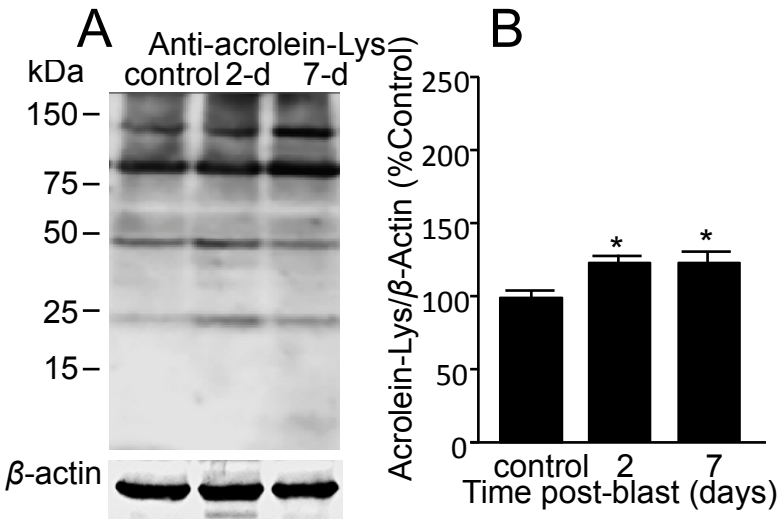

Figure 15. Acrolein-lysine adducts increase in whole brain preparation after mild bTBI. (A) Western Blot image of acrolein-lysine modified proteins (FDP-Lys) and β-actin for each group at control, 2-day and 7-day post-blast. All bands on the acrolein-lysine blot were used for analysis for each group. (B) Quantification demonstrated significant difference between control, 2-day post-injury, and 7-day post-injury [F(2,22)=5.20, p=0.014]. Data are relative, normalized as percent control and presented as mean ± SEM. Tukey's post-hoc test. *p<0.05.

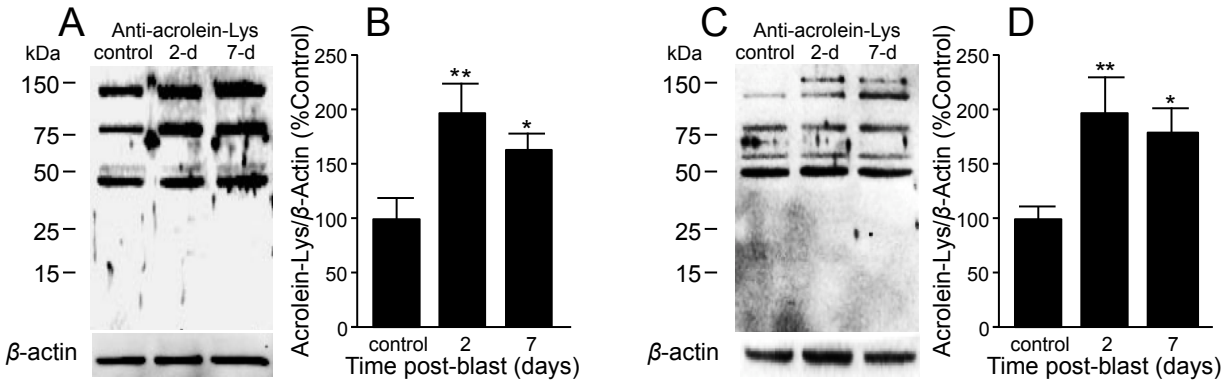

Figure 16. Acrolein-lysine adducts increase in striatum after mild bTBI. (A) Western Blot image of acrolein-lysine modified proteins (FDP-Lys) and β-actin for each group at control, 2-day and 7-day post-blast of the B5 (anterior) striatal region. All bands on the acrolein-lysine blot were used for analysis for each group. (B) Quantification demonstrated significant difference between control, 2-day post-injury, and 7-day post-injury [F(2,9)=6.58, p=0.017]. (C) Western Blot image of acrolein-lysine modified proteins (FDP-Lys) and β-actin for each group at control, 2-day and 7-day post-blast of the C5 (posterior) striatal region. (B) Quantification demonstrated significant difference between control, 2-day post-injury, and 7-day post-injury [F(2,10)=6.22, p=0.018]. Data are relative, normalized as percent control and presented as mean ± SEM. Fisher's LSD post-hoc test. *p<0.05, **p<0.01.

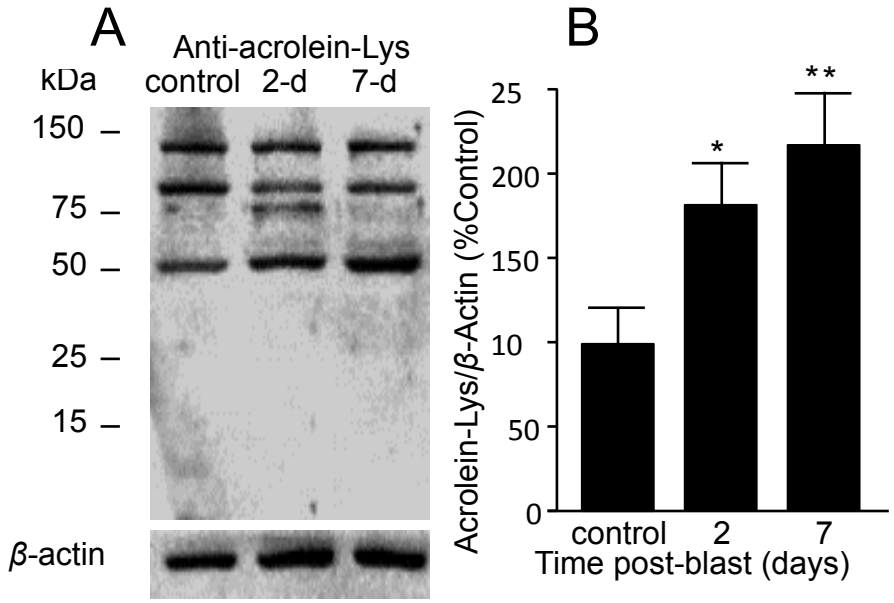

Figure 17. Acrolein-lysine adducts increase in substantia nigra region after mild bTBI. (A) Western Blot image of acrolein-lysine modified proteins (FDP-Lys) and β-actin for each group at control, 2-day and 7-day post-blast. All bands on the acrolein-lysine blot were used for analysis for each group.(B) Quantification demonstrated significant difference between control, 2-day post-injury, and 7-day post-injury [$F(2,10)=5.61$, $p=0.023$]. Data are relative, normalized as percent control and presented as mean ± SEM. Fisher's LSD post-hoc test. *$p<0.05$, **$p<0.01$.

2.2.3.4. Aberrant α-synuclein levels post-mild TBI

α-syn is the main protein present in the Lewy bodies (LB) of the surviving dopaminergic neurons in PD patients. It is a small soluble protein at 14 kDa that is highly localized in the presynaptic terminals and can be essential in the normal brain function. [157-160]. We measured the α-syn protein levels using Western blotting in the whole, striatal, and substantia nigral brain region lysates (Fig. 18a, 19a,e, 20a). We observed two consistent bands of the α-syn protein at 25 kDa and 19 kDa (19 kDa is the predicted size of the antibody used, per mfr. BD Transduction). These bands were confirmed to be species of α-syn by blocking the antibody with α-syn purified protein before incubating the blots (Fig. 21). All values were normalized using β-actin and expressed as percent control. In the whole brain lysates analysis of the 25 kDa band ANOVA shows a significant group effect [$F(2,21)=5.77$, $p=0.01$] and pairwise comparison show a

significant increase in the 2-day (47.21 ± 11.10 %, n=9), 7-day (54.81 ± 15.61 %, n=7) post-injury groups compared to the control (100 ± 10.39 %, n=8; *p<0.05, **p<0.01) as shown in Fig. 18b. On the other hand, in the whole brain lysates at 19 kDa α-syn band a significant group effect is observed [F(2,24)=6.56, P=0.005] and pairwise comparison shows a significant decrease in the 2-day (44.54 ± 5.62 %, n=9), 7-day(59.12 ± 5.78 %, n=7) post-injury groups compared to the control (100 ± 18.8 %, n=8; *p<0.05, **p<0.01) as shown in Fig. 18c. Ratio analysis of the 25 kDa and 19 kDa α-syn bands showed statistically significant increase in the proportion of over all α-syn accounted for by the 25 kDa α-syn species [F(2,20)=5.83, p=0.01] and pairwise comparison show increase levels in the 2-day (132.80 ± 17.62 %, n=9) and 7-day (118.72 ± 55.75 %, n=6) post-injury groups compared to the control (100 ± 12.57 %, n=8; *p<0.05, **p<0.01) as shown in Fig. 18d.

In the striatal regions, B5 (anterior) the levels of α-syn protein levels at 25 kDa show a significant group effect [F(2,9)=5.05 p=0.034] and pairwise comparison shows a significant increase in 2-day (49.50 ± 17.04 %, n=4), 7-day (63.07 ± 18.28 %, n=4) post-injury compared to the control (100 ± 5.47 %, n=4; *p<0.05, **p<0.01) as shown in Fig. 19b. In the C5 (posterior) region a significant group effect [F(2,10)=7.97 p=0.008] and pairwise comparison shows a significant increase in 2-day (111.36 ± 37.08 %, n=4), 7-day (84.87 ± 10.64 %, n=4) post-injury compared to the control (100 ± 8.89 %, n=5; *p<0.05, **p<0.01) as shown in Fig. 19f. α-syn protein levels at 19 kDa show significant decrease in both B5 and C5 striatal regions. In B5 (anterior), a significant group effect [F(2,9)=6.24 p=0.020] and pairwise comparison shows a significant decrease in 2-day (34.23 ± 0.49 %, n=4), 7-day (41.76 ± 8.17 %, n=4) post-injury compared to the control (100 ± 13.69 %, n=4; *p<0.05, **p<0.01) as shown in Fig. 19c. In C5 (posterior), a significant group effect [F(2,10)=10.27 p=0.004] and pairwise comparison shows a significant decrease in 2-day (46.33 ± 5.0 %, n=4), 7-day (51.75 ± 9.70 %, n=4) post-injury compared to the control (100 ± 11.14 %, n=5; *p<0.05, **p<0.01) as shown in Fig. 19g. The ratio analysis of the 25 kDa and 19 kDa bands shows a statistically significant increase in the proportion of overall α-syn protein accounted for by the 25 kDa α-syn species in both B5 and C5 striatal region. In B5 (anterior), [F(2,9)=6.46, p=0.018] pairwise comparison show a significant increase in 2-day (71.68 ± 28.39 %, n=4), 7-day (116.68 ± 27.70, n=4) post-injury compared to the control group (100 ± 5.74, n=4; *p<0.05, **p<0.01) as shown in Fig. 19d. In C5 (posterior), [F(2,10)=23.74, p=0.000] and pairwise comparison show a significant increase in 2-day (232.13

± 48.60 %, n=4), 7-day (301.83 ± 26.79, n=4) post-injury compared to the control group (100 ± 23.72, n=5; *p<0.05, **p<0.01) as shown in Fig. 19h.

Consequently, the α-syn protein levels at 25 kDa in the substantia nigral region show a significant group effect [F(2,10)=5.15 p=0.02] and pairwise comparison shows a significant increase in 2-day (42.08 ± 15.73 %, n=4), 7-day (58.75 ± 19.61 %, n=4) post-injury compared to the control (100 ± 5.18 %, n=5; *p<0.05, **p<0.01) as shown in Fig. 20b. A significant group effect is also observed in the 19 kDa band [F(2,10)=12.9, P=0.002] and pairwise comparison show a decrease in 2-day (28.23 ± 12.64 %, n=4), and significant increase in 7-day (64.82 ± 20.39 %, n=4) post-injury compared to the control (100 ± 2.81 %, n=5, *p<0.05, **p<0.01) as shown in Fig. 20c. Similarly, The ratio analysis of the 25 kDa and 19 kDa bands shows a statistically significant increase in the proportion of overall α-syn protein accounted for by the 25 kDa α-syn species in the SN region (E8) [F(2,10)=9.87, p=0.004] and pairwise comparison show a significant increase only in 2-day (105.11 ± 20.69 %, n=4) and a trend of increase in 7-day (19.77 ± 25.4, n=4) post-injury compared to the control group (100 ± 5.24, n=5; *p<0.05, **p<0.01) as shown in Fig. 20d.

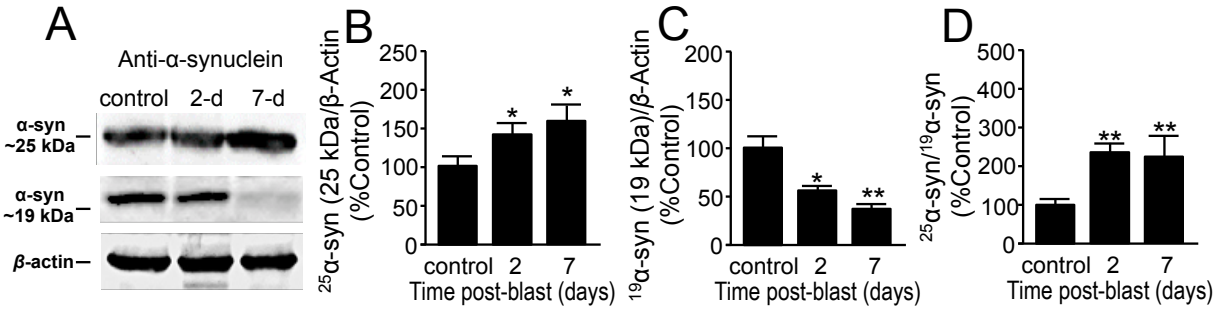

Figure 18. Aberrant expression of α-synuclein in whole brain preparation after mild bTBI. (A) Western Blot image of α-syn at approximately 25kDA, α-syn at 19kDA, and β-actin at control, day 2 and day 7 post-blast. There are significant differences between control and 2-day post-injury, and 7-day post-injury in both (B) 25 kDa α-syn from [F(2,21)=5.77 p=0.01] and (C) 19 kDa α-syn form [F(2,24)=6.56, p=0.005]. (D) The normalized ratio of the 25 kDa and 19 kDa α-syn at control, 2 and 7 days post-blast indicates an increase in the proportion of 25 kDa α-syn [F(2,20)=5.83, p=0.01). Data in B-D are relative, normalized as percent control, and presented as mean ± SEM. Tukey's post-hoc test.

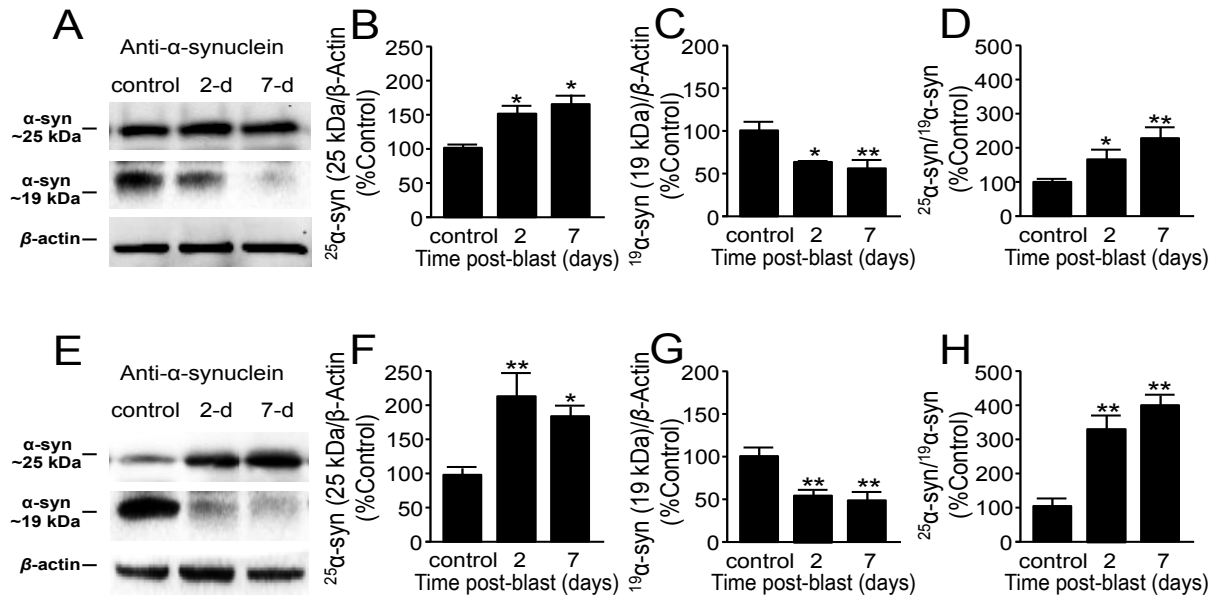

Figure 19. Aberrant expression of α-synuclein in striatal region after mild bTBI. (A) B5 (anterior) striatal region Western blot image of α-syn at approximately 25kDA, α-syn at 19kDA and β-actin for control, day 2 and day 7 post-blast. There were significant differences between control, 2-day post-injury, and 7-day post-injury in both (B) 25 kDa [$F(2,9)=5.05$ $p=0.034$] and (C) 19 kDa [$F(2,9)=6.24$, $P=0.020$] forms of α-syn. (D) The normalized ratio of the 25 kDa and 19 kDa forms of α-syn at control, 2 and 7 days post-blast indicates an increase in the proportion of 25kDa form of α-syn [$F(2,9)=6.46$, $p=0.018$]. (E) C5 (posterior) striatal region Western blot image of α-syn at approximately 25kDA, α-syn at 19kDA and β-actin for control, day 2 and day 7 post-blast. There were significant differences between control, 2-day post-injury, and 7-day post-injury in both (F) 25 kDa [$F(2,10)=7.97$ $p=0.008$] and (G) 19 kDa [$F(2,10)=10.27$, $P=0.004$] forms of α-syn. (H) The normalized ratio of the 25 kDa and 19 kDa forms of α-syn for control, 2 and 7 days post-blast indicates an increase in the proportion of 25kDa form of α-syn [$F(2,10)=23.74$, $p=0.000$]. Data in B-D and F-G are relative, normalized as percent control, and presented as mean ± SEM. Fisher's LSD post-hoc test. *$p<0.05$, **$p<0.01$.

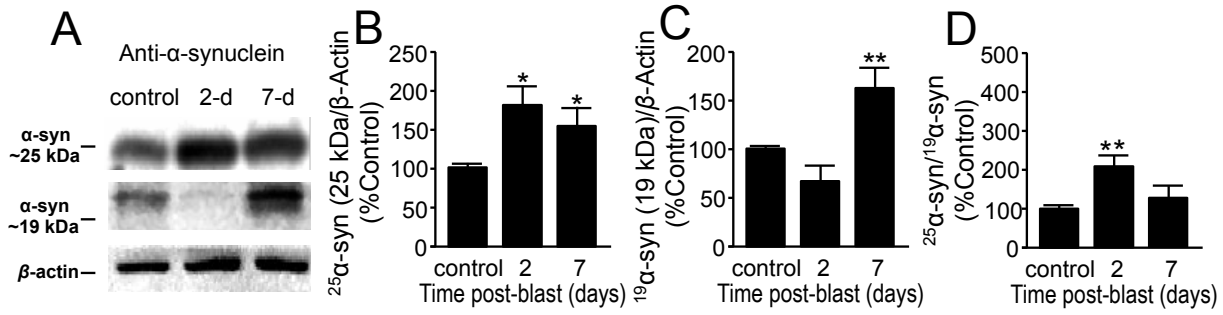

Figure 20. Aberrant expression of α-synuclein in substantia nigra region after mild bTBI. (A) Western Blot image of α-syn at approximately 25kDA, α-syn at 19kDA and β-actin at control, day 2 and day 7 post-blast. There were significant differences between control, 2-day post-injury, and 7-day post-injury in both (B) 25 kDa [F(2,10)=5.15 p=0.02] and (C) 19 kDa forms of α-syn [F(2,10)=12.9, P=0.002]. (D) The normalized ratio of the 25 kDa and 19 kDa forms of a α-syn at control, 2 and 7 days post-blast indicates an increase in the proportion of 25 kDa α-syn [F(2,10)=9.87, p=0.004]. Data in B-D are relative, normalized as percent control, and presented as mean ± SEM. Fisher's LSD post-hoc test. *p<0.05, **p<0.01.

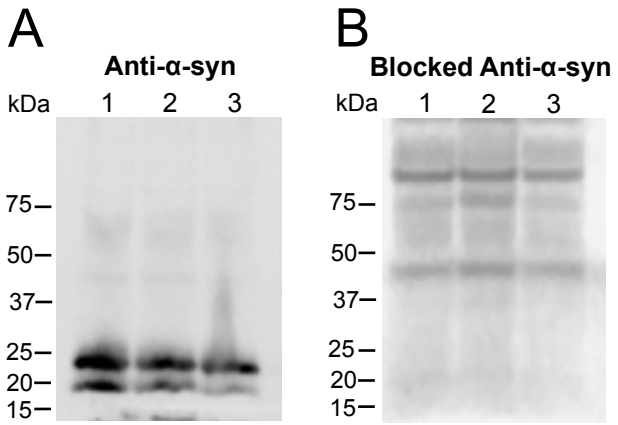

Figure 21. Western Blot confirming the 25 kDa and 19 kDa forms α-Synuclein. Whole brain protein lysates from rats were used at the same concentration for samples 1-3. Blots were run simultaneously. **(A)** Western blot image of samples 1-3 incubated with the α-syn antibody. **(B)** Western blot image of samples 1-3 incubated with the blocked α-syn antibody. The antibody was blocked with purified α-syn protein for 2 hours at 4^{o}C prior to blot incubation. The absence of distinct bands at 25 kDa and 19 kDa confirmed that these were α-syn protein species.

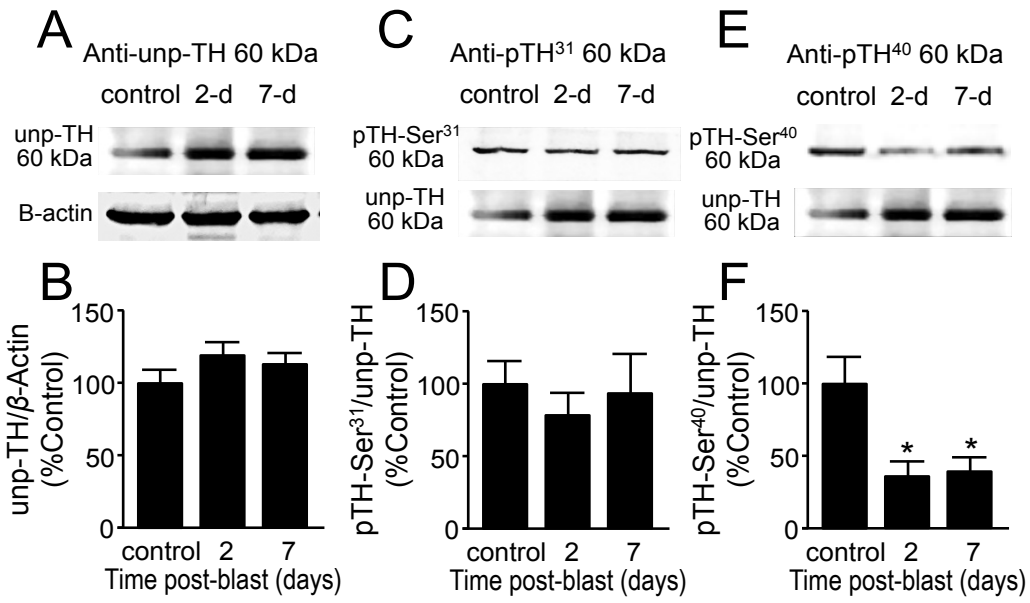

Figure 22. Decreased phosphorylation of tyrosine hydroxylase (TH) at Ser^{40} suggests reduced TH activity after mild bTBI in whole brain preparation. (A,C,E) Western Blot images of un-phosphorylated TH (A), phosphorylated TH at Ser^{31} (B), phosphorylated TH at Ser^{40} (C), and β-actin for each group at control, 2 and 7 days post-blast. (B,D,F) Comparisons were made between control, 2-day post-injury, and 7-day post-injury in all three forms of TH. No changes were observed in (B) un-phosphorylated or (D) Ser^{31}-phosphorylated TH. (F) Phosphorylation at Ser^{40}, TH's primary activation site, demonstrated significant reductions at both 2 and 7 days post-injury [$F(2,21)=5.24$, $p=0.014$]. Data in B,D,F is relative, normalized as percent control, and presented as mean ± SEM. Tukey's post-hoc test. *$p<0.05$.

2.2.3.5. Acute alterations of tyrosine hydroxylase protein post-mild TBI

Tyrosine hydroxylase (TH) is the rate limiting enzyme in the production of dopamine from the amino acid tyrosine. In PD patients the TH activity is decreased in the nigro-striatal area resulting in decrease dopamine levels. We measured the protein levels of TH and its phosphorylation sites at serine 31 and serine 40 post-injury in the whole brain (Fig. 22), striatal (Fig. 23) and susbstantia nigral (Fig. 24) region protein lysates using Western blotting. The un-phosphorylated from of TH (Unp-TH) were normalized using β-actin and the phosphorylated TH, pSer31 and pSer40, were normalized with the unp-TH, and values were expressed as percent control. In the whole brain lysates (Fig. 22a, c, e), there were no significant changes in the TH protein levels [$F(2,24)=1.53$, $p=0.23$] (Fig. 22b) and TH pSer31[$F(2,21)=0.037$, $p=0.69$] (Fig. 22d), respectively. However, there was a significant group effect of TH pSer40 [$F(2,21)=5.24$, $p=0.014$ and pairwise comparison show significant decrease in 2-day (62.70 ± 9.09 %, n=8) and 7-day (60.10 ± 9.74 %, n=7) post-injury groups compared to control (100 ± 21.74 %, n=9; *$p<0.05$, **$p<0.01$) (Fig. 22f).

In the striatal brain region lysates, there were no significant changes in the TH protein levels [$F(2,10)=0.216$, $p=0.81$], [$F(2,10)=0.665$, $p=0.53$] in both B5 (anterior, Fig. 23a,b) and C5 (posterior) regions respectively (Fig 23g,j). TH pSer31 expression showed no significant changes in B5 (anterior, Fig. 23c,d) [$F(2,10)=1.04$, $p=0.38$] (Fig. 23d) and C5 (posterior) [$F(2,10)=0.524$, $p=0.60$] (Fig. 23h,k). However, there was a significant group effect of TH pSer40 in B5 (anterior) region [$F(2,10)=6.24$, $p=0.02$] (Fig. 23e,f) and pairwise comparison showed significant increase in 2-day (85.03 ± 27.01 %, n=4) and 7-day (103.57 ± 20.22 %, n=5) post-injury groups compared to control (100 ± 17.81 %, n=5; *$p<0.05$, **$p<0.01$) as shown in Fig. 23f. Similarly in the C5 (posterior) region [$F(2,10)=6.41$, $p=0.016$] pairwise comparison showed significant increase in 2-day (167.99 ± 33.67 %, n=4) and 7-day (167.36 ± 61.26 %, n=4) post-injury groups compared to control (100 ± 20.96 %, n=5; *$p<0.05$, **$p<0.01$) as shown in Fig. 23i,l.

In the substantia nigral region, TH protein (Fig. 24a) and its phosphorylation sites at serine 31(Fig. 24c) and serine 40 (Fig. 24e) were also measured using Western blotting. A significant group effect was observed in the TH protein levels [$F(2,10)=5.61$, $p=0.033$] and pairwise comparison indicated significant increase in the 2-day (114.84 ± 40.08 %, n=4) and 7-day (96.47 ± 26.29 %, n=5) post-injury groups compared to the control group (100 ± 20.20 %, n=4) as shown in Fig. 24b. TH protein levels at serine 31 phosphorylation site showed a significant

group effect [F(2,10)=5.96, p=0.02] and pairwise comparison showed significant decrease in 2-day (38.17 ± 3. 62 %, n=4) and 7-day (37.28 ± 5.04 %, n=5) post-injury groups compared to control (100 ± 12.66 %, n=4; *p<0.05, **p<0.01) as shown in Fig. 24d. Similarly, TH protein levels at serine 40 phosphorylation site showed a significant group effect [F(2,10)=12.81, p=0.002] and pairwise comparison showed significant decrease in 2-day (60.87 ± 18.33 %, n=4) and 7-day (77.98 ± 6.81 %, n=5) post-injury groups compared to control (100 ± 8.43 %, n=4; *p<0.05, **p<0.01) as shown in Fig. 24f.

2.2.3.6. Acrolein induces α-syn protein oligomerization and aggregation in vitro

The effects of acrolein on the α-syn protein were studied *in vitro* using a purified protein provided by the Rochet lab at Purdue University. Purified α-syn protein samples were treated with acrolein for 20 hrs. All sample groups were run in triplicates. Western blot detection using anti-α-syn (Fig. 25a) indicates the protein at 15 kDa becomes broader with increasing acrolein concentrations and at 1 mM acrolein this band starts to fade as the acrolein concentration increases. Quantification of this band is shown in Fig. 25b. Similarly, quantification of the band at 37 kDa, which is a species of α-syn protein, follows the same trend as the 15 kDa band (Fig. 25a, b). In addition, speculated oligomerized and aggregated forms α-syn were observed at 125 μM up to1 mM of acrolein and faded with higher concentrations of acrolein (red arrows, Fig. 25a). Quantification of these observed bands is shown in Fig. 25b (bands above 37 kDa).

Similarly, Western blot detection using anti-acrolein-lys adduct antibody (Fig. 25c) demonstrates that the acrolein-modified α-syn protein bands at 15 kDa becomes broader with increasing acrolein concentrations and starts to decrease at 10 mM of acrolein. Quantification of these bands is shown in Fig. 25d. Acrolein-modified proteins were also observed at 250 μM up to 1 mM of acrolein (arrows, Fig. 25c). Quantification of these bands is shown in Fig. 25d. These data suggest that the α-syn aggregation and oligomerization is dose-dependent to acrolein concentrations; and the native α-syn protein seems to either a) degrade at the higher concentrations of acrolein or b) be modified so extensively by acrolein that the antibody binding sites are blocked.

2.2.3.7. Increased interaction and co-localization between α-syn and acrolein post-mild blast TBI

Coimmunoprecipitations (co-IPs) were conducted on the whole brain lysates of the control, 2-day, and 7-day post-injury groups with antibodies against α-syn and acrolein-lysine adducts. Consequently, immunoblotting (IBs) using the same antibodies were performed to detect co-localization of these two molecules in each sample group. In the acrolein-lys-precipitated (Acr-IP) row for each sample group, α-syn species were detected in the α-syn IB (Fig. 26a), particularly distinct bands at around 50 and 75 kDa (two arrows) were observed and these bands are intensified in the 2-day and 7-day post-injury groups. Notably, the α-syn IP (Fig. 26a, single arrow) was also relatively increased in the post-injured groups compared to the control group. Similarly, in the Acr-Lys adducts IB (Fig. 26b), bands in the α-syn IP row (arrow) were detected and the intensity of this is increased in the 2-day and 7-day post-injured groups. In addition, the Acr IP row (arrow) intensity is also increased in the injured groups at around 50-75 kDa. Furthermore, immunofluorescence staining show increased co-localization of α-syn protein and acrolein-lysine adducts in the striatum (Fig 26c) and substantia nigra (Fig 26d) in both the 2-day and 7-day post-injury groups. These data suggest increasing levels of α-syn protein and acrolein-lysine adducts, and provide direct visual confirmation of their co-localization after blast injury, supporting the in vitro (Fig. 25) and in vivo (Fig. 26a,b) protein analyses suggesting such a relationship may be possible.

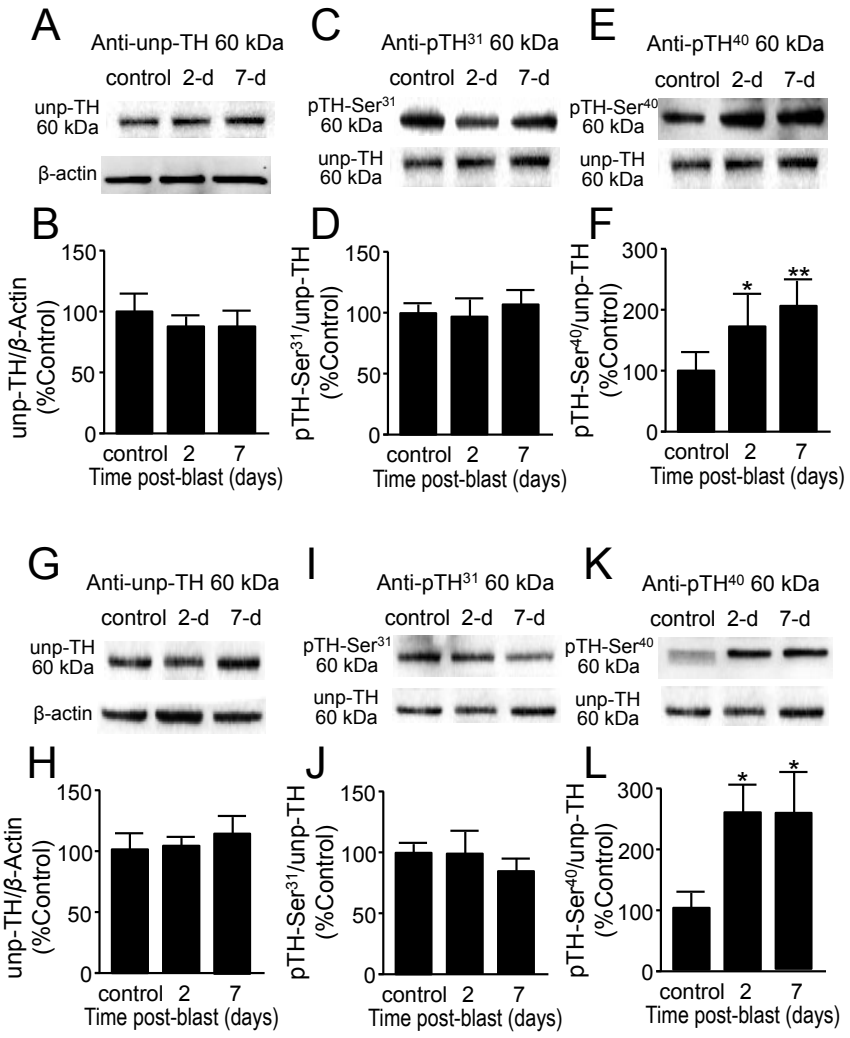

Figure 23. Increased phosphorylation of tyrosine hydroxylase (TH) at Ser^{40} suggests increased TH activity in the striatum after mild bTBI. (A,C,E) B5 (anterior) striatal region Western Blot images of (A) un-phosphorylated TH, (C) phosphorylated TH at Ser^{31}, (E) phosphorylated TH at Ser^{40}, and β-actin for each group at control, 2 and 7 days post-blast. (B,D,F) Comparisons were made between control and 2-day post-injury, as well as 7-day post-injury in al three forms of TH. (B) There were no significant changes in the un-phosphorylated TH at 2 and 7 days post-blast [$F(2,10)=0.216$, $p=0.81$]. (D) There were no significant changes in the Ser^{31}-phosphorylated TH [$F(2,10)=1.04$, $p=0.38$] and (F) There is a significant increase in the Ser^{40}-phosphorylated TH [$F(2,10)=6.24$, $p=0.02$]. (G,I,K) C5 (posterior) striatal region Western Blot images of (G) un-phosphorylated TH, (I) phosphorylated TH at Ser^{31}, (K) phosphorylated TH at Ser^{40}, and β-actin for each group at control, 2 and 7 days post-blast. (H,J,L) Comparisons were made between control and 2-day post-injury, as well as 7-day post-injury in al three forms of TH. (H) There were no significant changes in the un-phosphorylated TH at 2 and 7 days post-blast [$F(2,10)=0.665$, $p=0.53$]. (J) There were no significant changes in the Ser^{31}-phosphorylated TH [$F(2,10)=0.524$, $p=0.60$] and (L) There was a significant increase in the Ser^{40}-phosphorylated TH [$F(2,10)=6.41$, $p=0.016$]. Data in B,D,F and J,K,L is relative, normalized as percent control, and presented as mean ± SEM. Fisher's LSD post-hoc test. *$p<0.05$, **$p<0.01$.

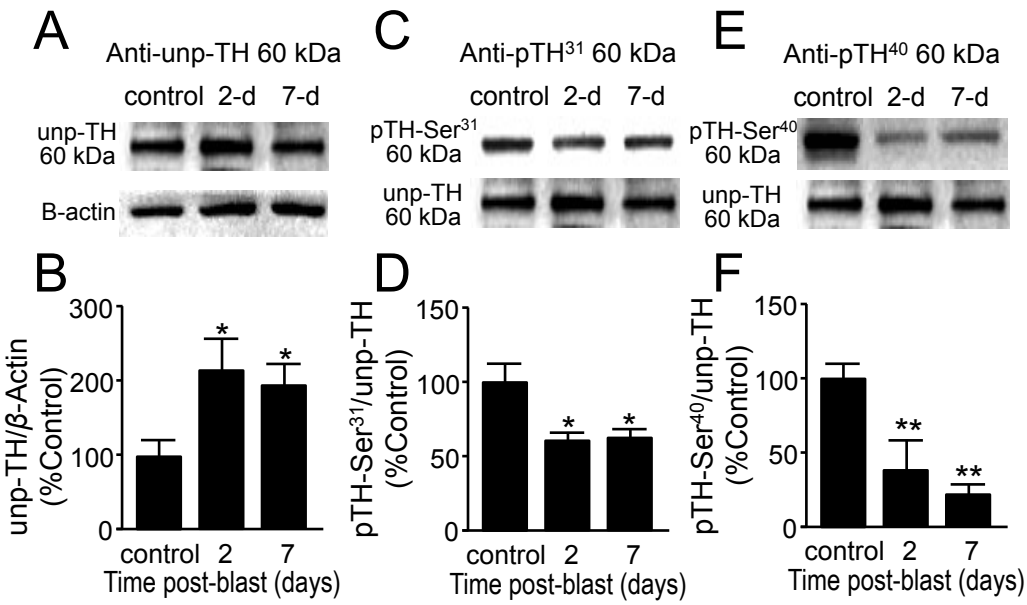

Figure 24. Decreased phosphorylation of tyrosine hydroxylase (TH) at Ser^{40} and Ser^{31} suggest reduced TH activity in the substantia nigra region after mild bTBI. (A,C,E) Western Blot images of (A) un-phosphorylated TH, (C) phosphorylated TH at Ser^{31}, (E) phosphorylated TH at Ser^{40}, and β-actin for each group at control, 2 and 7 days post-blast. (B,D,F) Comparisons were made between control and 2-day post-injury, as well as 7-day post-injury in al three forms of TH. (B) Un-phosphorylated TH was significantly increased at 2 and 7 days post-blast [$F(2,10)=5.61$, $p=0.033$]. (D) Ser^{31}-phosphorylated TH [$F(2,10)=5.96$, $p=0.02$] and (F) Ser^{40}-phosphorylated TH [$F(2,10)=12.81$, $p=0.002$], TH's two most common activation sites, both demonstrated significant reductions at 2 and 7 days post-injury. Data in B,D,F is relative, normalized as percent control, and presented as mean ± SEM. Fisher's LSD post-hoc test. *$p<0.05$, **$p<0.01$.

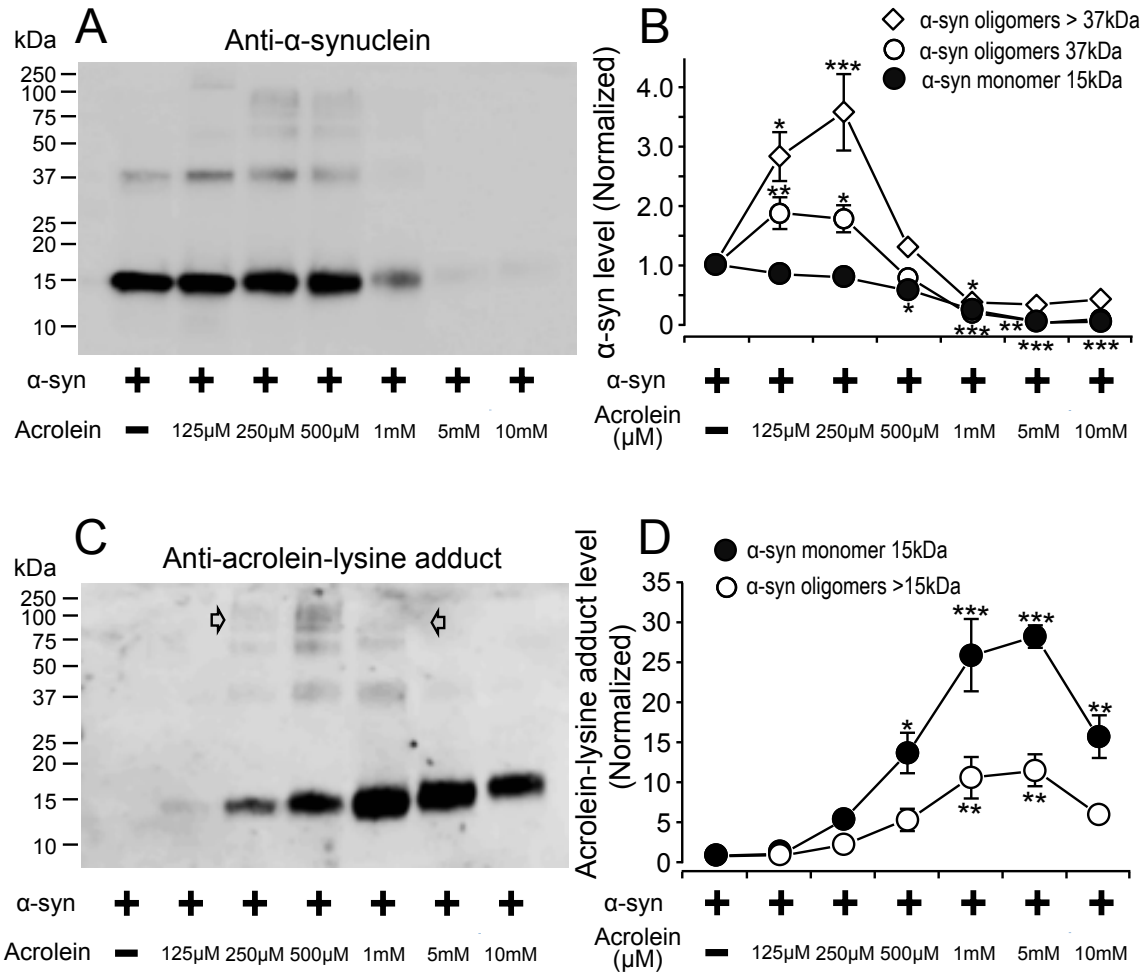

Figure 25. Acrolein induces α-synuclein oligomerization and aggregation *in vitro*. α-synuclein (2.5 μM) was incubated alone and in the presence of ACR at different concentrations (0.125, 0.25, 0.5, 1, 5, and 10 mM) at 37^{o}C for 20h. All samples were run in triplicates. Samples were separated by SDS-PAGE and blotted using either α-syn (A,B) or acrolein-lysine antibodies (C,D). (A) Immunoblotting image using anti-α-syn. (B) Quantification of the image in (A). Comparison of immunoreactivity for bands at 15 kDa [$F(6,20)=32.16$; $p<0.001$], 37 kDa [$F(6,20)=31$; $p<0.001$], and >37kDa [$F(6,20)=19.83$, $p<0.001$] showed significant effect across different acrolein concentrations. Compared to isolated α-syn incubation, there was a significant increase in α-syn oligomers when incubated with 125μM and 250μM acrolein, as well as a decrease in monomers for all acrolein concentrations ≥500μM. (C) Immunobloting images using anti-acrolein-lysine. (D) Quantification graph of the image on (C). Analysis of the bands at 15 kDa [$F(6,20)=23.7$; $p<0.001$] and >15 kDa [$F(6,20)=8.8$; $p<0.001$] showed significant effects. Compared to isolated α-syn incubation, there was a significant change in acrolein-modified α-syn levels with the addition of acrolein. Significant increases in acrolein-modified α-syn monomers were observed at all concentrations ≥500μM acrolein, while acrolein-modified α-syn oligomers significantly increased at 1 and 5 mM acrolein. Data in B,D is relative, normalized as percent control, and presented as mean ± SEM. Tukey's post-hoc test. *$p<0.05$, **$p<0.01$, ***$p<0.001$.

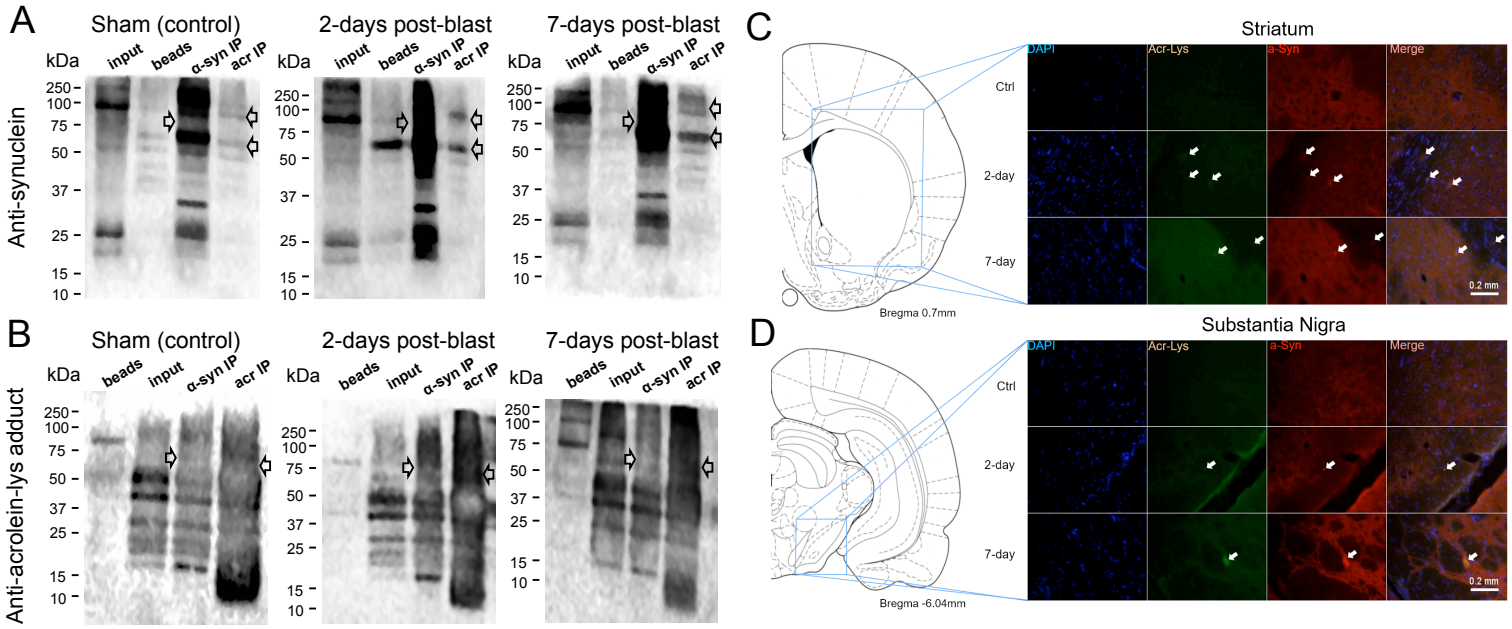

Figure 26. Increased acrolein and α-synuclein interaction and co-localization *in vivo* after mild bTBI. **(A-B)** Whole brain lysates from control, 2 and 7 day post-blast rats were homogenized and immunoprecipitated with either α-syn or acrolein-lysine antibodies. Then, samples were subjected to SDS-PAGE and immunoblotting detection using anti-α-syn (A) or anti-acrolein-lysine (B) to complete the co-immunoprecipitation procedure. (A) Immunoblotting using α-syn antibody from each group's brain lysate. Arrows indicate bands of interest that are acrolein-modified α-syn proteins and show increased expression in injured rats. (B) Immunoblotting using acrolein-lysine antibody from each group's brain lysate. Arrows indicate acrolein-modified α-syn proteins and show increased expression after blast injury, reinforcing the result from (A). Representative immunofluorescence staining data showed increased co-localization of FDP-lysine and α-syn immunoreactivities in the striatum (C) and substantia nigra (D) 2-day and 7-day post-blast injury.

2.2.3.8. Tau Neuropathogy post-mild TBI

Tau protein is one of the major microtubule associated proteins (MAPs) and plays an essential function in the modulation and spatial organization of microtubules [161-165]. This protein is the main component of the neurofibrillary tangles (NFT's), one of the pathological hallmarks of Alzheimer's disease (AD) [161], however tau protein neuropathy (tauopathy) is also observed in PD and can be found in the Lewy bodies, hallmark of PD [166-170]. We measured the levels of tau post-blast injury using an antibody to detect paired helical filaments, abnormal form of tau, at Ser202/Thr205 phosphorylation sites. In the whole brain lysates (Fig. 27a, b) there was a significant increase 2 days (58.54 ± 33.82 %, n=5), post injury and sustained until 7 days (41.65 ± 29.51 %, n=5), compared to the control group (100 ± 6.41 %, n=5); [$F(2,12)=4.79$, $p=0.030$]. Similarly in the SN area (E8), (Fig. 27 c, d) there was a significant increase 2 days (108.17 ± 30.64 %, n=4) and sustained increase 7 days (61.29 ± 14.97 %, n=4) post injury compared to the control group (100 ± 18.43 %, n=5); [$F(2,10)=6.73$, $p=0.016$]. In the anterior STR (B5) (Fig 27e, f) there was a significant increase 2 days (48.56 ± 9.21 %, n=4) and 7 days (26.83 ± 7.08 %, n=5) post injury compared to the control (100 ± 6.16 %, n=4); [$F(2,10)=9.55$, $p=0.005$]. In the posterior STR (C5) (Fig 27g, h) there was a significant increase 2 days (69.28 ± 8.97 %, n=4) and 7 days (81.11 ± 20.21 %, n=5) post injury compared to the control (100 ± 14.88 %, n=4); [$F(2,10)=6.88$, $p=0.013$].

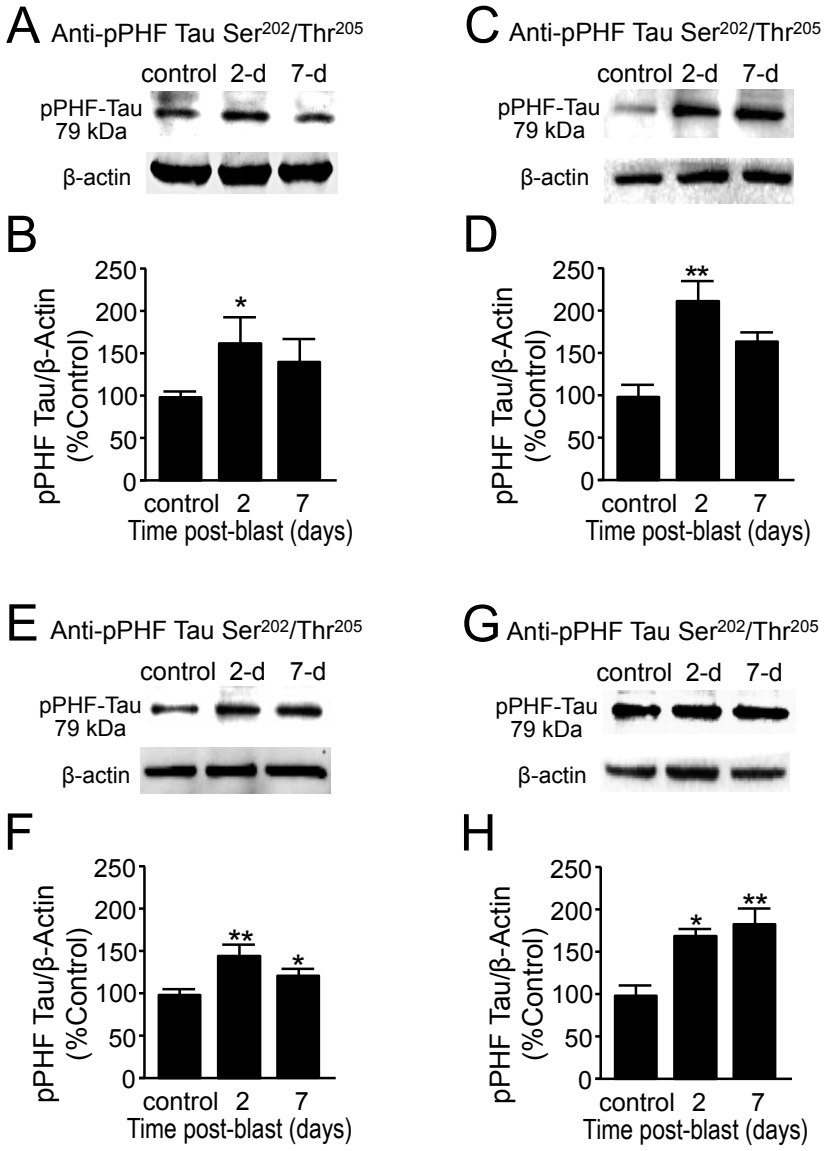

Figure 27. Increased pPHF Tau Ser^{202}/Thr^{205} in the whole brain, SN and STR region. Comparisons of pPHF Tau were made between control and post-blast in these brain areas. (A) Western Blot image of pPHF Tau Ser202/Thr205 and β-actin for each group at control, 2 and 7 days post-blast in the whole brain. (B) pPHF Tau Ser202/Thr205 significantly increased at 2 and a trend of increased at 7 days post-blast [$F(2,12)=4.79$, $p=0.030$]. (C) Western Blot image of pPHF Tau Ser202/Thr205 and β-actin for each group at control, 2 and 7 days post-blast in the SN (E8). (D) pPHF Tau Ser202/Thr205 significantly increased at 2 and a trend of increased at 7 days post-blast [$F(2,10)=6.73$, $p=0.016$]. (E) Western Blot image of pPHF Tau Ser202/Thr205 and β-actin for each group at control, 2 and 7 days post-blast in the B5 STR region. (F) pPHF Tau Ser202/Thr205 significantly increased at 2 and a trend of increased at 7 days post-blast [$F(2,10)=9.55$, $p=0.005$]. (G) Western Blot image of pPHF Tau Ser202/Thr205 and β-actin for each group at control, 2 and 7 days post-blast in the C5 STR region. (H) pPHF Tau Ser202/Thr205 significantly increased at 2 and a trend of increased at 7 days post-blast [$F(2,10)=6.88$, $p=0.013$]. Data in B,D,F is relative, normalized as percent control, and presented as mean ± SEM. Either Tukey's or Fisher's LSD post-hoc test were used. *$p<0.05$, **$p<0.01$.

2.2.4. Discussion

TBI has been associated with an increased risk for Parkinson's disease [26, 118, 119, 171-173]. PD-like neuropathologies, such as α-syn aggregation and tyrosine hydroxylase dysregulation have been observed in animal models of TBI [139, 174, 175]. However, pathophysiological mechanisms leading to PD-like neurodegenerative processes after TBI are currently not well-characterized. In the present investigation, we report the first direct evidence indicating the ability of acutely upregulated post-TBI oxidative stress / lipid peroxidation-related reactive aldehydes, namely acrolein, to modify α-syn, both *in vitro* and *in vivo*. We also demonstrate dysregulation of the primary dopamine synthesis pathway via alterations in TH phosphorylation sites in the whole brain and more specifically the nigrostriatal pathway. We assert that early post-injury oxidative stress / lipid peroxidation products after TBI play an important role in initiating and perpetuating neurodegenerative processes mimicking those observed in idiopathic PD, perhaps accelerating onset or heightening the susceptibility to Parkinsonian pathologies in TBI patients. Together, these data provide insight into putative biochemical mechanism/s, which may link the acute and subacute pathophysiology of TBI to known PD-relevant neurodegenerative processes.

2.2.4.1. Oxidative stress and lipid peroxidation, as observed via increased acrolein, play a key role in secondary injury progression after TBI

We observed significant increases of 3-HPMA, an acrolein metabolite (Fig. 14), in the urine 1-7 days post injury, and acrolein-lysine adducts in post-mortem whole brain (Fig. 15), STR (Fig. 16) and SN (Fig. 17) regions at 2 and 7 days post-injury. These data support and expand the results of our previous study where we established a consistent animal mbTBI model mimicking the human condition and observed brain elevation of acrolein-lysine adducts at 1 and 5 days post-injury alongside urine 3-HPMA elevation at 1 and 2 days post-injury[137]. It has been demonstrated that acrolein and the other reactive aldehydes are elevated in TBI and their levels have long been associated with the mortality rate in TBI, suggesting this class of molecules as putative surrogate biomarkers for the injury [176-180].

In the central nervous system, the majority of oxidative stress is manifested by lipid peroxidation, which leads to the generation of reactive aldehydes such as acrolein, 4-hydroxy-2-nonenal (HNE), and malondialdehyde (MDA) [41-43]. Acrolein is the most reactive of the α,β-unsaturated aldehydes produced endogenously, has a longer half-life in comparison to reactive

oxidative stress molecules [57, 58], and has been independently associated with PD [146], Alzheimer's disease [49, 181], and spinal cord injury (SCI) pathophysiology [54]. Our lab has studied SCI in depth, demonstrating that acrolein levels correlated with post-SCI deficit severity and, further, administration of acrolein-scavenging pharmacophores ameliorated SCI-induced impairments [51-53, 55]. With acrolein's relatively long half-life and its proven neurotoxicity in the context of neuronal trauma and degenerative diseases [46, 54], we speculate that similar biochemical changes and damages occur in brain tissue after TBI.

We have established that mechanical trauma during mbTBI, in a similar fashion to SCI, can provide an initial spike of acrolein in the lipid-rich environment of the brain – a phenomenon which can likely be attributed to abundance of myelin and axonal membrane as substrates for lipid peroxidation. Acrolein and related reactive aldehydes are known to exert numerous potentially neurotoxic effects including disrupting intracellular signaling pathways, dysregulating mitochondrial function and cellular metabolism, and binding and modifying structure and function of nucleic acids, lipids, and proteins. It has been reported that overproduction of acrolein significantly elevates oxidative stress through depletion of glutathione [156, 182, 183]. This leads to a self-regenerative feed-forward cycle, where oxidative stress via lipid peroxidation leads to more production of acrolein, which itself can perpetuate oxidative stress [44, 184, 185].

On proteins, specifically, acrolein preferentially binds to three functional groups with high affinity: the sulfhydryl group of cysteine, the amino group of lysine, and imidazole group of histidine, forming covalent adducts [47, 186, 187] which can subsequently affect protein expression and function. TBI has been documented to alter the proteome, namely via post-translational modifications (PTMs) of key proteins such as microtubule-associated proteins (MAP2A/2B), hexokinase, and ubiquitin carboxy-terminal hydrolase L1 protein (UCHL-1) [188-190]. These PTMs can lead to the dysfunction of the proteins and increase the risk of diseases [41, 176]. Our data suggest PTMs by acrolein and subsequent dysregulation of PD-related proteins (α-syn and TH, discussed in more detail below) in the nigrostriatal regions after TBI as a possible point of convergence between brain trauma and PD. More broadly, our findings implicate oxidative stress as a common post-TBI phenomenon capable of triggering a biochemical cascade altering protein structure and function which, left unmitigated, could lead to long-term post-TBI consequences including neurodegeneration.

2.2.4.2. Acrolein affects expression and promotes oligomerization of α-syn: A PD-like post-TBI neuropathology

α-Syn is the main protein present in the Lewy Bodies found in the surviving dopaminergic neurons of PD patients. It is a small, soluble protein that is highly localized in presynaptic terminals [191, 192], and can be essential to normal brain function [157-160]. While its exact function(s) are not completely understood, α-syn has been reported to facilitate membrane trafficking, dopamine regulation, and synaptic plasticity [193]. Overexpression of α-syn has been observed in animal models of TBI [119, 172, 173, 194], but the mechanisms by which PD-like neuropathologies are exacerbated by TBI remain ambiguous.

In this study we observed, in the whole brain, STR and the SN areas, two species of α-syn protein: 25 kDa and predicted form at 19 kDa. Confirmatory experiments have shown that both of these bands are α-syn (Fig. 21). In the whole brain (Fig. 18b), STR (Fig. 19b,f), and SN (Fig. 20b) regions the expression of the 25 kDa α-syn was increased post-injury. Similarly the ratio of the 25 kDa to 19 kDa forms (Figs. 18d, 19d,h, 20d) was elevated. These data indicate an increase in the proportion of overall α-syn accounted for by the 25 kDa form of α-syn in the whole brain, STR and SN regions 2 and 7 days post-mbTBI. These results are in accordance with preclinical and clinical studies where TBI promoted the overexpression of α-syn [26, 118, 119, 171-173]. In contrast, we observed a gradual significant decrease in levels of 19 kDa predicted form of α-syn in the whole brain (Fig. 18c) and the STR (Figs.19c, g) post-injury. Interestingly, in the SN-area there was a decrease in 19 kDaα-syn two days after blast and a significant increase seven days post injury (Fig. 20c). We suspect that the 19 kDa predicted form α-syn is the "native/normal" state of the protein and our data suggest that this is decreasing post-injury. Consequently, we speculate the 25 kDa to be a post-translationally modified (PTM) form of α-syn and this form is increasing post-injury. However, the nature of this species of α-syn needs to be further investigated. Together, these results suggest a spatiotemporally dynamic, aberrant expression pattern of α-syn occurs after mbTBI.

Currently, little is known about the mechanism leading to the post-TBI aggregation of α-syn; however, one study suggests PTMs and protein dimerization can be a rate-limiting step of its aggregation en route to LB formation [195]. The structure of α-syn may be one reason this protein is particularly vulnerable to PTMs by reactive aldehyde species, namely acrolein. The protein structure of α-syn contains seven imperfect repeats of 11 amino acids, which form N-

terminal helices, a central hydrophobic domain, and acidic rich C-terminus. The amino acid lysine makes up 13.39% of the total amino acids of the α-syn proteome. These lysine-rich regions are ubiquitination sites, a common PTM event for α-syn, and contribute to the structural stability of the protein [196, 197]. We speculate disruption of these lysine residues, one of the aforementioned high-affinity targets for acrolein-protein binding, are potentially interrupting the structural stability of the protein leading to PTM and oligomerization as observed in our mbTBI rats. In support of this notion, we observe that acrolein induces α-syn oligomerization *in vitro* (Fig. 25) and modifies/co-localizes with α-syn *in vivo* post-blast TBI (Fig. 26). These results resemble the familial mutants of α-syn that promote its toxic oligomerization and aggregation, a critical step in Lewy body (LB) formation [198, 199].

To our knowledge, these findings document the first evidence of acrolein co-localization with α-syn after TBI. Interestingly, however, acrolein-α-syn co-localization has previously been observed in LBs within the SN of PD patients [146] and injection of acrolein into the SN induces α-syn aggregation and cell death [200], further suggesting acrolein is a capable and likely causal factor promoting α-syn aggregation. We thus emphasize that the elevation of acrolein may be a critical secondary injury process in promoting PD-like degenerative processes after TBI, specifically via α-syn oligomerization/aggregation

2.2.4.3. Disruption of dopaminergic synthesis via dysregulation of tyrosine hydroxylase

Tyrosine hydroxylase (TH) is the key enzyme for dopamine (DA) synthesis in the dopaminergic neurons and its terminals. TH function is regulated via its phosphorylation sites, mainly at serine 30 and serine 40 [201, 202]. In PD patients, TH activity is decreased in the nigro-striatal area, which results in the reduction of dopamine levels leading to the cardinal symptoms of PD [203]. In addition, decreased TH is an indirect indication of dopaminergic neuron damage/death in the SN in TBI rodent models [119, 172].

In our study, whole brain levels of TH pSer40 (Fig. 22f), were significantly decreased after mbTBI while total TH and TH pSer30 (Figs. 22b, d) were not affected. In the SN-area, both TH pSer30 and pSer40 sites (Figs. 24d,f) levels were decreased and the total TH protein (Fig. 24b) showed significant increase. The decreased levels of TH pSer40, the most studied and directly implicated phosphorylation / activation site of DA synthesis, suggest decreased activity of TH after injury in the whole brain and SN. Furthermore the changes observed in the TH protein and

TH pSer30 in the SN (Figs. 24b,d) is perhaps due to the specific function of these neurons. The dopaminergic neurons of the SN mainly regulate motor function via the nigrostriatal projections into the striatum [204]. Interestingly, in the STR region TH pSer40 levels were significantly increased post injury (Figs. 23f,l). There have been conflicting results regarding striatal TH activity after TBI [205, 206] The increase of striatal TH activity is thought to be a compensatory action of the striatum [206]. The different levels of TH and its phosphorylation sites we observed post-injury may be due to the complexity of the dopaminergic neurotransmission, specifically in the SN and STR. The TH protein is found to be expressed much greater in the terminal fields compared to the somatodendritic compartments of the nigrostriatal pathways [207, 208]. Furthermore, dopaminergic neurons in the SN are known to be more susceptible to oxidative processes than dopaminergic neurons found elsewhere in the brain [209-212]. Differential mechanical injury profiles between brain regions could also contribute, wherein the SN experiences more injurious loading conditions than the STR, as our lab's computational biomechanics work in this mbTBI model has suggested. Regardless of the underlying mechanism, these data suggest differential localization and regulation of the TH protein between different brain loci, in a similar fashion to the α-syn protein, after injury. Our data suggest a putative mechanism for disruption of the brain's supply of dopamine, but the source of the disruption remains unclear. To our knowledge, this is the first time that the expression of TH protein levels and its phosphorylation sites have been quantified in the whole brain, STR, and SN-area after a single mild blast TBI. This study provides further evidence that the dopaminergic system is acutely altered by TBI.

The decrease of TH activity as measured by the protein levels specifically on its pSer40 and pSer30 phosphorylation sites in the whole brain and SN-area after mbTBI may occur through several mechanisms. Possibly the most important regulatory protein of TH activity is α-syn, which is also directly implicated in PD pathology as discussed above. The abnormal expression of α-syn has been demonstrated to inhibit TH expression and activity in both *in vitro* and *in vivo* studies [191]. TH function is hindered in both transgenic mice overexpressing α-syn and in dopaminergic cells transfected with α-syn [213, 214]. Additionally, transfection of α-syn in MES 23.5 dopaminergic cell line induces cell injury and decreases TH gene expression and protein levels [215]. Furthermore, α-syn has similar protein homology to adapter protein 14-3-3, which promotes TH activation and is thought to function as a chaperone protein [158, 159, 216-218].

The 14-3-3 chaperone protein enhances the major kinases' function to activate TH at pSer40, thereby increasing DA synthesis [219-221]. We speculate that the overall increased of aberrant α-syn levels post mbTBI may affect TH regulation as observed in our study.

It is also possible that acrolein can modulate the structure and function of TH directly, as we observed for α-syn, or indirectly by altering entangled signaling pathways or molecules involved in dopamine synthesis. For the indirect option, TH is an enzyme in which its activity is regulated by many kinases and phosphatases. The main activating kinases that regulate TH phosphorylation at Ser40 are the cAMP-dependent protein kinase A (PKA) and the mitogen-activated protein kinase-activated protein kinase 2 (MAPKAP-K2) [191, 222, 223]. In contrast, protein kinase C (PKC), which is highly expressed in SN dopaminergic neurons and co-localizes with TH [191, 224], has been shown to decrease TH activity and DA synthesis. Many of acrolein's documented effects on biological systems are attributed to activation of kinases similar to those mentioned above [225, 226], however the exact mechanisms remain unknown [225-227]. Such pathways would be logical targets to investigate how acrolein may impact TH activity-modifying molecules.

The potential of oxidative stress, specifically mediated by acrolein, to modulate any of the aforementioned proteins may be critical for PD progression and/or induction of PD-like pathologies resulting from TBI. We speculate that the aberrations of α-syn after mbTBI due to acrolein elevation play a role in the dysregulation of TH in the whole brain and SN-area. In relation to the interplay between the kinases and phosphatases mentioned above, TH and α-syn alterations in the presence of acrolein need to be further validated and investigated in depth to fully understand how TBI pathophysiology can potentiate PD-like degenerative processes.

2.2.4.4. Tau Neuropathology post-mild TBI

Tau protein is one of the major microtubule associated proteins (MAPs) and plays an essential function in the modulation and spatial organization of microtubules [161-165]. This protein is the main component of the neurofibrillary tangles (NFT's), one of the pathological hallmarks of Alzheimer's disease (AD) [161], however tau protein neuropathy (tauopathy) is also observed in PD and can be found in the Lewy bodies, hallmark of PD [166-170]. This suggests that both AD and PD have overlapping neuropathology. The paired helical filaments (PHF) found in the NFT's are consist of abnormally hyperphosphorylated tau protein. The hyperphosphorylation of tau is a critical event leading to abnormal aggregation and disruption of

the normal function of tau. Tau protein is regulated at multiple phosphorylation sites and its microtubule stabilizing activity are dependent on its phosphorylation; thus implicating a balance of kinases and phosphatases for its proper regulation [161]. Closed traumatic brain injury such as blast TBI induces diffused axonal injuries leading to the disruption of neuronal integrity in which microtubules are the key players [228]. Furthermore, in blast injury biochemical changes such as oxidative stress is upregulated therefore can induce a cascade of events [14, 28, 229] (Fig. 1) and can directly or indirectly affect the function of Tau protein.

We observe a significant and overall increase of the PHF Tau protein in the whole brain (Fig. 27a, b), SN area (Fig. 27c, d) and both STR anterior (Fig. 27e, f) and posterior (Fig. 27g, h) 2 and 7 days post injury, suggesting a neurodegenerative-like neuropathology following our blast model injury. This further supports the idea that perhaps the oxidative stress from brain injuries dysregulates key proteins such as tau and if not mitigated can lead to neurodegneration. The successful development of true biochemical markers of blast injury, particularly mild-bTBI could help distinguish from other type of brain trauma and help find therapeutic targets post-mild bTBI.

In conclusion, this study provides insight into potential pathophysiological responses of the brain after a single mild blast traumatic brain injury that may lead to Parkinson's disease-like neurodegenerative processes. These studies were aimed to evaluate the role of oxidative stress, a-synuclein, and nigrostriatal DA regulation after a mild-blast traumatic brain injury. We found that the endogenous reactive aldehyde acrolein may play a key role in increasing PD susceptibility after TBI by inducing PD-like pathology, specifically α-syn oligomerization and dopaminergic dysregulation. Our data indicate that increased levels of acrolein are associated with α-syn aberrations after exposure to a single, mild blast event and, further, that acrolein can directly modify and oligomerize α-syn *in vitro* and *in vivo*. Furthermore, we show dysregulation of TH activity post-injury, indicating dopaminergic neuron disturbance.

Increased acrolein levels in our mbTBI rat model indicate ongoing acute to subacute oxidative stress and lipid peroxidation cascades in the brain post-TBI consistent with prior reports, suggesting these pathways may be critical initiators of later stage TBI pathophysiology including inflammatory and degenerative processes. As demonstrated herein, acrolein may serve as a pathological link between TBI and PD, opening new avenues for therapeutic targets to mitigate the long-term consequences in TBI patients. These findings warrant further

investigation into the clinical relevance of acrolein and related aldehydes, as well as its direct role in and mechanisms for modifying α-syn post-injury. We hope this study sparks new avenues for mechanistic and translational research, particularly for preventative therapeutic interventions targeting oxidative stress and/or lipid peroxidation after TBI.

2.3. Long-Term Mild bTBI Biochemical Assessment

2.3.1. Rationale

The lack of neuromotor deficits in the acute (24-hr and 48-hr post-injury) time period post injury validates our mild bTBI model. Furthermore, we have detected morphological and biochemical abnormalities at these time points post-injury. We have shown through confocal imaging an elevation of the blood-brain barrier disruption, activation of microglial/macrophage inflammation, and an increased levels of acrolein, a marker of oxidative stress in our acute post-mild bTBI model [230]. Our acute neuropathological assessment post-injury (Section 2.2), show evidence of role of acrolein post-mild injury and its role in inducing PD-like neuropathology. These initial assessments provide essential information regarding the biochemical changes in the brain post-mild bTBI injury. However, for a better diagnostic and therapeutic interventions to help alleviate or prevent long-term consequences post-injury, a more thorough assessment at different time points of the injury is warranted and especially PD neuropathology has a later onset. Specifically, we propose a biochemical characterization focusing on acrolein and PD-pathology markers post-mild bTBI. We hypothesize that the biochemical events flowing chronic mild-bTBI, especially acrolein, plays an integral role in the development of PD post-injury. The aim of this study is to obtain a more comprehensive biochemical assessment of the mild-blast injury at a chronic stage focusing on PD-pathology.

2.3.2. Brief Methods

2.3.2.1. Post-mortem brain tissue preparation and Western blotting

Rats were sacrificed for Western blot at 4 weeks, 6weeks post-mild blast TBI and sham group. After deeply anesthetized with 80 mg/kg ketamine and 20 mg/kg xylazine cocktail, animals were transcardially perfused with Krebs solution and decapitated. Whole brains were quickly removed and frozen on dry ice and stored in the -80^{o}C until processed. Tissue from the striatal regions (STR: B5 (anterior), C5 (posterior)) and substantia nigral region (SN: E8) was dissected out according to Paxinos & Watson's The Rat Brain Atlas as a reference guide for the

regional assessment. Similar protein isolation and Western Blot methods were employed as mentioned in Section 2.2.2.

2.3.2.2. Detection of acrolein (3-HPMA Measurements)

The quantification of acrolein and its metabolites in urine has recently been established using liquid chromatography-mass spectroscopy (LC/MS); providing a non-invasive detection to monitor acrolein and investigate its pathological role in brain injuries and other diseases [45, 58, 147-151]. Similar methods mentioned in Section 2.2.2 was used to assessed urine samples 2-days and 20-days post-blast injury.

2.3.3. Results and Discussion

2.3.3.1. Biochemical assessment of acrolein metabolite, 3-HPMA, and acrolein-lys protein adducts

A stable acrolein metabolite, 3-HPMA[231], was analyzed by LC-MS/MS in the urine of blast exposed animals at 2 and 20 days post injury (Fig 28). 3-HPMA, a product of the reaction of acrolein and glutathione[231], showed significant elevated levels in the urine at 2 days (1.83 ± 0.29 %, n=5) post-injury (Fig. 28) when compared to the sham group (0.47 ± 0.19) %, n=4) ($p=0.009$), but not 20 days (0.88 ± 0.12 %, n=4) post injury compared to sham group (0.76 ± 0.39 %, n=4) (Fig 28). Western blotting technique using homogenized whole brain tissue from rats sacrificed at four (99.20 ± 20.31 %, n=4) and six (94.42 ± 19.70 %, n=4) weeks post-blast indicated no significant elevations of acrolein-lysine adducts compared to the control (100 ± 15.62 %, n=5) (Fig. 29) [$F(2,10)=0.02$, $p=0.974$]. This suggests that oxidative stress is elevated on a subacute timescale in the central nervous system (CNS) following blast exposure.

In the anterior STR (B5) area (Fig 30a, b) there was a trend of increased of acrolein-lys protein adducts at 4-weeks (83.36 ± 16.15 %, n=5) and 6- weeks (65.41 ± 24.86 %, n=5) post injury compared to the control (100 ± 20.95 %, n=4), but not significant [$F(2,11)=3.99$, $p=0.05$]. In the posterior STR (C5) (Fig. 30c, d) acrolein-lys adducts levels were significantly increased 4-weeks (102.37 ± 34.87 %, n=5) and elevated 6-weeks (58.03 ± 19.81 %, n=5)post-injury compared to the control (100 ± 13.56 %, n=5) [$F(2,12)=4.41$, $p=0.03$]. Consequently, in the SN region (E8) (Fig. 31) acrolein-lys adducts levels were increased 4-weeks (21.35 ± 5.60 %, n=5) and significantly elevated 6-weeks (52.64 ± 10.14 %, n=5) post-injury compared to the control group (100 ± 17.08 %, n=5) [$F(2,12)=4.93$, $p=0.02$].

Our data suggest that systemic and whole brain levels of acrolein were not significantly increased 4- and 6- weeks post-injury. However, the significant elevations in the STR and SN area suggest that these regions are more vulnerable after the injury and that the levels of acrolein were sustained suggesting that a PD-like neuropathology.

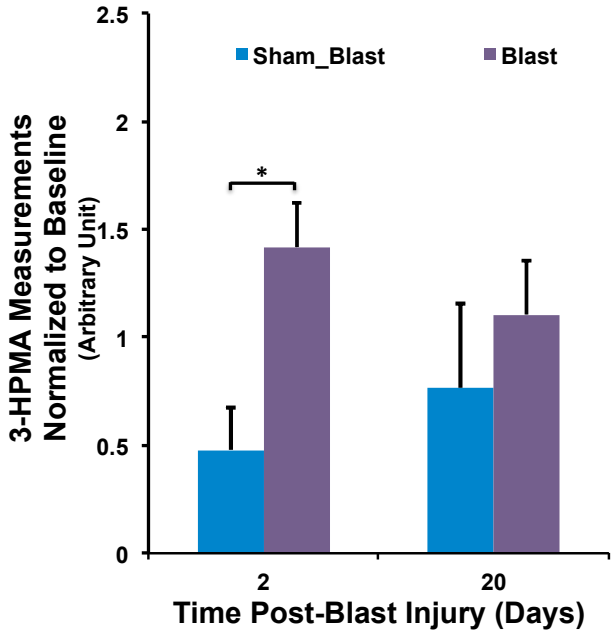

Figure 28: 3-HMPA Measurements Post-Blast Injury, an acrolein metabolite. Data expressed as mean (±S.E.M.) and normalized to their baseline. Group treatment summary: Sham_Blast is the control group (anesthesized and placed in the room where the blast occurs), Blast (as described on the Methods section). There is a significant increase of 3-HPMA levels two days post blast. Tukey's post-hoc indicates significant increase in the blast (*$p<0.05$). Measurements twenty days post-blast injury show no significant increase of 3 HPMA levels. Error bars represent SEM.

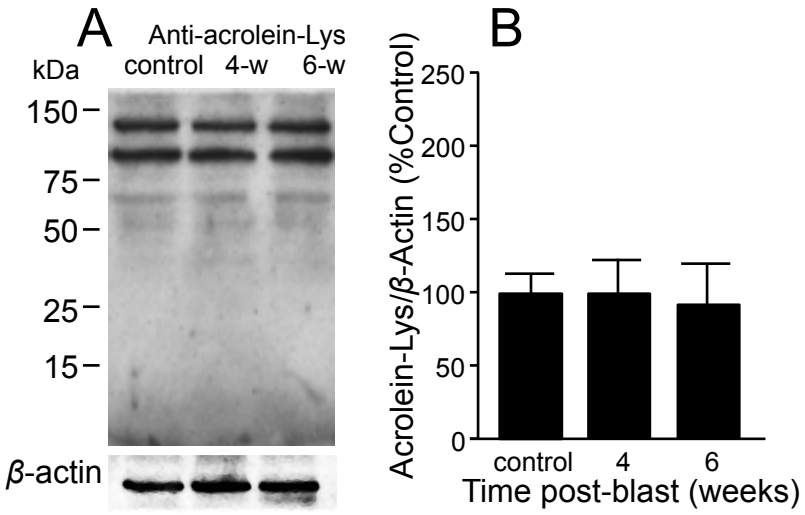

Figure 29. Acrolein-lysine adducts in whole brain preparation after mild bTBI. (A) Western Blot image of acrolein-lysine modified proteins (FDP-Lys) and β-actin for each group at control, 4-week and 6-week post-blast. (B) Quantification demonstrated no significant difference between control, 4-week and 6-week post-injury [F(2,10)=0.02, p=0.974]. Data are relative, normalized as percent control and presented as mean ± SEM.

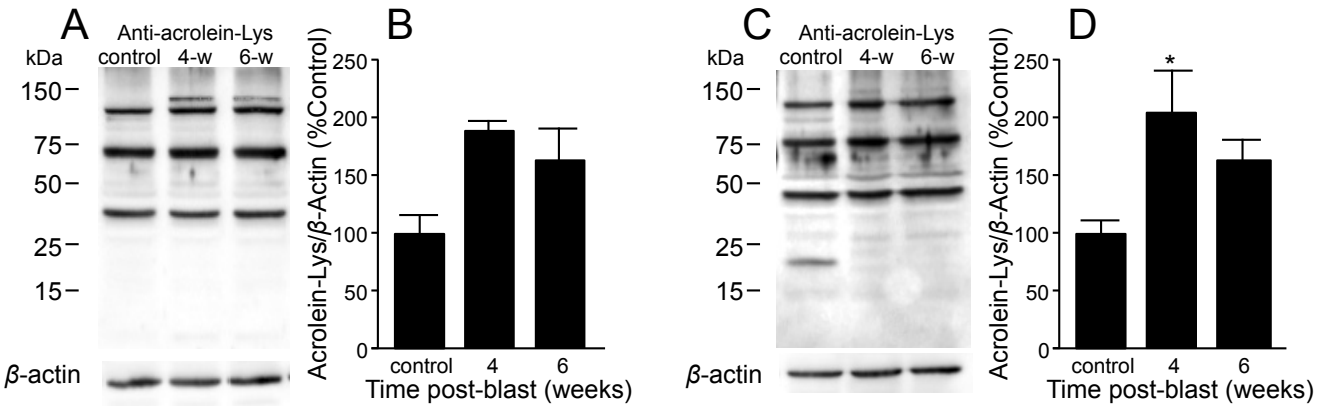

Figure 30. Acrolein-lysine adducts increase in striatum after mild bTBI. (A) Western Blot image of acrolein-lysine modified proteins (FDP-Lys) and β-actin for each group at control, 4-week and 6-week post-blast of the B5 striatal region. (B) Quantification demonstrated no significant difference between control, 4-week and 6-week post-injury [F(2,11)=3.99, p=0.05]. (C) Western Blot image of acrolein-lysine modified proteins (FDP-Lys) and β-actin for each group at control, 4-week and 6-week post-blast of the C5 striatal region. (B) Quantification demonstrated significant difference between control and 4-week, but not at 6-week post-injury [F(2,12)=4.41, p=0.03]. Data are relative, normalized as percent control and presented as mean ± SEM. Tukey's post-hoc test. *p<0.05, **p<0.01.

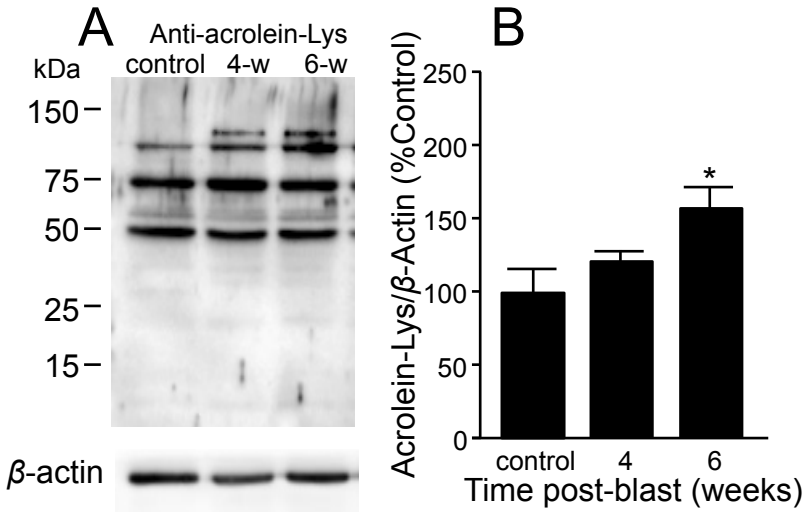

Figure 31. Acrolein-lysine adducts increase in substantia nigra region after mild bTBI. (A) Western Blot image of acrolein-lysine modified proteins (FDP-Lys) and β-actin for each group at control, 4-week and 6-week post-blast. (B) Quantification demonstrated no significant difference between control and 2-day post-injury, but a significant increase at 6-week post-injury [F(2,12)=4.93, p=0.02]. Data are relative, normalized as percent control and presented as mean ± SEM. Tukey's post-hoc test. *p<0.05, **p<0.01.

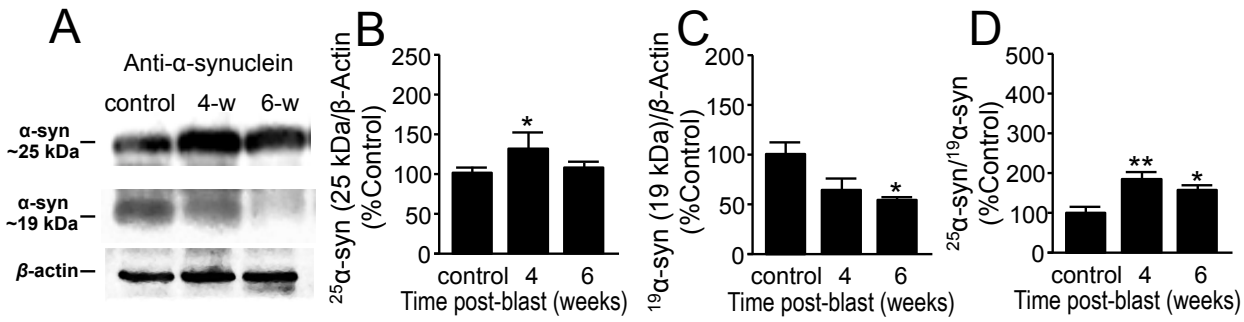

Figure 32. Aberrant expression of α-synuclein in whole brain preparation after mild bTBI. (A) Western Blot image of α-syn at approximately 25kDA, α-syn at 19kDA, and β-actin at control, week 4 and week 6 post-blast. (B) There is a significant increase of the 25 kDa α-syn 4 weeks post-blast [F(2,11)=4.31 p=0.04] but not 6 weeks. (C) Decreased levels of the 19 kDa α-syn at 4 weeks and significant decrease at 6 weeks post blast. [F(2,11)=5.53, p=0.02]. (D) The normalized ratio of the 25 kDa and 19 kDa α-syn at control, 4 and 6 weeks post-blast indicates an overall increase of α-syn [F(2,12)=10.21, p=0.003). Data in B-D are relative, normalized as percent control, and presented as mean ± SEM. Tukey's post-hoc test. *p<0.05, **p<0.01.

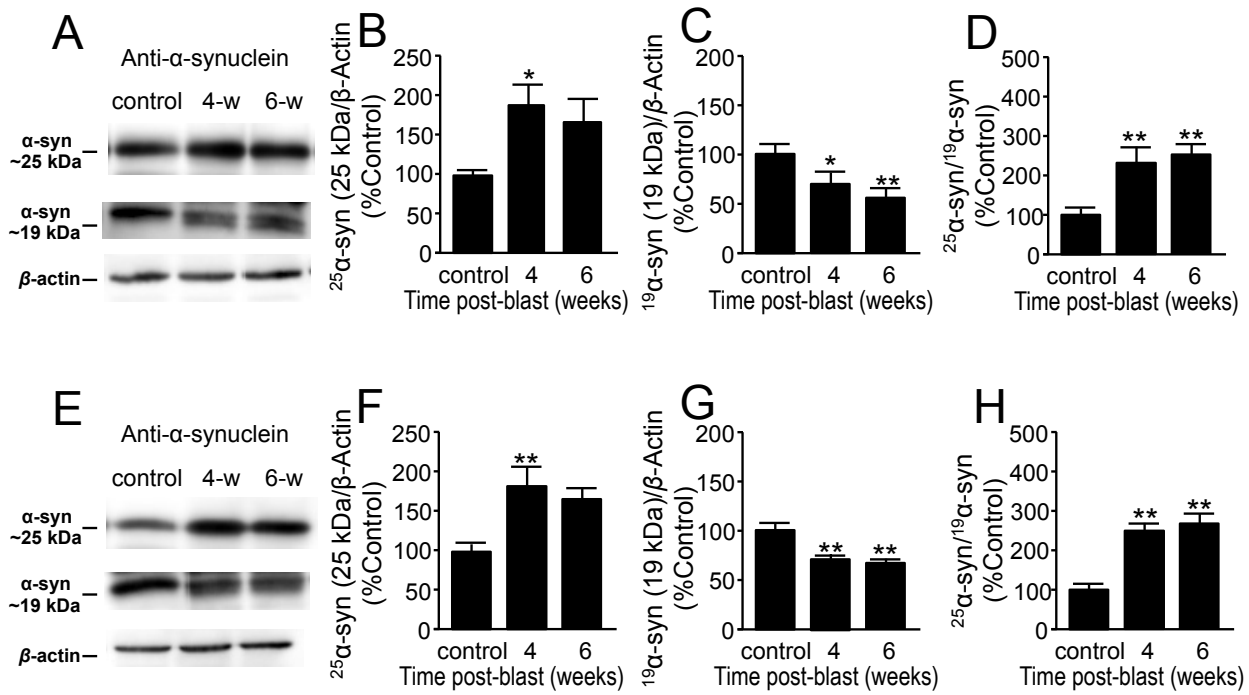

Figure 33. Aberrant expression of α-synuclein in striatal region after mild bTBI. (A) B5 striatal region Western blot image of α-syn at approximately 25kDA, α-syn at 19kDA and β-actin for control, week 4 and week 6 post-blast. (B) There is a significant increase at 25 kDa α-syn [$F(2,12)=4.38$ $p=0.03$] 4-weeks post-injury. (C) There is a significant decrease at of 19kDa α-syn [$F(2,11)=7.97$, $p=0.007$] 4- and 6-weeks post-injury. (D) The normalized ratio of the 25 kDa and 19 kDa forms of α-syn indicates an overall increased levels of α-syn [$F(2,12)=37.72$, $p=0.00$] post-injury. (E) C5 striatal region Western blot image of α-syn at approximately 25kDA, α-syn at 19kDA and β-actin for control, week 4 and week 6 post-blast. (F) There is a significant increase at 25 kDa α-syn [$F(2,12)=7.45$ $p=0.008$] 4-weeks post-injury. (G) There is a significant decrease at of 19kDa α-syn [$F(2,11)=17.91$, $p=0.000$] 4- and 6-weeks post-injury. (H) The normalized ratio of the 25 kDa and 19 kDa forms of α-syn indicates an overall increased levels of α-syn [$F(2,12)=58.21$, $p=0.000$] post-injury. Data in B-D and F-G are relative, normalized as percent control, and presented as mean ± SEM. Tukey's post-hoc test. *$p<0.05$, **$p<0.01$.

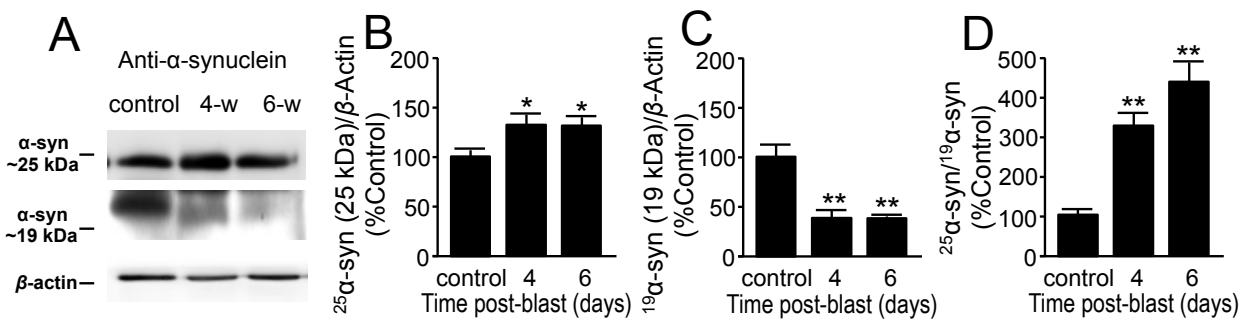

Figure 34. Aberrant expression of α-synuclein in substantia nigra region (E8) after mild bTBI. (A) Western Blot image of α-syn at approximately 25kDA, α-syn at 19kDA and β-actin at control, week 4 and week 6 post-blast. (B) There is a significant increase at 25 kDa α-syn [$F(2,9)=9.11$ $p=0.007$] 4- and 6-weeks post-injury. (C) There is a significant decrease at of 19kDa α-syn [$F(2,9)=26.7$, $p=0.000$] 4- and 6-weeks post-injury. (D) The normalized ratio of the 25 kDa and 19 kDa forms of α-syn indicates an overall increased levels of α-syn [$F(2,9)=62.40$, $p=0.000$] post-injury. Data in B-D are relative, normalized as percent control, and presented as mean ± SEM. Tukey's post-hoc test. *$p<0.05$, **$p<0.01$.

2.3.3.2. Chronic aberrant levels of α-synculein post-mild bTBI

α-Synuclein is the main protein present in the Lewy Bodies (LB) found in the surviving dopaminergic neurons of PD patients. It is a small soluble protein (14 kDa) that is highly localized in the presynaptic terminals [191, 192], and can be essential in normal brain function. However, the exact function and neurotoxic level of α-synuclein remains unclear. α-Synuclein is very sensitive to environmental factors and genetic modifications which trigger its misfolding and an eventual loss of normal function. Point mutations in the α-synuclein gene can enhance its aggregation and thus contributes to the development of the familial and rare forms of PD. Currently, little is known about the mechanism leading to the aggregation of α-synuclein, however one study suggests that the dimerization of the protein can be a rate-limiting step in its aggregation leading to the formation of LBs [195]. The ubiquitin proteasome system (UPS) and oxidative stress are two mechanisms, which can promote α-synuclein aggregation. UPS is the main biochemical pathway for degrading both normal and abnormal (mutated, misfolded) intracellular proteins [232, 233], such as α-synuclein. Malfunction of this system leads to protein accumulation and cell death [234, 235]. Several studies have shown that in PD this ubiquitin-dependent protein degradation is impaired [233]. In vivo post-translational modifications such as phosphorylation and ubiquitination can interfere with the function and

degradation of α-synuclein and alter its native state in a way that enables aggregation. Tofaris et al. (2003) used a two-dimensional gel electrophoresis approach to characterize the pathogenic species of α-synuclein in LBs isolated from the post-mortem brain tissue of PD individuals [220]. They found a highly modified species of α-synuclein at 22-24 kDa that was ubiquitinated. This species was conjugated with at least 1-3 ubiquitins. Furthermore, this 22-24 kDa α-synuclein species was hyperphosphorylated on its serine residues. The phosphorylation of α-synuclein at Ser-129 has been highly associated with LB α-synucleins and accelerates neurodegeneration in a rat model of PD [236]. In addition, as mentioned previously, this Ser129 site can also regulate TH activity and further implicates these post-translational modifications of α-synuclein in the pathogenesis of PD.

Our Western blots consistently showed two distinct bands of α-synuclein, at around 19 kDa and 25 kDa (Fig. 32, Fig. 33, Fig. 34). We speculate that the band observed at 19 kDa is the monomeric form of α-synuclein, which is the "normal" unmodified form, and the 25 kDa is the modified form of α-synuclein, possibly by post-translational modifications. We measured the α-syn protein levels using Western blotting in the whole, striatal (STR), and substantia nigral (SN) brain region lysates. All values were normalized using β-actin and expressed as percent control. In the whole brain lysates analysis (Fig 32b) of the 25 kDa band ANOVA shows a significant group effect [$F(2,11)=4.31$ $p=0.04$] and pairwise comparison show a significant increase in the 4-week (34.73 ± 17.71 %, n=4) but not 6-week (7.29 ± 7.76 %, n=4) post-injury group compared to the control (100 ± 4.03 %, n=6; *$p<0.05$, **$p<0.01$) as shown in Fig. 32b. On the other hand, in the whole brain lysates at 19 kDa α-syn band a significant group effect is observed [$F(2,11)=5.53$, $p=0.02$] and pairwise comparison shows a decrease in the 4-week (37.02 ± 12.10 %, n=4), significant decrease 6-week (45.62 ± 0.67 %, n=4) post-injury groups compared to the control (100 ± 11.83 %, n=6; *$p<0.05$, **$p<0.01$) as shown in Fig. 32c. Ratio analysis of the 25 kDa and 19 kDa α-syn bands showed statistically significant increase in the proportion of over all α-syn accounted for by the 25 kDa α-syn species [$F(2,12)=10.21$, $p=0.003$) and pairwise comparison showed significant increase levels in the 4-week (82.33 ± 14.39 %, n=4 and 6-week (61.36 ± 9.10 %, n=4) post-injury groups compared to the control (100 ± 14.10 %, n=6; *$p<0.05$, **$p<0.01$) as shown in Fig. 32d.

In the striatal regions, B5 (anterior) the levels of α-syn protein levels at 25 kDa (Fig. 33b) show a significant group effect [$F(2,12)=4.38$ $p=0.03$] and pairwise comparison shows a

significant increase in 4-week (87.57 ± 26.58 %, n=5), but not in 6-week (67.18 ± 26.77 %, n=5) post-injury compared to the control (100 ± 3.47 %, n=5; *p<0.05, **p<0.01) as shown in Fig. 33b. In the C5 (posterior) region (Fig. 33f) a significant group effect [F(2,12)=7.45 p=0.008] and pairwise comparison shows a significant increase in 4-week (83.07 ± 23.17 %, n=5), but not in 6-week (58.97 ± 10.24 %, n=5) post-injury compared to the control (100 ± 9.62 %, n=5; *p<0.05, **p<0.01) as shown in Fig. 33f. α-syn protein levels at 19 kDa show significant decrease in both B5 and C5 striatal regions. In B5 (anterior) (Fig. 33c), a significant group effect [F(2,11)=7.97, p=0.007] and pairwise comparison shows a significant decrease in 4-week (30.34 ± 5.76 %, n=5), 6-week (40.01 ± 7.81 %, n=5) post-injury compared to the control (100 ± 7.74 %, n=4; *p<0.05, **p<0.01) as shown in Fig. 33c. In C5 (posterior) (Fig. 33g), a significant group effect [F(2,11)=17.91, p=0.000] and pairwise comparison shows a significant decrease in 4-week (33.96 ± 4.0 %, n=4), 6-week (38.70 ± 3.02 %, n=5) post-injury compared to the control (100 ± 6.89 %, n=5; *p<0.05, **p<0.01) as shown in Fig. 33g. The ratio analysis of the 25 kDa and 19 kDa bands shows a statistically significant increase in the proportion of overall α-syn protein accounted for by the 25 kDa α-syn species in both B5 and C5 striatal region. In B5 (anterior) (Fig. 33d), [F(2,12)=37.72, p=0.00] pairwise comparison show a significant increase in 4-week (137.02 ± 17.92 %, n=5), 6-week (146.58 ± 11.77, n=5) post-injury compared to the control group (100 ± 8.64, n=5; *p<0.05, **p<0.01) as shown in Fig. 33d. In C5 (posterior) (Fig. 33h), [F(2,12)=58.21, p=0.000] and pairwise comparison show a significant increase in 4-week (142.04 ± 8.24 %, n=5), 6-week (159.63 ± 15.93, n=5) post-injury compared to the control group (100 ± 8.53, n=5; *p<0.05, **p<0.01) as shown in Fig. 33h.

Consequently, the α-syn protein levels at 25 kDa in the substantia nigral region (Fig. 34b) show a significant group effect [F(2,9)=9.11 p=0.007] and pairwise comparison shows a significant increase in 4-week (26.94 ± 8.28 %, n=4), 6-week (22.91 ± 5.68 %, n=4) post-injury compared to the control (100 ± 5.98 %, n=4; *p<0.05, **p<0.01) as shown in Fig. 34b. A significant group effect is also observed in the 19 kDa band (Fig. 34c) [F(2,9)=26.7, p=0.000] and pairwise comparison show a significant decrease in 4-week (59.50 ± 3.60 %, n=4), and 6-week (66.97 ± 1.01 %, n=4) post-injury compared to the control (100 ± 11.70 %, n=5, *p<0.05, **p<0.01) as shown in Fig. 34c. Similarly, The ratio analysis of the 25 kDa and 19 kDa bands (Fig. 34d) shows a statistically significant increase in the proportion of overall α-syn protein accounted for by the 25 kDa α-syn species in the SN region (E8) [F(2,9)=62.40, p=0.000] and

pairwise comparison show a significant increase only in 4-week (212.48 ± 16.25 %, n=4) and a trend of increase in 6-week (324.95 ± 31.79, n=4) post-injury compared to the control group (100 ± 5.83, n=4; *p<0.05, **p<0.01) as shown in Fig. 34d.

Our data showed that the aberration of α-synuclein at weeks post injury is sustained similar to only days after injury in the whole brain and nigrostriatal pathway. This supports a PD-like neuropathology as a long-term consequence post-blast injury. It is essential to conduct further experiments to validate the 25 kDa α-synuclein bands on our results and the specific α-synuclein post-translational modification mechanism. We suspect that perhaps, the acrolein damage to the α-synuclein during days post-blast may not be reversed after weeks post-injury. We speculate that increased levels of modified of α-synuclein suggests a disruption of the physiological integrity of the cells and can also affect dopamine regulation. Similarly *in vitro* studies have demonstrated that overexpression of α-synuclein reduces the levels of TH mRNA and protein [237, 238] and thereby can regulates TH expression and affects dopamine synthesis in the brain, further exacerbating PD pathology.

2.3.3.3. Chronic alterations of tyrosine hydroxylase post-mild bTBI

TH catalyzes the amino acid tyrosine to Levodopa (L-dopa), which is the rate-limiting step in synthesizing the catecholamine dopamine [201, 202]. In PD patients, TH activity is decreased in the nigro-striatal area, which results in the reduction of dopamine levels [203]. TH is essential in the synthesis of dopamine and it is an essential biomarker implicated in the neurodegeneration process of PD. Our data suggest an overall dysregulation of TH in the whole brain (Fig. 35), STR (Fig. 36), and SN (Fig. 37) at 4-weeks and 6-weeks post-blast injury. This is similar trend of dysregulation shown in Section 2.2.3 suggesting a PD-like neuropathology. We speculate that the damage of the TH regulation early on after the injury, specifically acrolein, is sustained as a long-term consequence of the injury.

In the whole brain lysates (Fig. 35), there were no significant changes in the TH protein levels [$F(2,12)=0.62$], $p=0.55$] (Fig. 35b) and TH pSer31 [$F(2,11)=1.42$, $p=0.28$] (Fig. 35d), respectively. However, there was a significant group effect of TH pSer40 [$F(2,11)=4.37$, $p=0.04$] and pairwise comparison show significant increase in 4-week (41.92 ± 7.08 %, n=4) and but not in 6-week (23.33 ± 14.34 %, n=4) post-injury groups compared to control (100 ± 8.95 %, n=6; *p<0.05, **p<0.01) (Fig. 35f).

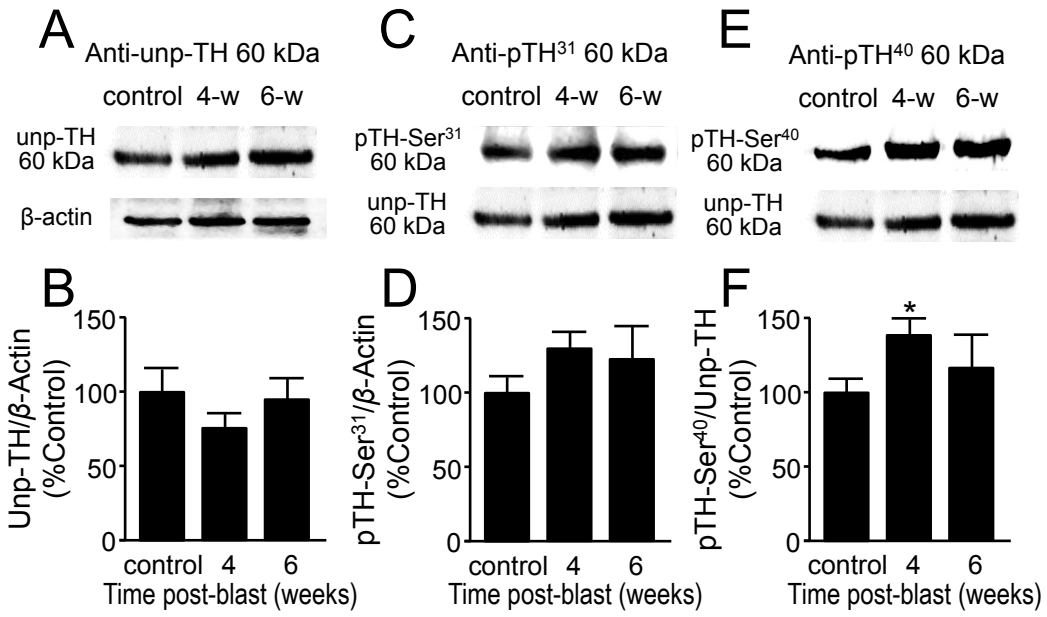

Figure 35. Increased phosphorylation of tyrosine hydroxylase (TH) at Ser^{40} after mild bTBI in whole brain preparation. (A,C,E) Western Blot images of un-phosphorylated TH (A), phosphorylated TH at Ser^{31} (B), phosphorylated TH at Ser^{40} (C), and β-actin for each group at control, 4 and 6 weeks post-blast. (B,D,F) Comparisons were made between control, 4-w and 6-w post-injury in all three forms of TH. No significant changes were observed in (B) un-phosphorylated [$F(2,12)=0.62$], $p=0.55$] or (D) Ser^{31}-phosphorylated [$F(2,11)=1.42$, $p=0.28$] TH. (F) Phosphorylation at Ser^{40}, TH's primary activation site, demonstrated significant increase at 4 weeks [$F(2,11)=4.37$, $p=0.04$], but not at 6 weeks post-injury. Data in B,D,F is relative, normalized as percent control, and presented as mean ± SEM. Tukey's post-hoc test. *$p<0.05$.

In the striatal brain region lysates, there were significant increase in the TH protein levels in the B5 (anterior) (Fig. 36b) [$F(2,12)=4.27$, $p=0.04$] and pairwise comparison show significant increase in 4-week (68.39 ± 14.60 %, n=5) and 6-week (74.69 ± 26.02 %, n=5) post-injury groups compared to control (100 ± 17.68 %, n=5; *$p<0.05$, **$p<0.01$) (Fig. 36b). Similarly in the C5 (posterior) (Fig. 36j) TH protein levels were significantly increase [$F(2,12)=6.62$, $p=0.01$] in 4-week (79.60 ± 21.43 %, n=5) and 6-week (71.83 ± 10.66 %, n=5) post-injury groups compared to control (100 ± 17.31 %, n=5; *$p<0.05$, **$p<0.01$) (Fig. 36j).

Interestingly, TH pSer31 levels in the B5 (Fig. 36d) region were significantly decrease [$F(2,11)=7.87$, $p=0.008$] in 4-week (23.63 ± 5.25 %, n=5) and 6-week (27.63 ± 6.02 %, n=5) post-injury groups compared to control (100 ± 2.25 %, n=4; *$p<0.05$, **$p<0.01$) (Fig. 36d). In the C5 (Fig. 36k) TH pSer31 levels were significantly increase $F(2,9)=4.43$, $p=0.04$] in 4-week (28.30 ± 7.10 %, n=4) and 6-week (23.54 ± 8.15 %, n=4) post-injury groups compared to control

(100 ± 6.19 %, n=4; *p<0.05, **p<0.01) (Fig. 36k). The TH pSer40 showed similar trend. In B5 (Fig. 36f) pSer40 levels were significantly decrease [F(2,11)=7.01, p=0.01] in 4-week (31.95 ± 4.47 %, n=5) and 6-week (35.88 ± 3.85 %, n=5) post-injury groups compared to control (100 ± 12.60 %, n=4; *p<0.05, **p<0.01) (Fig. 36f). In the C5 (Fig. 36l) TH pSer40 levels were significantly increase [F(2,9)=4.53, p=0.04] in 4-week (85.76 ± 23.55 %, n=4) and 6-week (92.91 ± 29.03 %, n=4) post-injury groups compared to control (100 ± 19.27 %, n=4; *p<0.05, **p<0.01) (Fig. 36l).

In the substantia nigral region, TH protein (Fig. 37a) and its phosphorylation sites at serine 31(Fig. 37c) and serine 40 (Fig. 37e) were also measured using Western blotting. Analysis on the TH protein levels showed no significant change [F(2,12)=1.18, p=0.24] Fig. 37b. TH protein levels at serine 31 phosphorylation site (showed a significant group effect [F(2,11)=4.65, p=0.03] and pairwise comparison showed significant increase in 4-week (55.68 ± 20.45 %, n=4) and but not in 6-week (31.54 ± 11.76 %, n=5) post-injury groups compared to control (100 ± 5.14 %, n=5; *p<0.05, **p<0.01) as shown in Fig. 37d. Similarly, TH protein levels at serine 40 phosphorylation site showed a significant group effect [F(2,11)=7.46, p=0.009] and pairwise comparison showed significant decrease in 4-week (31.28 ± 3.87 %, n=5) and 6-week (31.04 ± 8.69 %, n=5) post-injury groups compared to control (100 ± 8.77 %, n=4; *p<0.05, **p<0.01) as shown in Fig. 37f.

Due to the myelin content of brain tissue, lipid peroxidation (LPO) is a major process of neurodegeneration-related oxidative stress. Among the end products of LPO, acrolein is a far more reactive molecule compared to the other aldehydes products (Figure 1). Although acrolein has been shown to modify proteins *in vitro* [47, 148] and acrolein-modified proteins have been observed in PD brains [239], the mechanisms by which it interacts with TH remain unclear. It is possible that acrolein can modulate the function of TH through direct or indirect signaling that is thereby affecting dopamine synthesis. TH is an enzyme in which its activity is regulated by kinases and phosphatases, activators and deactivators respectively. The main kinases that regulate TH phosphorylation at Ser40 are the cAMP-dependent protein kinase A (PKA) and the mitogen-activated protein kinase-activated protein kinase 2 (MAPKAP-K2) [191, 222, 223]. In addition, the adapter protein, 14-3-3 enhances both kinases phosphorylation of TH at Ser40 and TH function [240]. On the other hand, protein kinase Cδ (PKCδ) has been shown to decrease TH activity and DA synthesis. PKCδ is also highly expressed in the nigral dopaminergic neurons

and co-localizes with TH [191, 224]. The potential of oxidative stress, specifically acrolein, to modulate any one of these proteins may be critical for PD progression.

Possibly the most important regulatory protein of TH is α-synuclein since it is directly implicated in PD pathology. The function of α-synuclein, the major protein found in the in Lewy body inclusions of PD, is not fully understood. However, the abnormal expression of α-synuclein has been demonstrated to inhibit TH gene expression and its activity in both *in vitro* and *in vivo* studies [191]. TH function is hindered in both transgenic mice overexpressing α-synuclein and in dopaminergic cells transfected with α-synuclein [213, 214]. Additionally, transfection of α-synuclein in MES 23.5 dopaminergic cell line induces cell injury and decreases TH gene expression and protein levels [215]. Furthermore, α-synuclein has similar protein homology as 14-3-3 and is thought to function as a chaperone protein [158, 159, 216-218]. The 14-3-3 chaperone protein enhances the kinase's function to activate TH at pSer40 thereby increasing DA synthesis [219-221]. Interestingly, α-synuclein is found to activate phosphatases, particularly phosphatase 2A (PP2A), leading to the inhibition of TH activity [241] and could explain the decrease in TH activity and gene expression in the aforementioned *in vitro* and *in vivo* studies. Further investigation of the exact mechanism underlying α-synuclein effects on TH and PP2A, particularly delineating its soluble forms, is need not only for PD targeted therapeutics but also to potentially regress or prevent the onset of PD following blast injury.

The mechanisms by which acrolein affects biological systems are not yet fully understood; however, many of its effects are attributed to activation of such kinases mentioned above, particularly (MAPKs) and c-Jun N-terminal kinase (JNK) [225, 226], as well as chemokine production and the induction of apoptosis [185, 226]. The reactive properties of acrolein allow it to readily target these proteins by Michael addition to the cysteine, lysine and histidine residues, and thereby can dysregulate their function and affect downstream signaling pathways, particularly the dopaminergic synthesis and neurotransmission. In relation to the interplay between the kinases and phosphatases mentioned above, TH and α-synuclein in the presences of acrolein needs to be further validated to fully understand the pathology of blast injury and how it can potentiate PD pathology.

Additionally PD pathology is marked by increased inflammation and levels of pro-inflammatory cytokines, such as TNF-α [242]. This event can trigger proteosomal degradation

of TH and contribute to reduce TH levels [243]. This implicates the role of inflammation in the regulation of TH, and with acrolein's pro-inflammatory role, increased acrolein levels post-mBINT may directly affect TH activity as observed in our blots. Our results present further investigation on the role of acrolein post-mBINT and on the mechanisms and pathways of TH activation and deactivation to further elucidate its contribution to PD pathology. Also, investigation of the multi-site phosphorylation of TH is warranted. Overall, our data show a dysregulation of TH levels as a long-term consequence of blast injury and contributing to a PD-like neuropathology.

2.3.3.4. Tau neuropathy post-mild bTBI

As mentioned in Section 2, Tau protein is one of the major microtubule associated proteins (MAPs) and plays an essential function in the modulation and spatial organization of microtubules [161-165]. It is protein is the main component of the neurofibrillary tangles (NFT's), one of the pathological hallmarks of Alzheimer's disease (AD) [161], however tau protein neuropathy (tauopathy) is also observed in PD and can be found in the Lewy bodies, hallmark of PD [166-170]. This suggests that both AD and PD have overlapping neuropathology. We assessed the tau neuropathy at 4-week and 6-week post-injury by measuring the PHF-Tau (pSer202/Thr205) in the whole brain and nigrotsriatal pathway (Fig. 38).

In the whole brain lysates (Fig. 38a, b) there is a significant decrease 4 weeks (39.33 ± 8.41 %, n=4), post injury and but not 6 weeks (31.92 ± 6.57 %, n=4), compared to the control group (100 ± 10.31 %, n=6); [$F(2,11)=5.38$, $p=0.02$]. In the SN area (E8), (Fig. 38c, d) there is a significant increase 4 weeks (66.38 ± 9.67 %, n=5) and sustained increase 6 weeks (72.77 ± 20.59 %, n=5) post injury compared to the control group (100 ± 17.45 %, n=5); [$F(2,12)=5.92$, $p=0.01$]. In the anterior STR (B5) (Fig 38e, f) there was a significant increase 4 weeks (76.49 ± 13.07 %, n=5) and 6 weeks (55.72 ± 19.29 %, n=5) post injury compared to the control (100 ± 7.69 %, n=4); [$F(2,11)=7.39$, $p=0.009$]. Similarly in the posterior STR (C5) (Fig 38g, h), there was a significant increase 4 weeks (97.89 ± 17.27 %, n=5) and 6 weeks (68.81 ± 68.81 %, n=4) post injury compared to the control (100 ± 10.76 %, n=5); [$F(2,11)=10.81$, $p=0.003$]. Our data showed an overall Tau neuropathy especially in the nigrostriatal pathway and supports a PD-like neuropathology as a long-term consequence of mild-blast TBI.

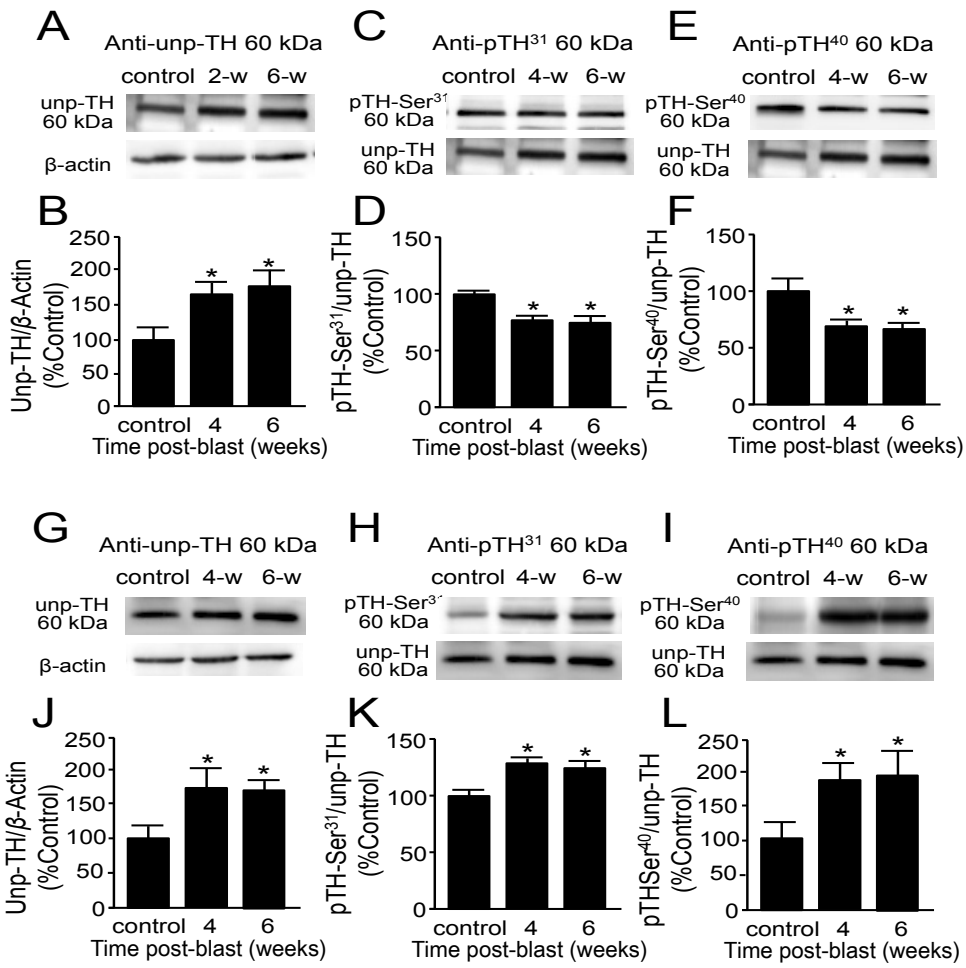

Figure 36. Dysregulation of tyrosine hydroxylase (TH) in the striatum after mild bTBI. (A,C,E) B5 striatal region Western Blot images of (A) un-phosphorylated TH, (C) phosphorylated TH at Ser^{31}, (E) phosphorylated TH at Ser^{40}, and β-actin for each group at control, 4 and 6 weeks post-blast. (B,D,F) Comparisons were made between control and 4-weeks, as well as 6-weeks post-injury in al three forms of TH. (B) There is significant increase of the un-phosphorylated TH at 4 and 6 weeks post-blast [$F(2,12)=4.27$, $p=0.04$]. (D) There is a significant decrease of Ser^{31}-phosphorylated TH [$F(2,11)=7.87$, $p=0.008$] post injury. (F) There is a significant decrease of the Ser^{40}-phosphorylated TH [$F(2,11)=7.01$, $p=0.01$]. (G,H,I) C5 striatal region Western Blot images of (G) un-phosphorylated TH, (H) phosphorylated TH at Ser^{31}, (I) phosphorylated TH at Ser^{40}, and β-actin for each group at control, 4 and 6 weeks post-blast. (J,K,L) Comparisons were made between control and 4-weeks, as well as 6-weeks post-injury in al three forms of TH. (J) There is a significant increase of the un-phosphorylated TH post-blast [$F(2,12)=6.62$, $p=0.01$]. (K) There is significant increase of the Ser^{31}-phosphorylated TH [$F(2,9)=4.43$, $p=0.04$] post-blast. (L) There is a significant increase of the Ser^{40}-phosphorylated TH [$F(2,9)=4.53$, $p=0.04$] post-blast. Data in B,D,F and J,K,L is relative, normalized as percent control, and presented as mean ± SEM. Fisher's LSD or Tukey's post-hoc test. *$p<0.05$, **$p<0.01$.

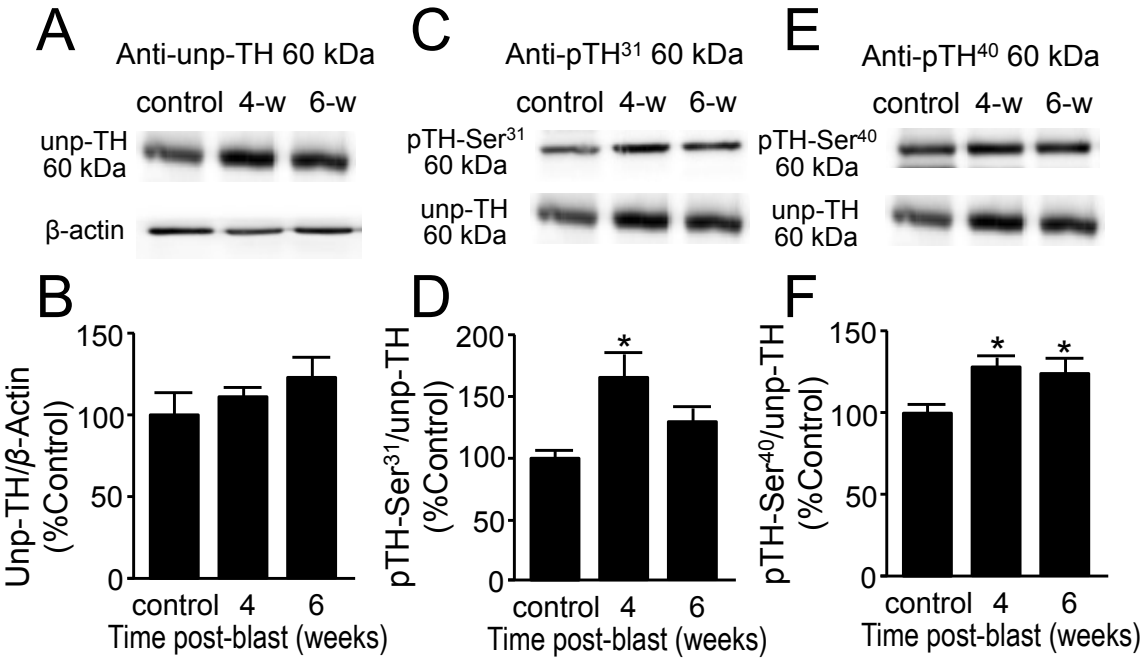

Figure 37. Increased phosphorylation of tyrosine hydroxylase (TH) at Ser[40] and Ser[31] in the substantia nigra region (E8) after mild bTBI. (A,C,E) Western Blot images of (A) un-phosphorylated TH, (C) phosphorylated TH at Ser[31], (E) phosphorylated TH at Ser[40], and β-actin for each group at control, 2 and 7 days post-blast. (B,D,F) Comparisons were made between control and 4-week and 6-week post-injury in all three forms of TH. (B) There is no significant change in the un-phosphorylated TH post-blast injury [$F(2,12)=1.18$, $p=0.24$]. (D) There is a significant increase of Ser[31]-phosphorylated TH [$F(2,11)=4.65$, $p=0.03$] 4 weeks post-injury. (F) There is a significant increase of Ser[40]-phosphorylated TH [$F(2,11)=7.46$, $p=0.009$] 4 and 6 weeks post-injury. Data in B,D,F is relative, normalized as percent control, and presented as mean ± SEM. Tukey's post-hoc test. *$p<0.05$, **$p<0.01$.

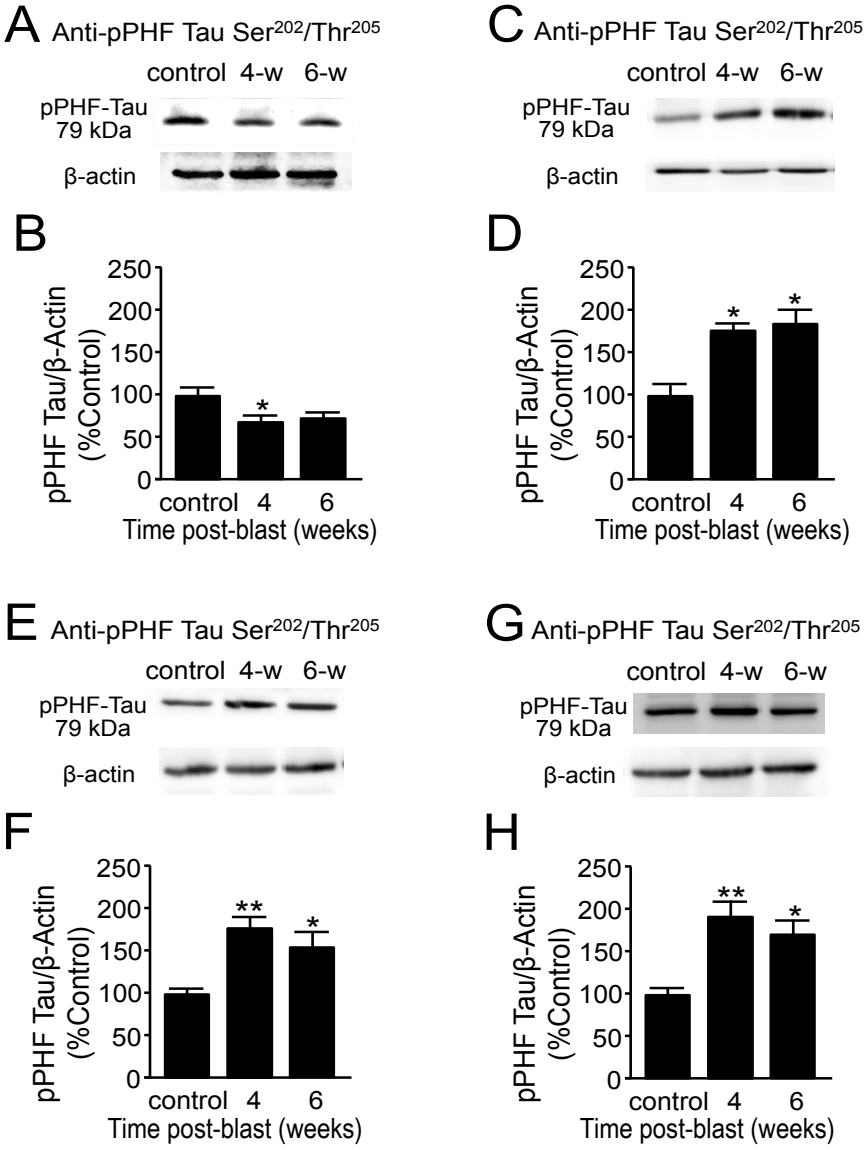

Figure 38. Increased pPHF Tau Ser^{202}/Thr^{205} in the whole brain, SN and STR region. Comparisons of pPHF Tau were made between control and post-blast in these brain areas. (A) Western Blot image of pPHF Tau Ser202/Thr205 and β-actin for each group at control, 4 and 6 weeks post-blast in the whole brain. (B) pPHF Tau Ser202/Thr205 significantly decreased at 4 and a trend of increased at 6 weeks post-blast [$F(2,11)=5.38$, $p=0.02$]. (C) Western Blot image of pPHF Tau Ser202/Thr205 and β-actin for each group at control, 4 and 6 weeks post-blast in the SN (E8). (D) pPHF Tau Ser202/Thr205 is significantly increased at 4 and 6 weeks post-blast [$F(2,12)=5.92$, $p=0.01$]. (E) Western Blot image of pPHF Tau Ser202/Thr205 and β-actin for each group at control, 4 and 6 weeks post-blast in the B5 STR region. (F) pPHF Tau Ser202/Thr205 is significantly increased at 4 and 6 weeks post-blast [$F(2,11)=7.39$, $p=0.009$]. (G) Western Blot image of pPHF Tau Ser202/Thr205 and β-actin for each group at control, 4 and 6 weeks post-blast in the C5 STR region. (H) pPHF Tau Ser202/Thr205 is significantly increased at 4 and 6 weeks post-blast [$F(2,11)=10.81$, $p=0.003$]. Data in B,D,F is relative, normalized as percent control, and presented as mean ± SEM. Tukey's post-hoc test were used. *$p<0.05$, **$p<0.01$.

3. SUSCEPTIBILITY OF PD-LIKE MOTOR DEFICITS FOLLOWING A MILD-bTBI

3.1. Gross Motor Behavior Tests and Biochemical Characterization of the Injury Models

3.1.1. Rationale

In light of these findings (Section 2), we propose that acrolein may be the underlying culprit rendering blast victims vulnerable to PD development. Additionally, *in vitro* studies performed in our laboratory show that acrolein enhances protein aggregation and promotes oligomerization of α –synuclein (data not shown). We postulate that elevated acrolein levels instigated by blast injury may synergistically work with some other possible factors to trigger or exacerbate PD pathology. With relevance to our animal models, we predict that the known event of post-blast injury, acrolein elevation, in combination with a sub-threshold 6-OHDA (sub clinical dose causing no behavioral deficits) may produce more severe PD like symptoms than either injury alone.

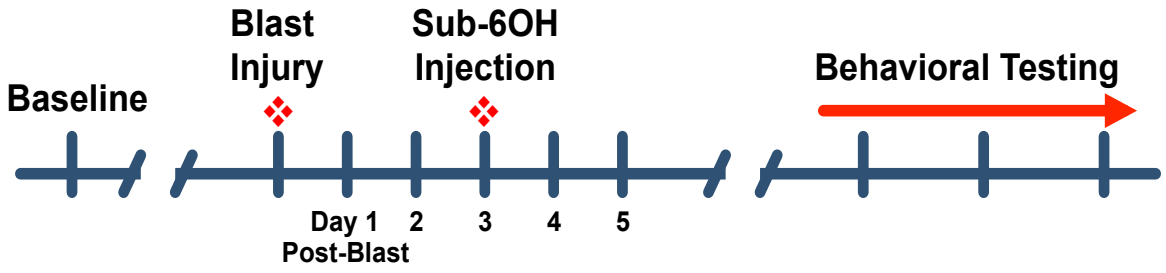

Figure 39: Section 3 Experimental Design and Timeline. Rats were trained on the rotarod and acclimated on the open box before collecting baseline readings. A blast injury was performed on the experimental group and 3 days after blast a sub-threshold dose of 6-OHDA was stereotaxically injected into the substantial nigra. Behavioral tests were performed for a certain period of time and animals were sacrificed according to PACUC guidelines after the study.

3.1.2. Brief Methods

3.1.2.1. Animal groups and numbers

Male Sprague Dawley rats (weight 350-450 grams) were used in this study. The rats were kept on a 12 h light/12 h darkness cycle and free access to water and food, and at controlled temperature of 25 ^{o}C. The experiments were performed under the strict accordance with PACUC guidelines. mBINT was performed as described in Fig. 3. Our time line for the mild-bTBI and sub-6-OHDA injection is shown in Fig. 39. The groups for this study:

Group 1: Sham_Blast (n=4)

Group 2: Mild-bTBI (n=5)

Group 3: Mild-bTBI + Sub-threshold_6-OHDA (n=5)

Group 4: Sub-threshold_6-OHDA only (n=5)

Group 5: 6-OHDA (n=5)

Group 6: Sham_6-OHDA (n=4)

3.1.2.2. Mild blast-traumatic brain injury model and behavioral assessments

Mild-blast TBI was administered as seen in Fig. 3. Rats were evaluated for locomotion on a rotarod. The rotarod speed increased gradually from 0-30 revolutions per minute over 3.5 minutes and remained at 30 rpm's until stopping at the 3.5-minute, 30 second mark or earlier if the rat fell. Criteria were developed to ensure animals were accustomed to the apparatus and testing before exposure. For pre-injury training, the rats had to successfully complete 2 out of 3 runs at 30 rpm (top speed). The average of the 3 runs per animal per test were recorded and used for analysis Then we measured further their locomotor and their exploratory behavior using the open field activity box as described in Koob et. al. [109]. The rat was placed in the center of a square 3 feet by 3 feet arena and allowed to explore for 15 minutes. Their exploratory activity was captured on a camera, and the motor metric analysis was conducted using Anymaze software (Stoelting Co., Wood Dale, IL). We collected data at least once a week on each animal up to 7 weeks post-injury. We evaluated their rotational activity, distance travelled, mean speed, immobility time, and rearing frequency. The blind analysis was employed in scoring of these parameters.

3.1.2.3. The 6-hydroxydomapine (6-OHDA) Rat Model

The 6-OHDA is one of the well-known PD animal models and it has been established in our lab. In brief, the 6-OHDA at 8μg diluted in sterile saline was administered using a Hamilton syringe with a stainless steel cannula gauge injector to obtain a unilateral nigrostriatal lesion. The rats were anesthetized with 100 mg/kg of ketamine and 10 mg/kg xylazine using intraperitoneal (i.p.) injections. A burr hole was made in the skull using a dermal drill, and after careful piercing of the dura mater; the needle was inserted vertically according to the stereotaxic coordinates using Paxinos as reference. Two microliters of the 6-OHDA solution was infused at a rate of 1 μL/min for 2 minutes. Sham-operated 6-OHDA rats (Group 6) rats received 2 microliters of saline delivered at the same rate. Sub-threshold 6-OHDA injection is induced laterally into the substantia nigra at this following coordinates: -5.4AP, +3.0ML, -8.2DV with a 6-OHDA concentration of 4μg/2μL and a full 6-OHDA with a higher concentration of at 8μg/2μL. The concentration of 6-OHDA has been previously used in our lab and the brain coordinates was followed according to Bergstrom et al., 2001 [244]. For Group 3, sub-threshold 6-OHDA was induced 3 days after blast. Since symptoms of PD do not present until dopamine loss in the putamen exceeds approximately 80%, the denervation produced by partial lesions as suggested is more suitable for investigating the compensatory adaption in the pre-symptomatic or preclinical phase of the disease [244].

3.1.3. Results and Discussion

3.1.3.1. Susceptibility of PD-like motor deficits following a blast injury and sub-threshold 6-OHDA injection

Loss of motor function is the predominant symptom of PD, which is observed in the most common 6-hydroxydopamine (6-OHDA) rat model of the disease. Our lab has established the 6-OHDA rat model by stereotaxically injecting 8 μg/2 μl of 6-OHDA into the substantia nigra (SN) to induce PD-like motor deficits. 6-OHDA promotes neurodegeneration of dopaminergic neurons in the substantia nigra further mimicking the pathology of PD. For our sub-threshold 6OHD group (Sub_6-OHDA) we injected at the same site (see methods for coordinates) but at a lower dosage of 6-OHDA (4 μg/2 μl). This is the first time we employed this sub-threshold dosage and expect to not show motor deficits. Sham_6-OHDA, injection of saline into the SN, is our negative control for this model. We trained each animal on the rotarod prior to collecting baseline measurements, which included three testing times per day and 210 seconds on the

rotarod was considered a perfect performance test. We averaged the motor performance for each animal (3 test per data point) and within groups, which was used to plot our data. We followed these animal groups' motor performance for approximately two months and collected data at different time points.

3.1.3.2. Motor activity assessment

The overall trend of motor performance on the rotarod for each of the six groups of animals is shown in Fig. 40a. Our motor performance test on the rotarod indicates that the combination of Blast+Sub_6-OHDA (172.2 ± 10.4 s) resulted in motor deficits similar to a full 6-OHDA PD model (180.1 ± 3.8 s) and is consistent throughout the study. However, the Blast only (204 ± 2.3 s) and Sub_6-OHDA (206 ± 1.8 s) alone did not show motor deficits. At the end of the study the motor performance test for each group was averaged and plotted on a bar graph (Fig. 40b). ANOVA shows a significant group effect [$F(5,22)$, $^{**}p<0.001$]. Post-hoc comparison between Blast and Blast+Sub_6-OHDA ($^{*}p<0.05$), Sub_6-OHDA and Blast+Sub_6-OHDA ($^{*}p<0.05$), and Sub_6-OHDA and 6-OHDA ($^{**}p<0.01$) all show statistically significant differences. The error bars represent SEM values. These results show that mild Blast can heighten the susceptibility to PD-like motor deficits. Motor deficits are absent in our mild Blast only and Sub_6-OHDA only groups, but the combination of these produce a PD-like motor deficits further supporting our hypothesis that mBINT can promote PD onset (Fig. 40). These data further validates our mild bTBI model, mimicking phenotypes typically observed in human mild-blast injury cases, and we have established an effective sub-threshold dosage of 6-OHDA.

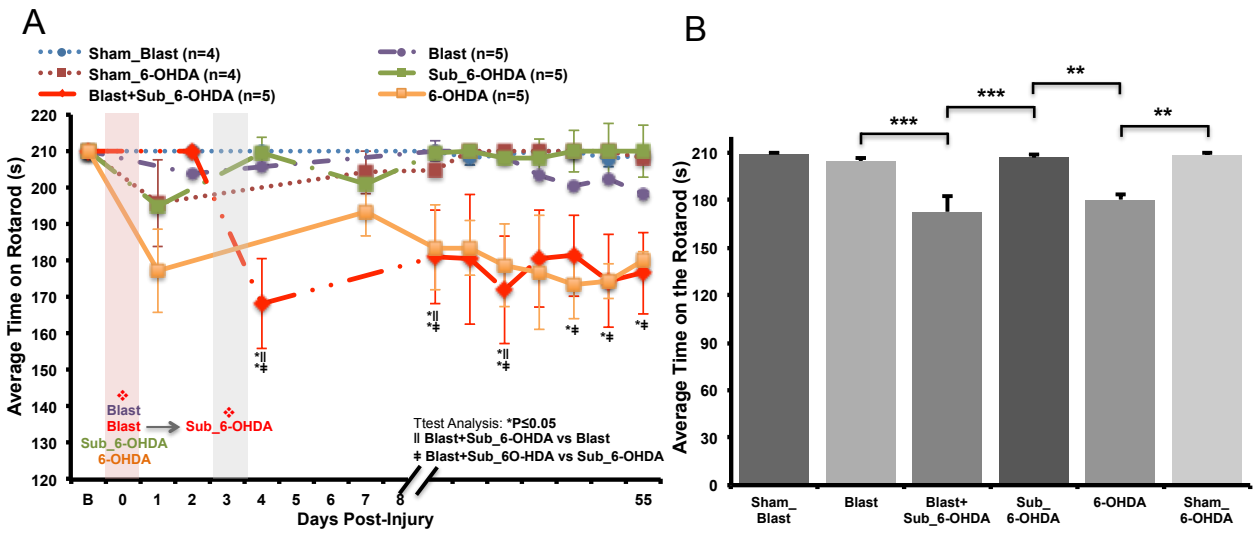

Figure 40: The combination of blast injury and sub-threshold 6-OHDA nigral injection induces a PD-like motor deficits. (A) The Sub_6-OHDA group and Blast only group show no motor deficits similar to the control groups (Sham_Blast and Sham_6-OHDA). However, when blast injury is combined with a Sub_6-OHDA injection to the substantia nigra (Blast+Sub_6-OHDA group) produce motor deficits similar to the 6-OHDA group, PD model. A comparison between Blast+Sub6OH vs Blast only and Blast+Sub6OH vs Sub6OH only show significant differences as indicated by the legends (*p≤0.05). Error bars represent SEM. (B) The combination of blast injury and sub-threshold 6-OHDA nigral injection induces a PD-like motor deficits. At the end of the study, the average motor activity tests for each rat within each group were calculated. ANOVA shows a significant group effect [F(2,22)=6.8, p=0.0005]. A post-hoc comparison using a two-sample t-test assuming equal variance was used to compare Blast and Blast+sub6OH and shows a statistically significant difference (p=0.02). The comparison between Sub-6OH and Blast+sub6OH show a statistically significant difference (p=0.02). In addition, the comparison between Sub-6OH and 6-OH (PD rat model) show statistically significant difference (p=0.001). Error bars represent SEM.

3.1.3.3. Spontaneous rotation

The unilateral 6-hydroxydopamine (6-OHDA) injection of rat model of PD has been a typical model in understanding the mechanisms underlying parkinsonian symptoms. It captures the changes in the neurocircuitry of the basal ganglia and the pharmacology of PD patients [245-250]. This model is assessed by measurement of spontaneous rotation with >70% ipsiversive (towards the lesioned side), indicating a >95% dopamine depletion in the striatum [249, 251]. We measured the spontaneous rotation amongst our groups using the open field and rotations were scored blindly. Figure 41a shows the average rotational preference (ipsiversive vs contraversive) amongst the groups measured at 4-5 weeks post- injury. In the 6-OHDA model there was a significant preference of ipsiversive rotation (81.0 ± 6.24 rotations/15-min, n=5) compared to contraversive rotation (52.0 ± 9.81 rotations/15-min, n=5, *p<0.05). ANOVA comparison of the ipsiversive rotation amongst group show s significant increase in the Blast+Sub_6-OHDA (73.50 ± 6.24 rotations/15-min, n=5) compared to the Blast group (45.10 ± 2.28 rotations/15-min, n=5) [F(5,21)=4.32, p=0.007, *p<0.05, **p<0.01]. Furthermore, in the 6-OHDA group (81.0 ± 6.24 rotations/15-min, n=5) show significant increase compared to the Sham-6-OHDA (50.25 ± 3.49 rotations/15-min, n=4). Analysis of spontaneous rotations 6-7 weeks post injury (Fig. 41b) show significant ipsiversive preference in the Blast+Sub_6-OHDA (86.2 ± 6.84 rotations/15-min, n=5, *p<0.05) similar to the 6-OHDA group (81.4 ± 9.81 rotations/15-min, n=5, *p<0.05). ANOVA analysis of the ipsiversive rotations amongst groups show significant group effect [F(5,21)=4.42, p=0.007, *p<0.05, **p<0.01], but no significance in the contraversive rotations [F(5,22)=0.99, p=0.44]. These data, together with the rotarod, support the synergistic effect of blast injury and injection of subthreshold 6-OHDA to induce a PD-like motor deficits similar to the 6-OHDA model.

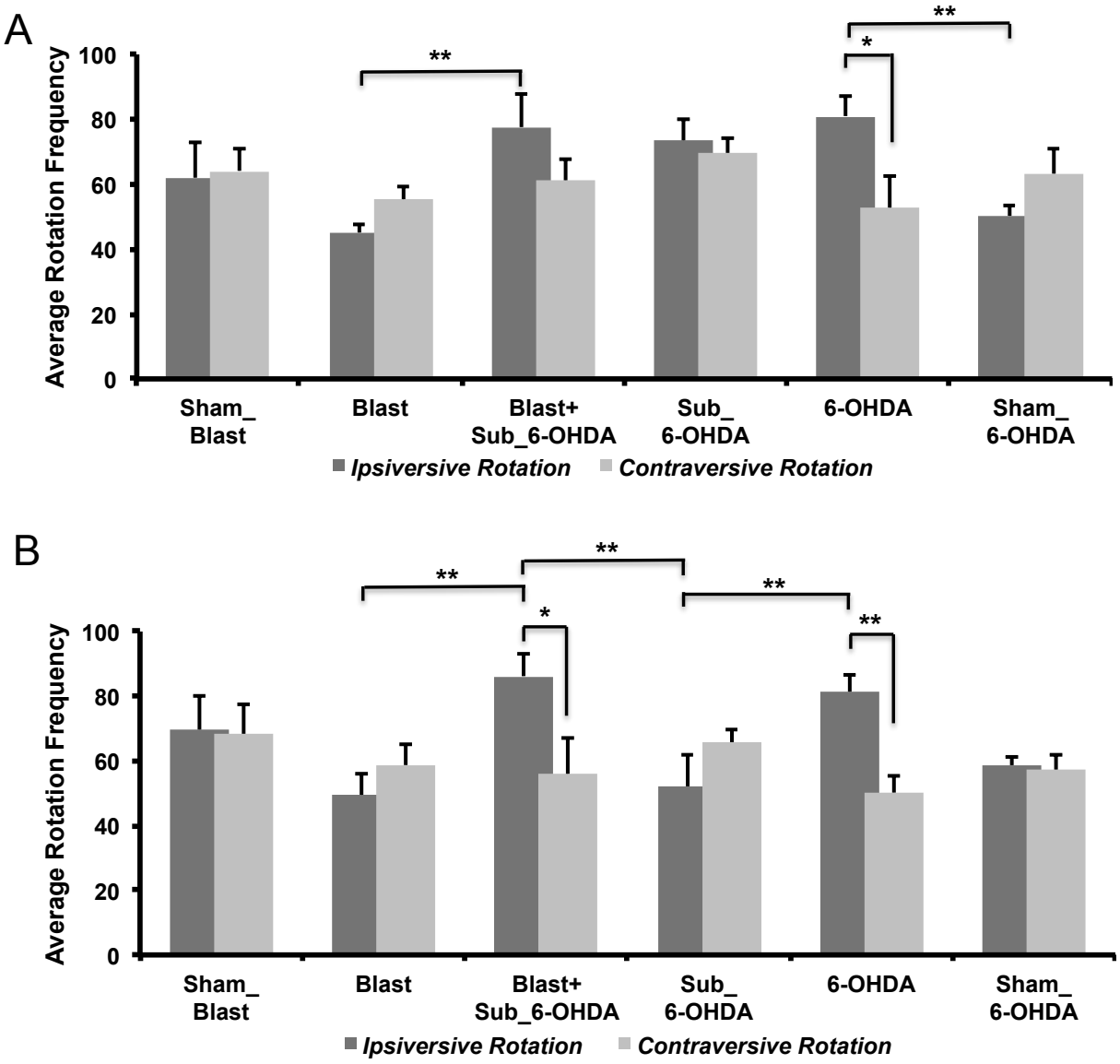

Figure 41: Assessment of rotational behavior amongst the group (A) Rotational assessment at 4-5 weeks post-injury. The 6-OHDA group shows significant ipsiversive preference (*p<0.05). ANOVA analysis of the ipsiversive rotation shows significant group effect [$F(5,21)= 4.321$, $p=0.007$]. Significant increase in the Blast+Sub_6-OHDA similar to the 6-OHDA compared to the Blast only and Sham_6-OHDA. (B) Rotational assessment at 6-7 weeks post injury. The Blast+Sub-6-OHDA group shows significant ipsiversive rotational preference similar to the 6-OHDA group. ANOVA analysis of the ipsiversive rotation indicates significant group effect [$F(5,21)= 4.421$, $p=0.007$]. Significant increase in the Blast+Sub_6-OHDA similar to the 6-OHDA compared to the Blast only and Sham_6-OHDA. Post-hoc Fisher's LSD; *p<0.05; **p<0.01, ***p<0.001. Error bars represent SEM.

3.1.3.4. Exploratory and locomotor activity: distance travelled, mean speed, immobility time and rearing frequency

Similarly, distance travelled and mean speed was assessed using the open field. Figure 42a shows the progression of their distance travelled up to 45 days post-injury. Average distance travelled was measured at 4-5 weeks post-injury showed no significant group effect [$F(5,22)=0.99$, $p=0.44$] (Fig. 42b). At 6-7 weeks post-injury a significant group effect was observed [$F(5,23)=5.30$, $p=0.002$, *$p<0.05$, **$p<0.01$]. Post-hoc analysis showed significant decrease in the Blast+Sub_6-OHDA group (39.34 ± 6.28 m/15-min, n=6) compared to the Sub_6-OHDA only (63.60 ± 5.06 m/15-min, n=6); similar to the 6-OHDA group (37.09 ± 5.56 m/15-min, n=5). This supports a synergistic effect of the blast and subthreshold 6-OHDA injection. However, the Blast only group (40.52 ± 3.86 m/15-min, n=5) show significant decrease when compared to the Sham_Blast group (54.07 ± 2.14 m/15-min, n=4); a similar trend to the 6-OHDA and Blast+Sub_6OHDA group.

We observed a similar trend in the mean speed assessment. At 4-5 weeks post-injury we observed a significant group effect [$F(5,22)=3.26$, $p=0.02$, *$p<0.05$, **$p<0.01$] (Fig. 43b). A significant decrease was observed in the Blast+Sub_6-OHDA (0.047 ± 0.005 m/s, n=5), 6-OHDA (0.045 ± 0.005 m/s, n=4), when compared to the Sub_6-OHDA only (0.068 ± 0.003 m/s, n=6). In addition, at 6-7 weeks post injury we observed a significant group effect [$F(5,22)=6.75$, $p=0.001$, *$p<0.05$, **$p<0.01$, ***$p<0.001$] (Fig. 43c). A significant decrease was observed in the Blast+Sub_6-OHDA (0.040 ± 0.007 m/s, n=5), 6-OHDA (0.034 ± 0.008 m/s, n=4), when compared to the Sub_6-OHDA only (0.070 ± 0.005 m/s, n=6) and the Sham_6OHDA (0.062 ± 0.004 m/s, n=4). Interestingly, a trend of decrease was observed in the Blast only group (0.044 ± 0.002 m/s, n=5) compared to the Sham_Blast group (0.060 ± 0.002 m/s, n=4).

Immobility time assessment showed no significant group effect [$F(5,23)=1.64$, $p=0.188$] at 4-5 weeks post-injury (Fig. 44b). However, at 6-7 weeks a significant group effect was observed [$F(5,23)=6.80$, $p=0.000$, *$p<0.05$, **$p<0.01$] (Fig. 44c). A significant increase was observed in the Blast+Sub_6-OHDA group (478.32 ± 60.39 s, n=6) similar to the 6-OHDA group (533.90 ± 80.65 s, n=4); when compared to the Sub_6-OHDA (254.45 ± 24.46 s, n=6) or the Sham_6-OHDA (299.07 ± 50.26 s, n=4). Interestingly, a significant increase was observed in the Blast group (559.47 ± 38.39 s, n=5) when compared to the Sham_Blast (343.81 ± 34.0 s, n=4).

Furthermore, a significant group effect was observed in the rearing frequency [$F(5,23)=7.23$, $p=0.000$, *$p<0.05$, **$p<0.01$, ***$p<0.001$] at 4-5 weeks post injury (Fig. 45b). Post-hoc analysis showed a significant decrease of rearing activity in the Blast+Sub_6-OHDA (35.10 ± 4.21 counts, n=5), similar to the 6_OHDA (33.83 ± 2.72 counts, n=6) when compared to the Sub_6-OHDA (55.10 ± 3.75 counts, n=5) and Sham_6-OHDA (48.66 ± 6.93 counts, n=3). Blast group (21.41 ± 4.45 counts, n=6) showed a significant decrease when compared to the Sham_Blast (39.37 ± 6.72 counts, n=4). In addition, a significant group effect [$F(5,23)=11.36$, $p=0.0001$, *$p<0.05$, **$p<0.01$, ***$p<0.001$] was also observed at 6-7 weeks post-injury (Fig. 45c). Post-hoc analysis showed a significant decrease of rearing activity in the Blast+Sub_6-OHDA (27.25 ± 4.99 counts, n=6), similar to the 6_OHDA (22.83 ± 1.03 counts, n=6) when compared to the Sub_6-OHDA (54.30 ± 4.08 counts, n=5) and Sham_6-OHDA (43.16 ± 6.58 counts, n=3). Blast group (17.25 ± 3.06 counts, n=6) showed a significant decrease when compared to the Sham_Blast (50.50 ± 10.75 counts, n=3).

Overall the assessment of distance travelled, mean speed, immobility time and rearing frequency showed significant behavioral deficits in the Blast+Sub-6-OHDA similar to the 6-OHDA group. These data support a synergistic effect, that when the mild-blast injury and sub-threshold 6-OHDA are combined, it produces overall locomotor and exploratory behavior impairments. However, the deficits observed in the Blast only group indicate a long-term consequence in the fine motor performance after the injury. Traumatic brain injury such as blast injury presents a very complex pathophysiology and individuals exposed to such injury suffer from long-term motor and cognitive functions and thus increasing their risk in developing neuropsychiatric and neurodegenerative diseases [252-257]. Similarly, animal models of TBI such as controlled cortical impact (CCI) and fluid percussion injury (FPI) also show the same long-term behavior deficits [139, 258-262]. Our rat mild-blast model show no significant motor and cognitive deficits acutely (Section 1), however approximately at one month after injury, they show behavioral deficits similar to what is observed in TBI victims and animal models of TBI.

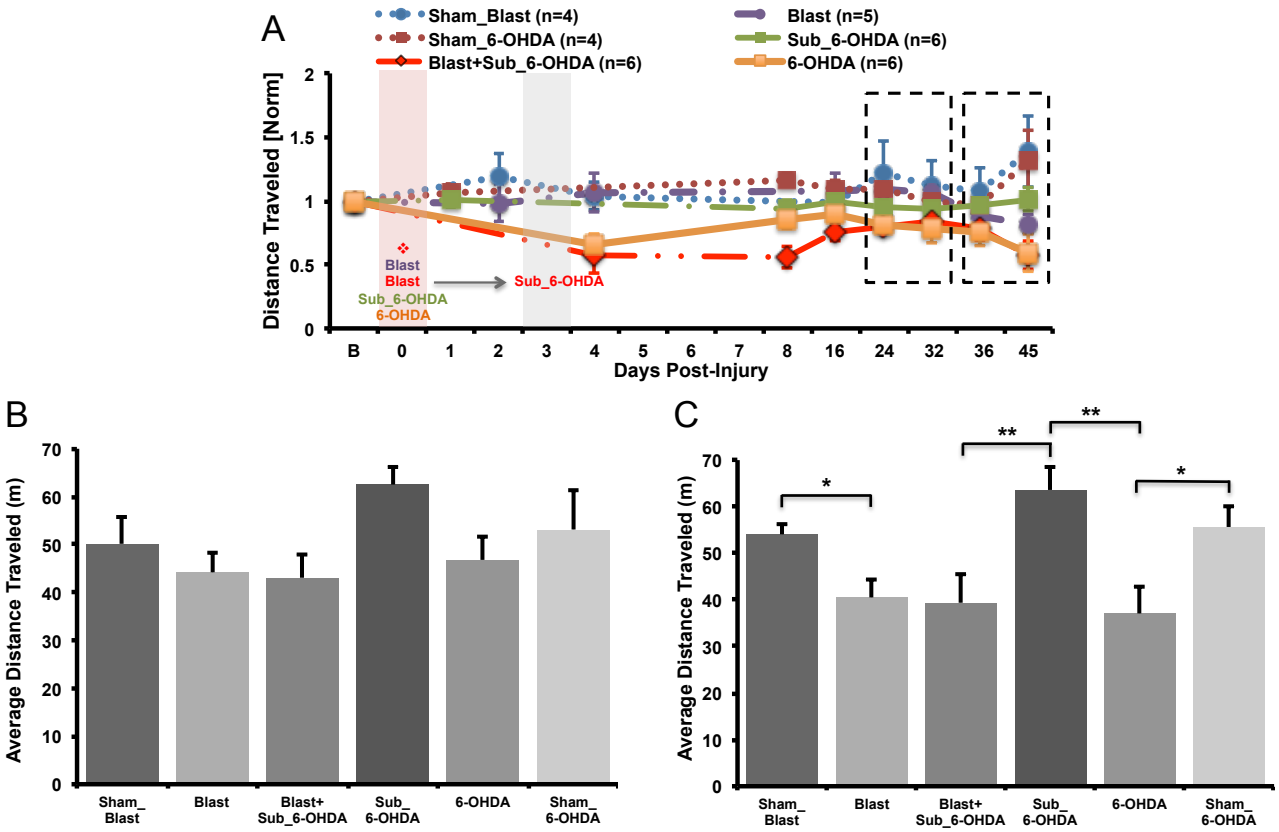

Figure 42: Differences in Total Distance Traveled. (A) Graph showing the progression of distance travelled (normalized to baseline) of all the groups throughout the study. (B) Average distance travelled at 4-5 weeks post-injury shows no significant group effect [$F(5,23)= 2.33$, $p=0.075$]. (C) Average distance travelled at 6-7 weeks post injury show significant group effect [$F(5,23)= 5.23$, $p=0.002$].The Blast+Sub-6-OHDA group shows significant decrease similar to the 6-OHDA group when compared to Sub_6OHDA and Sham_6-OHDA. The Blast only shows significant decrease compared to the Sham_Blast. Post-hoc Fisher's LSD; *$p<0.05$; **$p<0.01$, ***$p<0.001$.Error bars represent SEM.

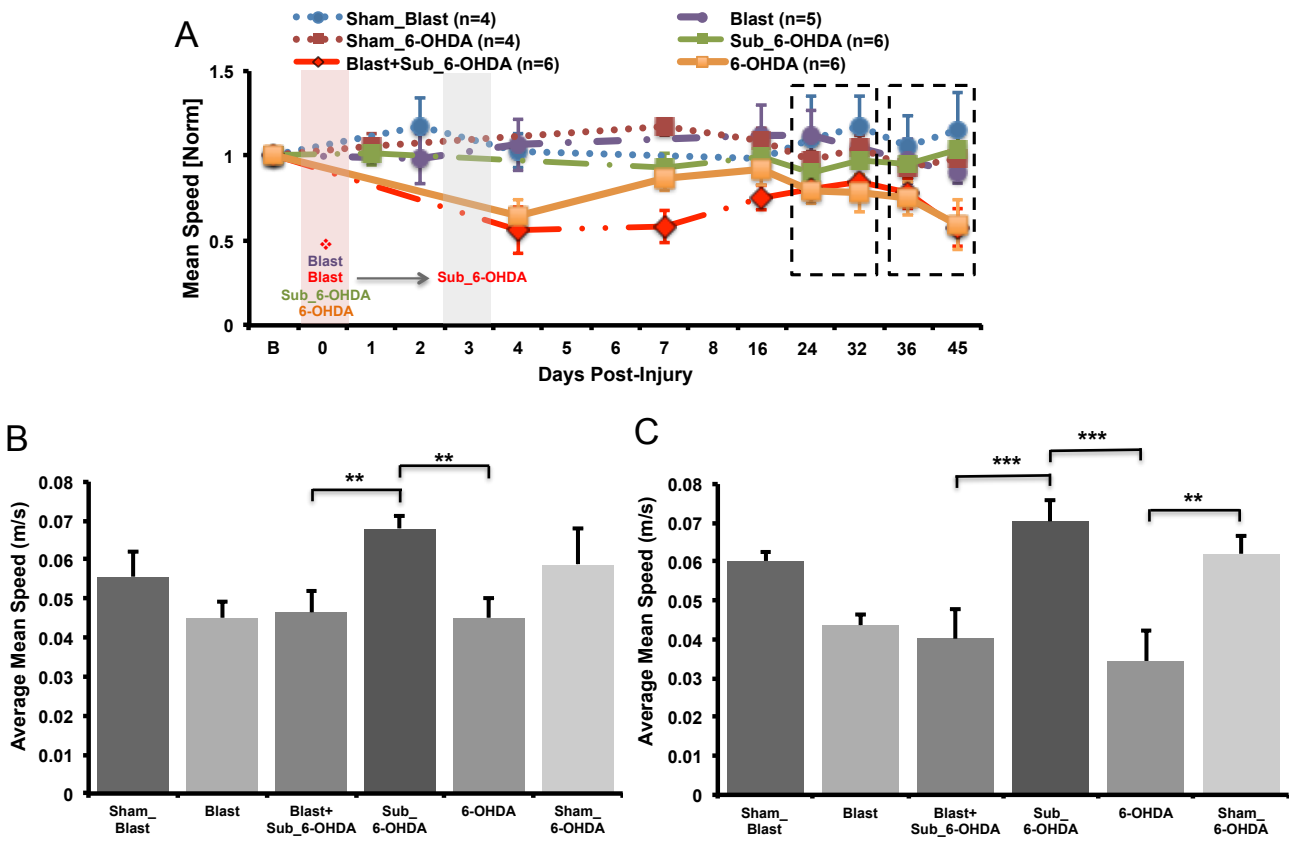

Figure 43: Differences in Average Mean Speed. (A) Graph showing the progression of mean speed (normalized to baseline) of all the groups throughout the study. (B) Average mean speed at 4-5 weeks post-injury shows significant group effect [$F(5,22)= 3.26$, $p=0.024$]. Blast+Sub_6-OHDA group shows significant reduction similar to 6-OHDA group when compared to Sub_6-OHDA .(C) Average mean speed at 6-7 weeks post injury show significant group effect [$F(5,22)= 6.75$, $p=0.001$]. The Blast+Sub-6-OHDA group shows significant reduction of speed similar to the 6-OHDA group when compared to Sub_6OHDA and Sham_6-OHDA. The Blast only shows significant decrease compared to the Sham_Blast. Post-hoc Fisher's LSD; *$p<0.05$; **$p<0.01$, ***$p<0.001$. Error bars represent SEM.

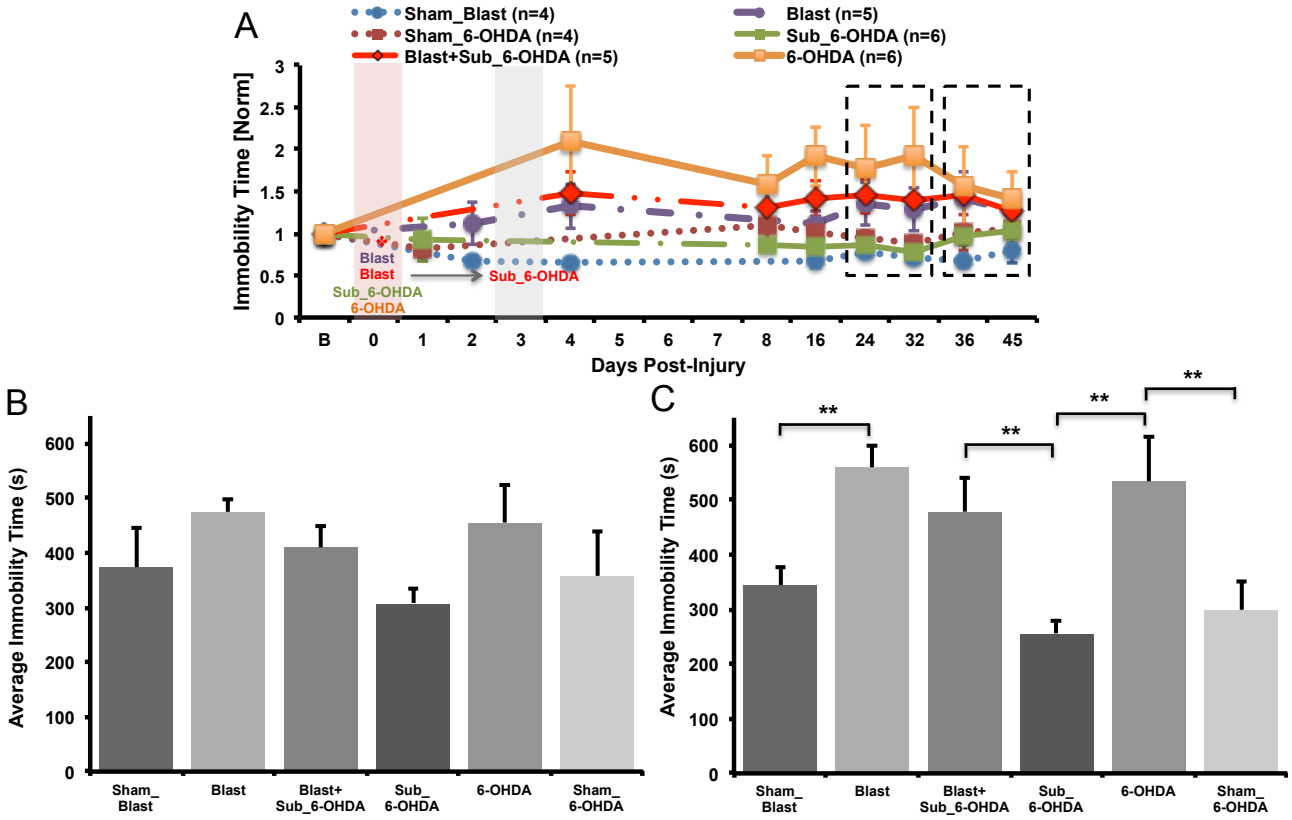

Figure 44: Differences in Immobility Time. (A) Graph showing the progression of immobility time (normalized to baseline) of all the groups throughout the study. (B) Average immobility time at 4-5 weeks post-injury shows no significant group effect [$F(5,23)= 1.64$, $p=0.18$]. (C) Average immobility time at 6-7 weeks post injury show significant group effect [$F(5,23)= 6.80$, $p=0.000$].The Blast+Sub-6-OHDA group shows significant increase of immobility time similar to the 6-OHDA group when compared to Sub_6-OHDA and Sham_6-OHDA. The Blast only shows significant increase compared to the Sham_Blast. Post-hoc Fisher's LSD; *$p<0.05$; **$p<0.01$, ***$p<0.001$.Error bars represent SEM.

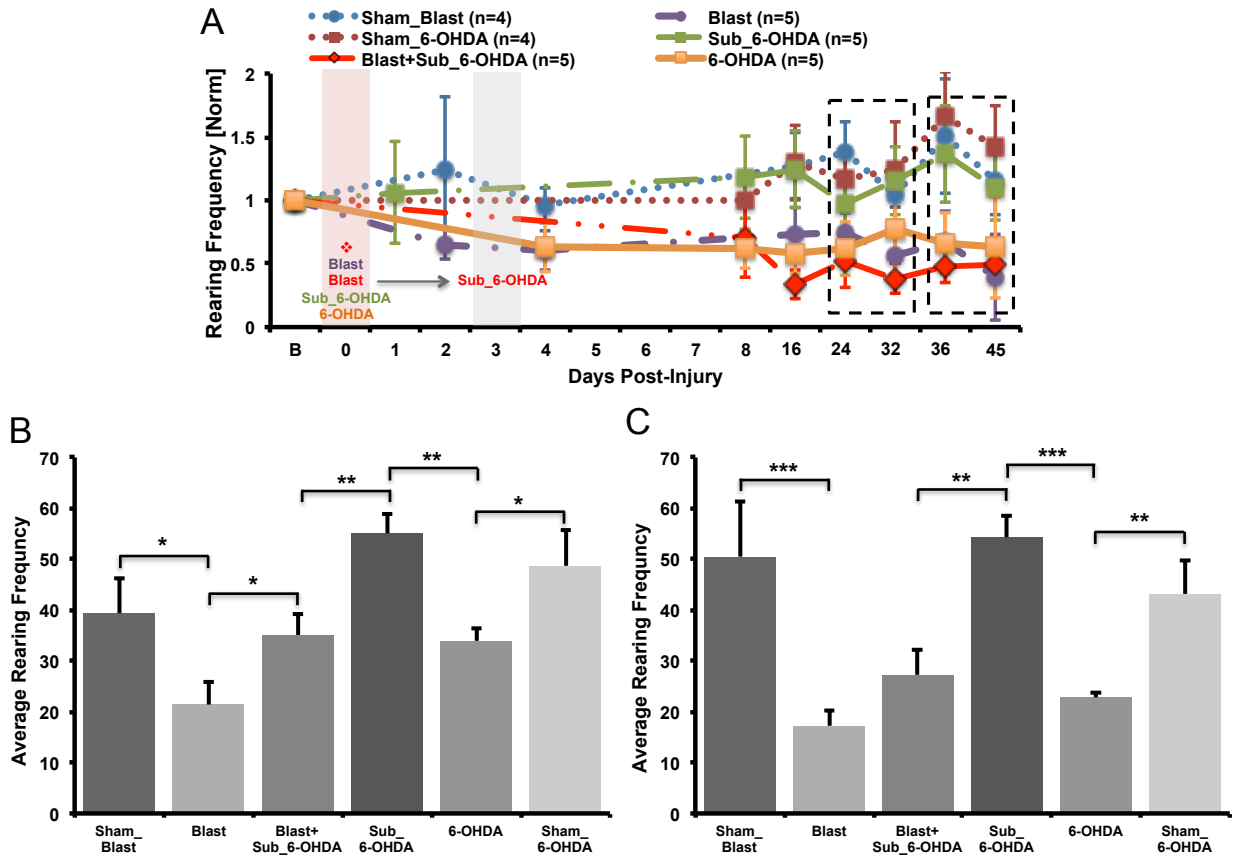

Figure 45: Differences in Rearing Frequency (A) Graph showing the progression of rearing frequency (normalized to baseline) of all the groups throughout the study. (B) Average rearing frequency at 4-5 weeks post-injury shows significant group effect [$F(5,23)= 7.23$, $p=0.0001$]. Blast+Sub_6-OHDA group show significant reduction of rearing frequency similar to 6-OHDA when compared to Sub_6-OHDA and Sham_6-OHDA. Blast group show significant reduction compared to the Sham_Blast. (C) Average rearing frequency at 6-7 weeks post injury show significant group effect [$F(5,23)= 11.36$, $p=0.0001$]. The Blast+Sub-6-OHDA group shows significant decrease of rearing frequency similar to the 6-OHDA group when compared to Sub_6-OHDA and Sham_6-OHDA. The Blast only shows significant decrease compared to the Sham_Blast. Post-hoc Fisher's LSD; *$p<0.05$; **$p<0.01$, ***$p<0.001$.Error bars represent SEM.

3.1.3.5. Role of acrolein in PD-like motor deficits in the 6-OHDA rat model and blast injury

Urine levels of the acrolein metabolite, 3-HMPA, were measured from each animal on each group. In Fig. 46 we show that 3-HPMA is elevated in the 6-OHDA group compared to the Sub_6-OHDA and the control, Sham_6-OHDA groups. The data are expressed as mean (±SEM) of their 3-HMPA measurements normalized to their baseline. We demonstrate that at five days post surgery there is an increasing trend of 3-HPMA levels, but no statistically significant group effect (Fig 46a). However fifteen days post-surgery there is a statistically significant group effect, ANOVA [$F(2,11)=8.08$, $p=0.007$]. Tukey's Post-hoc comparison between Sham_6-OHDA vs. 6-OHDA (*$p<0.05$) and Sub_6-OHDA vs. 6-OHDA (**$p<0.01$) show significant increased levels of 3-HPMA in the 6-OHDA group (Fig. 46b). This supports previous studies that oxidative stress, particularly acrolein, is increased in PD and perhaps is a major contributor of ROS production and if not mitigated leads to neurodegeneration. Additionally, these 3-HMPA measurements can be correlated to the motor and locomotor behavior deficits thus demonstrating that the increased levels of 3-HPMA induce motor deficits in the 6-OHDA PD rat model.

Furthermore, we monitored the 3-HMPA levels in the mild Blast+Sub_6-OHDA group (Fig. 47). Our data are expressed as mean (±SEM) of 3-HPMA quantity normalized to creatinine (μg/mg). There is a statistically significant increase of 3-HPMA in their urine after injury relative to their baseline measurements. ANOVA [$F(3,15)=8.88$, $p=0.001$] and Tukey's HSD post-hoc analysis show significant increase of 3-HPMA levels 2-Days Post-Blast (*$p<0.05$), 1 Day Post-Sub_6-OHDA Surgery (**$p<0.01$), and 20 Days Post-blast (*$p<0.05$) compared to their baseline levels. Additionally, when we compared Blast+Sub_6-OHDA group to the Sham_Blast and Blast only groups we show a statistically significant increased of 3-HPMA levels at two days ([$F(2,10)=7.71$, $p=0.009$]; Sham_Blast vs. Blast and Sham_Blast vs. Blast+Sub_6-OHDA(*$p<0.05$). Subsequently, twenty days post-injury the 3-HPMA levels are sustained (Fig. 18B). Here, we show that the combination of mild-blast TBI and sub_threshold 6-OHDA can potentiate the increase of 3-HPMA levels in the urine as compared to the mild-blast only and relatively to the sub_6-OHDA group, indicating that the combination of these two injuries increases oxidative stress similar to the 6-OHDA PD model. These levels of 3-HMPA

can also be correlated to the motor performance test (rotarod), and exploratory/locomotor measurements (open box).

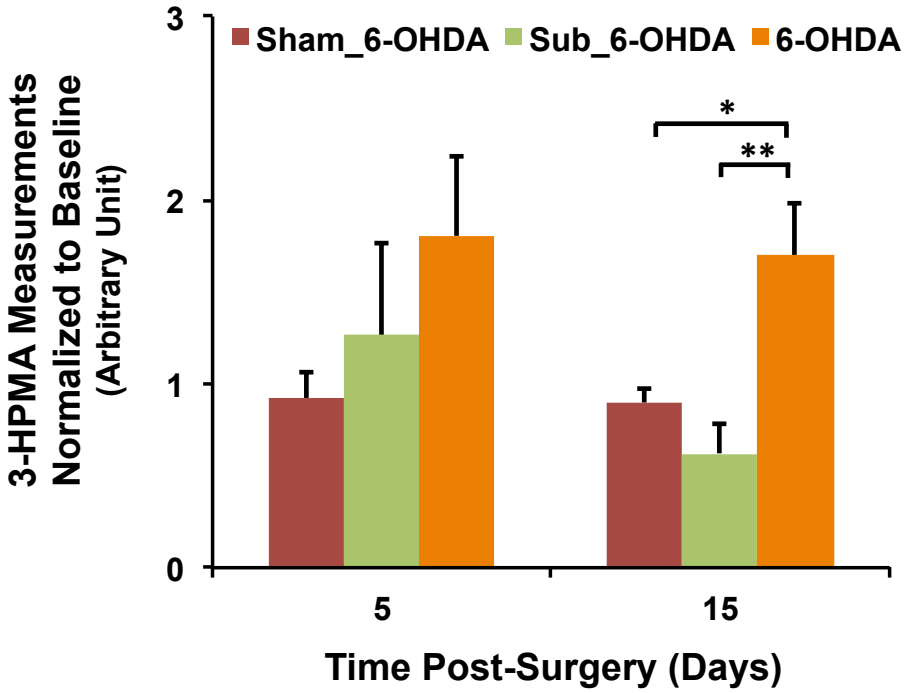

Figure 46: 3-HMPA, an acrolein metabolite, is increased in urine of the Parkinson's Disease rat model (6-OHDA). Data are expressed as mean (±S.E.M.) of the normalized 3-HPMA (µg/mg) levels to their respective baseline. Group treatment summary: Sham_6-OHDA is the control group (injection of saline in the SN), Sub_6-OHDA (4 µg/2µl injection of 6-OHDA toxin into the SN), and 6-OHDA (8µg/2µl injection of 6OHDA into SN). At 5 days post surgery, ANOVA shows no significant group effect [F (2,11)=1.08, p=0.37]. The ANOVA test 15 days post surgery show a significant group effect [F(2,11)=8.08, p=0.007]. A post-hoc comparison using Tukey's HSD was used to compare Sham_6OHDA vs. 6-OHDA (*$p<0.05$) and Sub_6-OHDA vs. 6-OHDA (**$p<0.01$) groups and showing significant differences between groups. Error bars represent SEM.

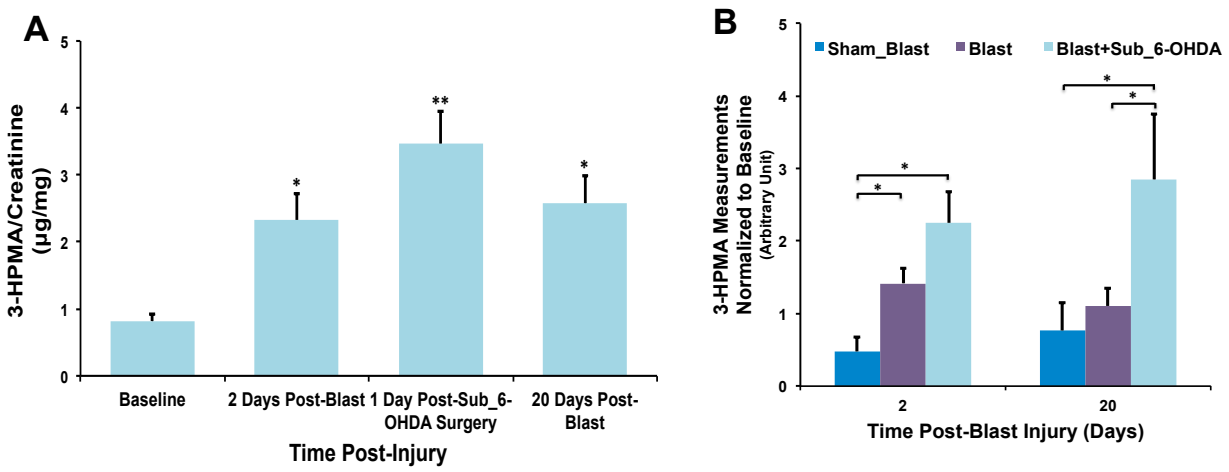

Figure 47: The combination of blast injury and sub-threshold 6OHDA nigral injection heightens the 3-HMPA, an acrolein metabolite, compared to only blast injured animals. (A) 3-HPMA measurements from the Blast+Sub_6-OHDA group, data are expressed as mean (±S.E.M.). ANOVA shows significant increase of 3-HPMA levels [$F(3,15)=8.88$, $p=0.001$]. Tukey's post-hoc test shows a significant increase of 3-HPMA levels 2-days post blast (*$p<0.05$), 1-day post surgery (**$p<0.01$), and 20-days post-blast (*$p<0.05$) relative to their baseline. (B) Data expressed as mean (±S.E.M.) and normalized to their baseline. Group treatment summary: Sham_Blast is the control group (anesthesized and placed in the room where the blast occurs), Blast (as described on the Methods section), Blast+Sub_6-OHDA (Blast and 3 days after a 4 µg/2µl 6OHDA was injected into the SN). There is a significant increase of 3-HPMA levels two days post blast (ANOVA [$F(2,10)=7.71$, $p=0.009$), Tukey's post-hoc indicates significant increase in the blast (*$p<0.05$) and blast+Sub_6-OHDA (*$p<0.05$). Measurements twenty days post-blast injury also show significant increase of 3_HPMA levels [$F(2,9)=5.44$, $p=0.02$], Tukey's post-hoc shows increased 3-HPMA levels in blast and blast+sub_6-OHDA groups relative to the sham_blast group (*$p<0.05$). Error bars represent SEM.

4. NEUROPROTECTIVE ROLE OF PHENELZINE, AN ACROLEIN SCAVENGER, POST-MILD-bTBI

4.1. Behavioral Assessment and Biochemical Characterization in the Blast+sub_threshold_6-OHDA Injury Model with Phenelzine Treatment

4.1.1. Rationale

Previous experiments from our lab demonstrate that acrolein scavengers, such as phenelzine, can mitigate motor deficits in the PD-6OHDA rat model. In addition, we show that injection of acrolein to the brain induces PD-like motor deficits. To further investigate the role of acrolein post-mild bTBI and its susceptibility to PD-like motor deficits and neuropathology, we used phenelzine as a therapeutic acrolein scavenger to mitigate motor deficits observed in the mild bTBI+Sub_threhshold 6-OHDA (results from Section 3). We instigate that the excessive acrolein production post-blast injury exacerbates the biochemical events in the brain and can potentiate further damage leading to the contribution to the PD-like pathology.

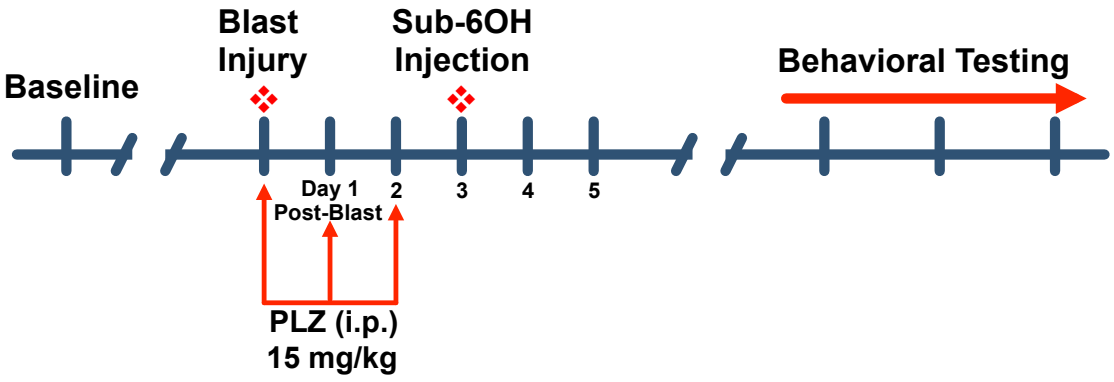

Figure 48: Section 4 Experimental Design and Timeline. Rats were trained on the rotarod and acclimated on the open box before collecting baseline readings. A blast injury was performed on the experimental group and 5 minutes after blast an injection of phenelzine (PLZ) at 15 mg/kg was administered intraperotineally (i.p.). Phenelzine was administered again 24 and 48 hours post-blast. On Day 3, a sub-threshold dose of 6-OHDA (4 µg/2µL 6-OHDA) was stereotaxically injected into the substantia nigra. Behavioral tests were performed for a certain period of time and animals were sacrificed according to PACUC guidelines after the study.

4.1.2. Brief Methods

The same animal models were used as previously described in sections 2 and 3. Male Sprague Dawley rats (weight 350-450 grams) were used in this study. The rats were kept on a 12 h light/12 h darkness cycle and free access to water and food, and at controlled temperature of 25 ^{o}C. The experiments were performed under the strict accordance with PACUC guidelines. Blast injury was performed as described in Aim 1 and sub-threshold 6-OHDA in Aim 2. A dose of 15 mg/kg of phenelzine was administered to each animal post-mBINT. Fig. 48 shows a time line of the experiment for this aim.

4.1.3. Results and Discussion

4.1.3.1. Phenelzine alleviates PD-like motor deficits: rotarod activity and spontaneous rotations

Fig. 49a shows that the treatment of phenelzine post-mild TBI, before induction of sub-6-OHDA (Blast/PLZ/Sub6OH group; 208 ± 4.8 s) shows an improvement of motor performance compared to the non-phenelzine treated group (Blast+sub-6-OHDA; 172 ± 10.4 s). The average motor performance was calculated at the end of the study and represented on each bar (Fig. 49b). ANOVA analysis shows significant group effects [$F(2,9)=5.88$, $P<0.05$] and a post-hoc comparison between blast/PLZ/sub-6-OHDA (203 ± 4.8 s) and Blast+sub-6-OHDA (172 ± 10.4 s) shows a statistically significant improvement in motor performance in the PLZ treated group ($p<0.05$). Therefore, we show that phenelzine treatment post-blast can be effective for alleviating these deficits. These data further implicate the role of acrolein post-mBINT and perhaps with other factors can contribute to the susceptibility to PD-like motor deficits and supports the therapeutic properties of phenelzine as shown in our previous studies.

Figure 50a shows the average rotational preference (ipsiversive vs. contraversive) amongst the groups measured at 4-5 weeks post- injury. There is an observed increase ipsiversive rotational preference in the Blast+Sub_6-OHDA (77.76 ± 10.12 rotations/15-min, n=5) compared to contraversive rotation (61.2 ± 6.43 rotations/15-min, n=5) but not significant. However, at 6-7 weeks post injury Blast+Sub_6-OHDA group (Fig. 50b) showed a significant ipsiversive rotational preference 86.20 ± 6.84 rotations/15-min, n=5) compared to its contraversive rotations (55.75 ± 11.42 rotations/15-min, n=4, *$p<0.05$). Consequently the Blast+PLZ+Sub_6-OHDA did not show a significant ipsiversive (65.00 ± 7.07 rotations/15-min,

n=4) preference as compared to its contraversive rotations (78.20 ± 3.45 rotations/15-min, n=5). ANOVA comparison of the ipsiversive rotation amongst group shows significant group effect [F(2,9)=4.90, p=0.036, *p<0.05, **p<0.01]. The phenelzine treated group, Blast+PLZ+Sub_6-OHDA, showed improvement (65.00 ± 7.07 rotations/15-min, n=4), compared to the non-PLZ treated group, Blast+Sub_6-OHDA (86.20 ± 6.84 rotations/15-min, n=5). The PLZ group only (57.66 ± 4.69 rotations/15-min, n=3).

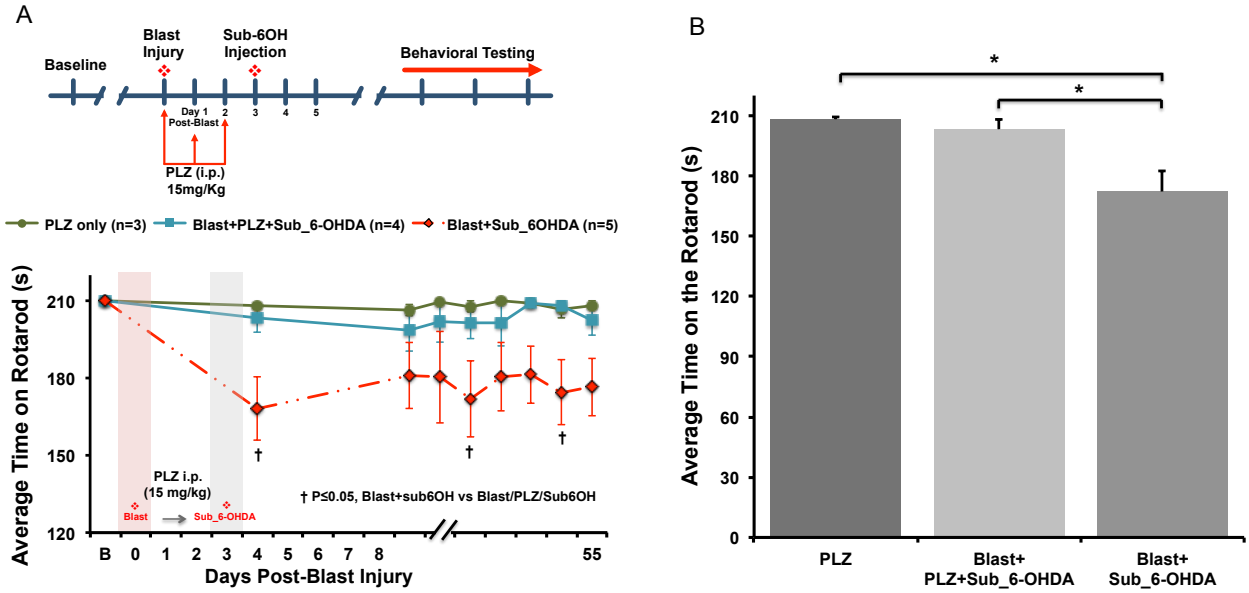

Figure 49: The treatment of phenelzine post-blast improves motor performance on the rotarod. **(A)** Shows that Phenelzine treatment (15 mg/kg, i.p.) after blast injury shows improvement of motor performance (Blast/PLZ/Sub-6OH group) compared to the non-phenelzine treated group (Blast+Sub6OH) . **(B)** The average motor performance of each animal on each group were calculated and represented on each bar. ANOVA shows significant group effects [F=5.88, p=0.02]. A post-hoc comparison using a two-sample t-test assuming equal variance was used to compare Blast/PLZ/Sub-6OH vs. Blast+Sub6OH (*p<0.05) show significant differences in motor activity. Error bars represent SEM.

4.1.3.2. Phenelzine alleviates exploratory and locomotor activity: distance travelled, mean speed, immobility time and rearing frequency

Distance travelled assessment showed no significant group effect [$F(2,10)=1.12$, $p=0.36$] at 4-5 weeks post injury (Fig. 51a) However at 6-7 weeks post-injury showed significant group effect [$F(2,10)=4.27$, $p=0.046$, $*p<0.05$] (Fig 51b). Post-hoc analysis showed a significant improvement of distance travelled in the phenelzine treated group, Blast+PLZ+Sub_6-OHDA, (53.51 ± 3.83 rotations/15-min, n=5), compared to the non-PLZ treated group, Blast+Sub_6-OHDA (35.64 ± 6.21 rotations/15-min, n=5). The PLZ group only (51.57 ± 0.18 rotations/15-min, n=3).

Similarly, the mean speed assessment showed no significant group effect [$F(2,10)=1.92$, $p=0.19$] (Fig. 52a) at 4-5 weeks post injury at 4-5 weeks post injury. However at 6-7 weeks post-injury showed near significant group effect [$F(2,10)=3.84$, $p=0.05$, $*p<0.05$] (Fig 52b). Post-hoc analysis showed a significant improvement of mean speed in the phenelzine treated group, Blast+PLZ+Sub_6-OHDA, (0.06 ± 0.004 m/s, n=5), compared to the non-PLZ treated group, Blast+Sub_6-OHDA (0.04 ± 0.007 m/s, n=5). The PLZ group only (0.05 ± 0.0003 m/s, n=3).

Immobility time assessment showed significant group effect [$F(2,11)=5.45$, $p=0.023$, $*p<0.05$] at 4-5 weeks post-injury (Fig. 53a). Post-hoc analysis showed a significant improvement of immobility time assessment in the phenelzine treated group, Blast+PLZ+Sub_6-OHDA, (289.0 ± 21.41 s, n=5), compared to the non-PLZ treated group, Blast+Sub_6-OHDA (409.85 ± 40.30 s, n=6). The PLZ group only (259.43 ± 25.47 s, n=3). Consequently, a significant group effect [$F(2,11)=5.57$, $p=0.021$, $*p<0.05$] at 6-7 weeks post injury (Fig 53b). Post-hoc analysis showed a significant improvement of immobility time assessment in the phenelzine treated group, Blast+PLZ+Sub_6-OHDA, (292.83 ± 20.02 s, n=5), compared to the non-PLZ treated group, Blast+Sub_6-OHDA (478.32 ± 60.39 s, n=6). The PLZ group only (280.63 ± 29.02 s, n=3).

The rearing frequency assessment showed no significant group effect [$F(2,9)=3.70$, $p=0.06$] (Fig. 54a) at 4-5 weeks post injury at 4-5 weeks post injury. However at 6-7 weeks post-injury showed a significant group effect [$F(2,11)=4.43$, $p=0.03$, $*p<0.05$] (Fig 54b). Post-hoc analysis showed a significant improvement of mean speed in the phenelzine treated group, Blast+PLZ+Sub_6-OHDA, (41.80 ± 3.0 counts, n=5), compared to the non-PLZ treated group,

Blast+Sub_6-OHDA (27.25 ± 4.99 counts, n=6). The PLZ group only (48.66 ± 8.44 counts, n=3).

The complex pathophysiology of traumatic brain injuries, such as blast injuries, presents difficulties in developing therapeutic targets and interventions. The current surgical interventions and supportive treatments do not directly address secondary neurological abnormalities [254, 256]. Current animal treatment studies have examined short survival time points and lack long-term assessment effects of TBI [259, 261, 263]. More importantly, early therapeutic intervention may be a key step to prevent these long-term consequences especially with the mild form of traumatic brain injury where behavioral symptoms are undetectable during the early stages of the injury. Here we present data supporting a key role of acrolein scavengers, such as phenelzine, as an effective therapeutic target post-mild blast injury. Our data show, early treatment of phenelzine post-blast injury improved the long-term behavioral consequences as measured in the rotarod activity and open-box parameters. These data also further implicate the role of secondary injures post-blast injury, such as acrolein, may be playing a key role in these behavioral deficits.

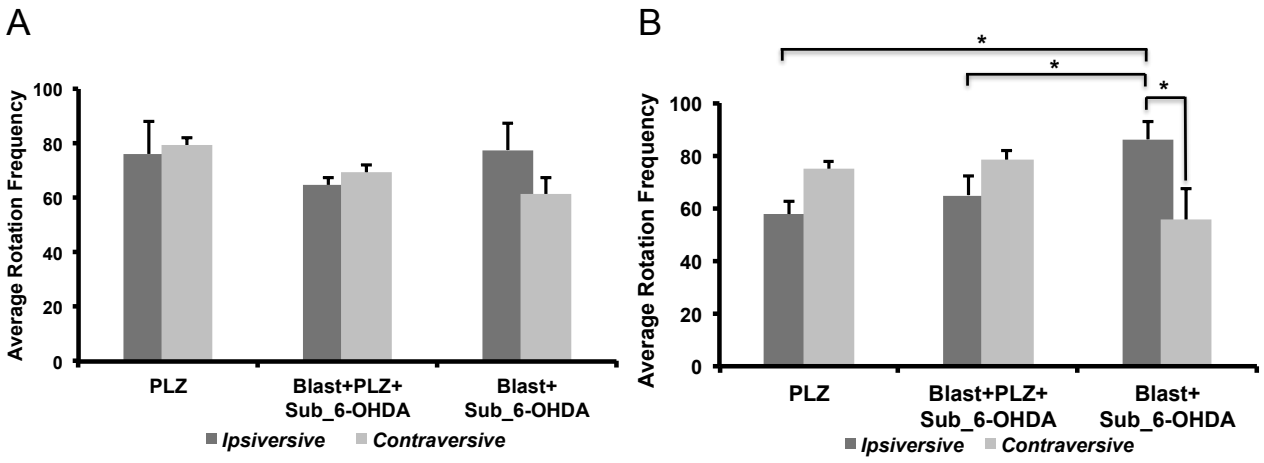

Figure 50: Assessment of rotational behavior in the phenelzine treated blast+sub_6-OHDA. (A) Rotational assessment at 4-5 weeks post-injury. The Blast+Sub_6OHDA group show a trend of increase ipsiversive rotational preference but not significant. ANOVA analysis of the ipsiversive rotation shows no significant group effect [$F(2,10)= 0.56$, $p=0.58$]. (B) Rotational assessment at 6-7 weeks post injury. The non-phenelzine treated group show significant ipsiversive rotational preference (*$p<0.05$), the phenelzine treated group, Blast+PLZ+Sub_6-OHDA did not show any rotational preference. ANOVA analysis of the ipsiversive rotation indicates significant group effect [$F(2,9)= 4.90$, $p=0.036$]. Significant decrease in the Blast+PLZ+Sub_6-OHDA compared to the Blast+Sub_6-OHDA. Post-hoc Fisher's LSD; *$p<0.05$; **$p<0.01$, ***$p<0.001$. Error bars represent SEM.

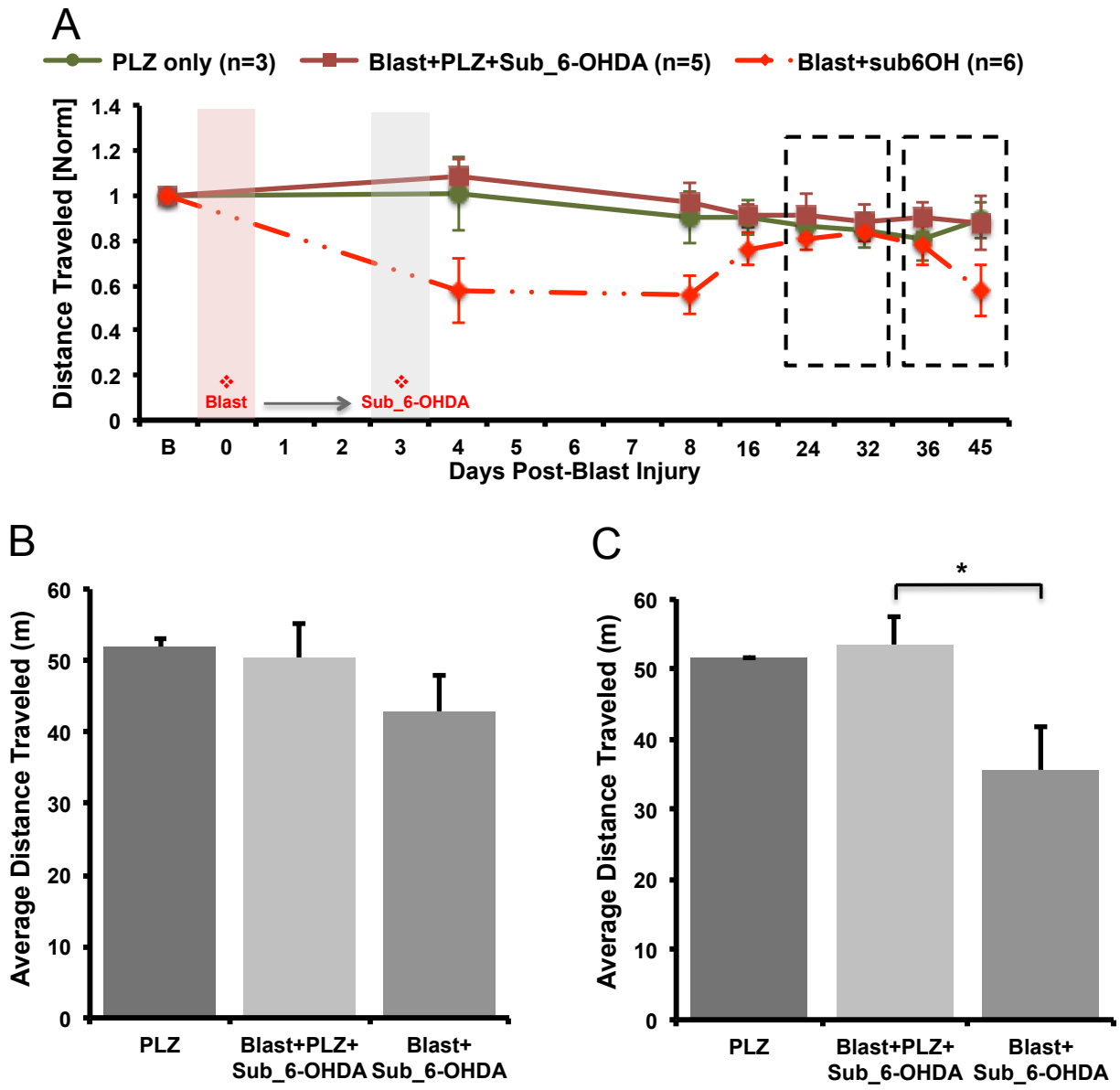

Figure 51: Total Distance Traveled in the Phenelzine Treated Blast+Sub_6-OHDA. (A) Graph showing the progression of distance travelled (normalized to baseline) of all the groups (B) Average distance traveled at 4-5 weeks post-injury shows no significant group effect [$F(2,10)= 1.12$, $p=0.036$]. (C) Average distance traveled at 6-7 weeks post injury show significant group effect [$F(2,10)= 4.27$, $p=0.04$]. The phenelzine treated group, Blast+PLZ+Sub-6-OHDA, shows significant increase compared to the non-phenelzine treated group, Blast+Sub_6-OHDA. Post-hoc Fisher's LSD; *$p<0.05$; **$p<0.01$, ***$p<0.001$. Error bars represent SEM.

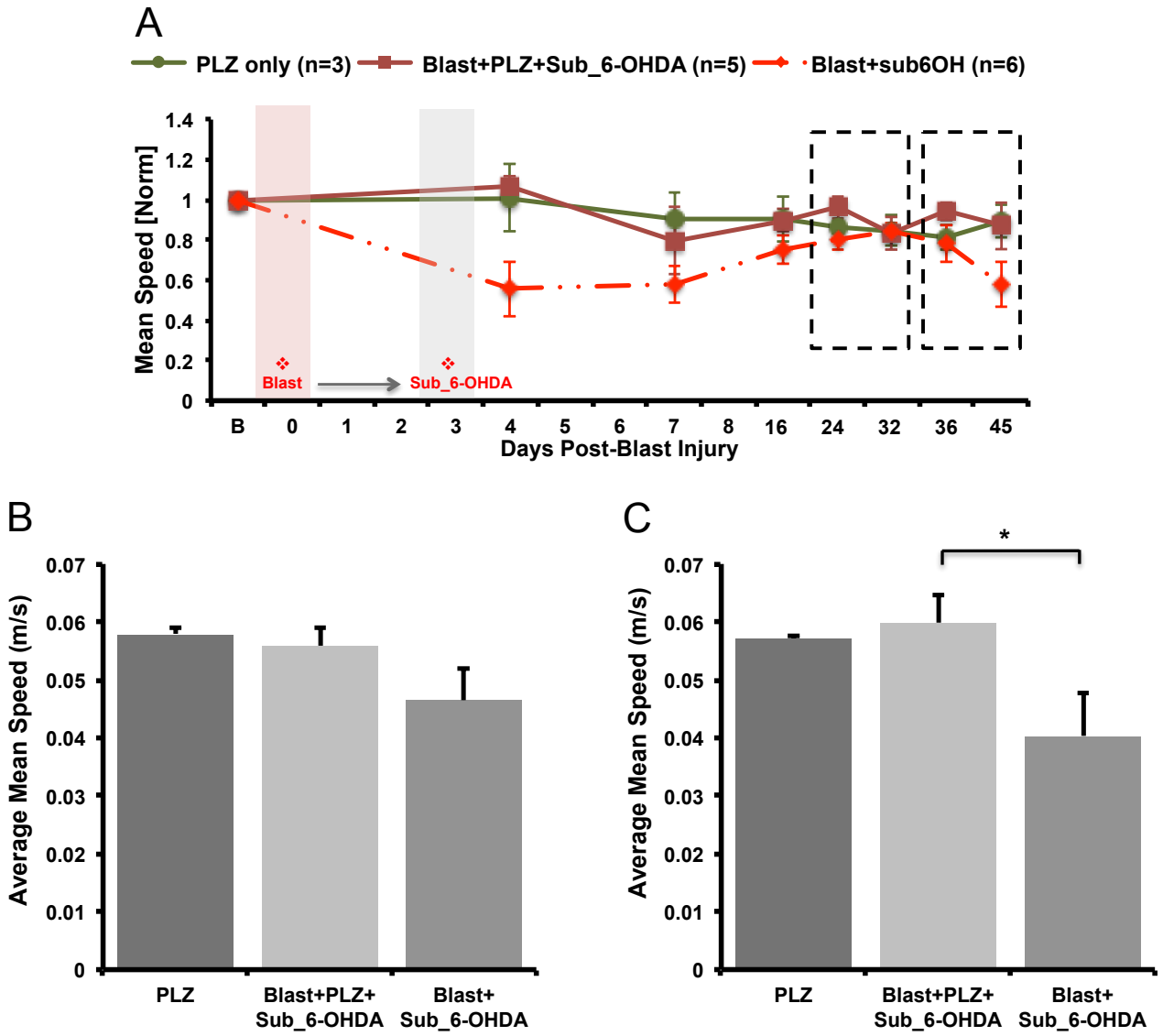

Figure 52: Mean Speed Assessment in the Phenelzine Treated Blast+Sub_6-OHDA. (A) Graph showing the progression of mean speed (normalized to baseline) of all the groups (B) Average mean speed at 4-5 weeks post-injury shows no significant group effect [$F(2,10)= 1.92$, $p=0.19$]. (C) Average mean speed at 6-7 weeks post injury show a near significant group effect [$F(2,10)= 3.84$, $p=0.05$]. The phenelzine treated group, Blast+PLZ+Sub-6-OHDA, shows significant increase compared to the non-phenelzine treated group, Blast+Sub_6-OHDA. Post-hoc Fisher's LSD; *$p<0.05$; **$p<0.01$, ***$p<0.001$.Error bars represent SEM.

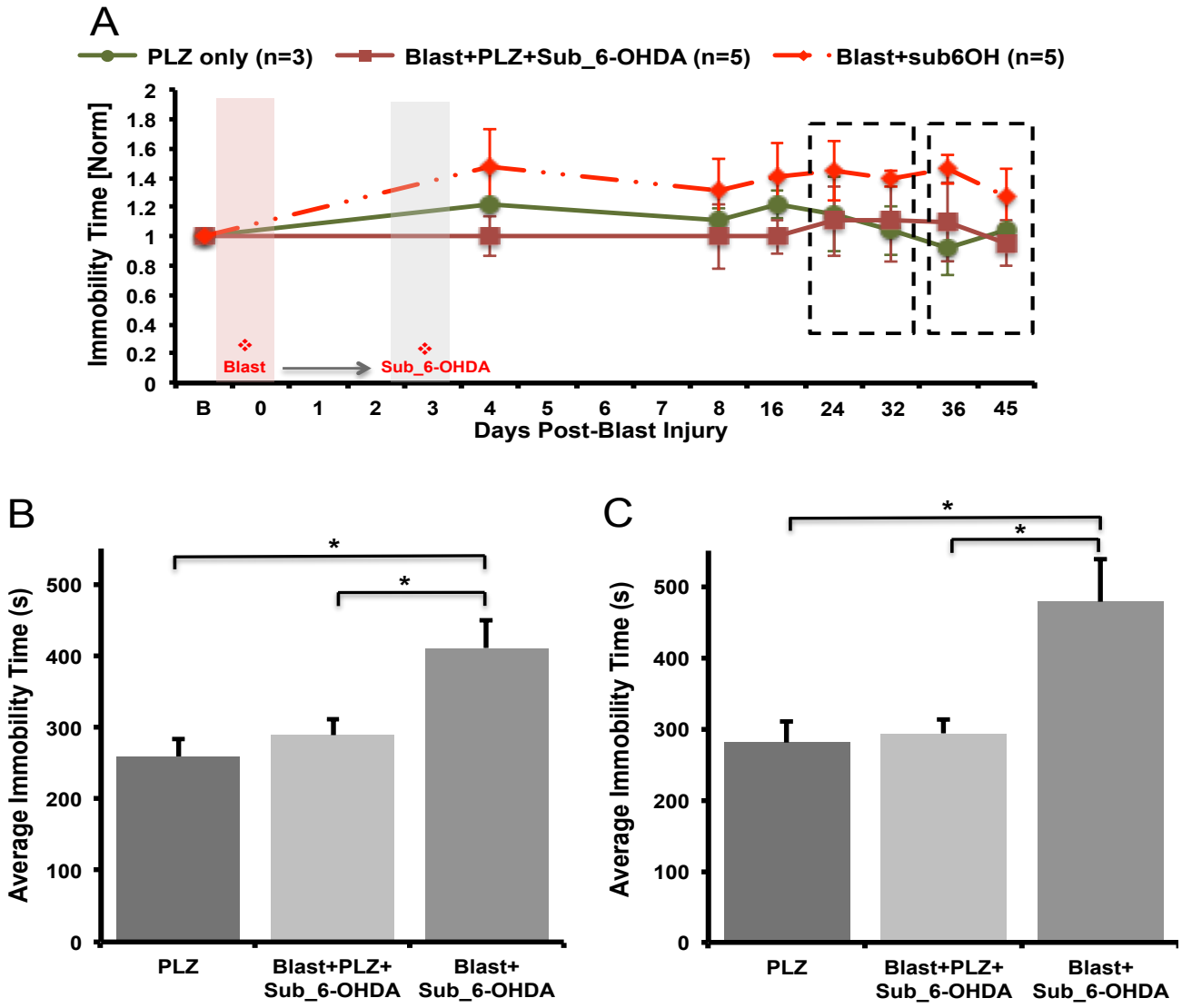

Figure 53: Immobility Time in the Phenelzine Treated Blast+Sub_6-OHDA. (A) Graph showing the progression of immobility time (normalized to baseline) of all the groups (B) Average immobility at 4-5 weeks post-injury shows significant group effect [$F(2,11)= 5.45$, $p=0.02$].The phenelzine treated group, Blast+PLZ+Sub_6-OHDA, shows significant decrease compared to the non-phenelzine treated group, Blast+Sub_6-OHDA. (C) Average immobility time at 6-7 weeks post injury show a significant group effect [$F(2,11)= 5.57$, $p=0.02$]. The phenelzine treated group, Blast+PLZ+Sub-6-OHDA, shows significant decrease compared to the non-phenelzine treated group, Blast+Sub_6-OHDA. Post-hoc Fisher's LSD; *$p<0.05$; **$p<0.01$, ***$p<0.001$.Error bars represent SEM.

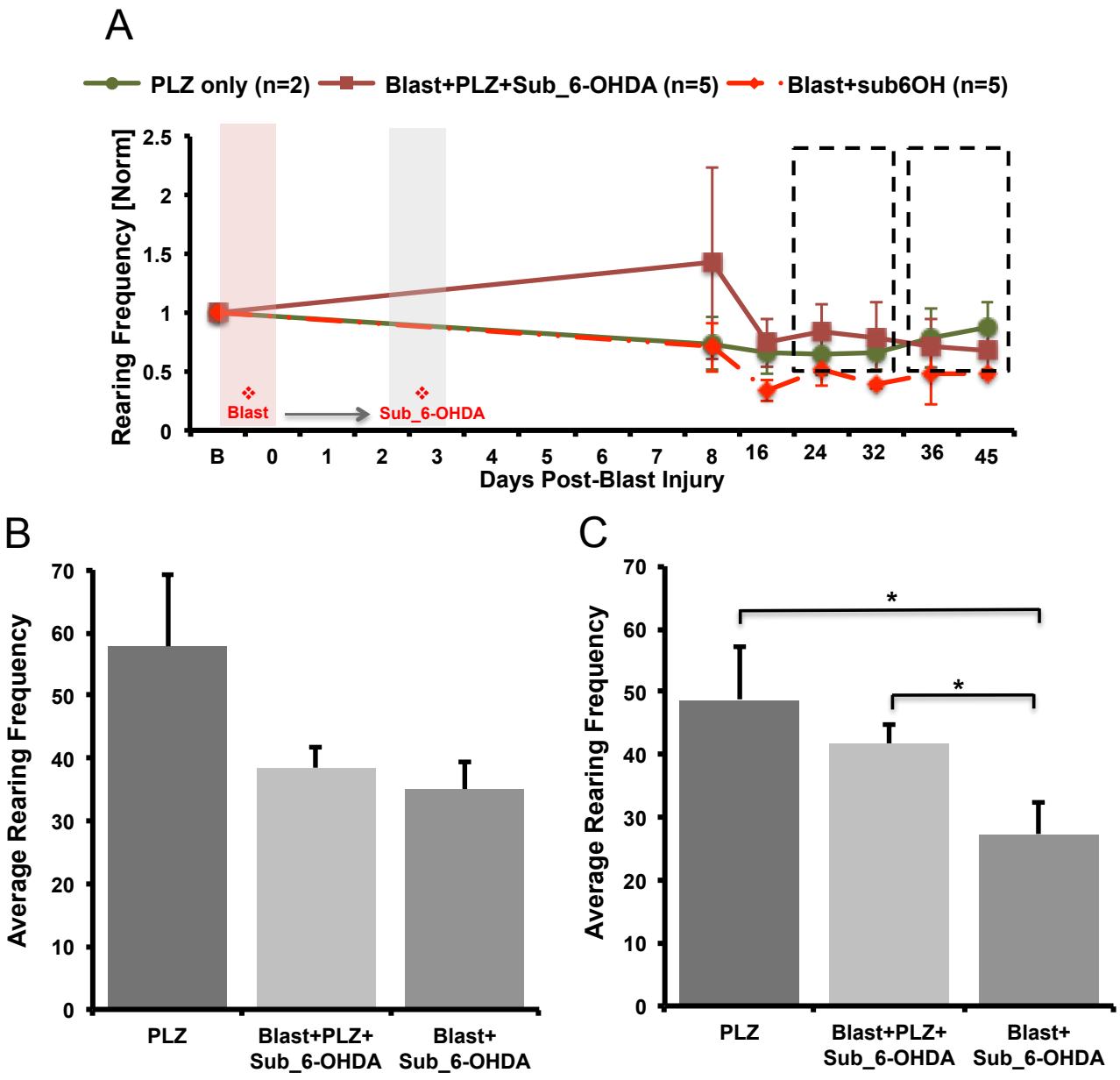

Figure 54: Rearing Frequency in the Phenelzine Treated Blast+Sub_6-OHDA. (A) Graph showing the progression of rearing frequency (normalized to baseline) of all the groups (B) Average rearing frequency counts at 4-5 weeks post-injury shows no significant group effect [$F(2,9)= 3.70$, $p=0.06$]. (C) Average rearing frequency at 6-7 weeks post injury show a significant group effect [$F(2,11)= 4.43$, $p=0.03$]. The phenelzine treated group, Blast+PLZ+Sub-6-OHDA, shows significant increase compared to the non-phenelzine treated group, Blast+Sub_6-OHDA. Post-hoc Fisher's LSD; *$p<0.05$; **$p<0.01$, ***$p<0.001$.Error bars represent SEM.

4.1.3.3. Phenelzine, acrolein scavenger, mitigation post-mild bTBI

Furthermore, we measured acrolein indirectly in the urine by detecting 3-HPMA from each sample group. Fig. 55 shows bar graph comparison of the normalized levels of 3-HPMA between non-phenelzine treated and phenelzine treated groups at different time points of the injury. Using at two-tailed t-test to compare between groups on each time point, we show a significant decrease of 3-HPMA levels in the phenelzine treated group compared to the non-phenelzine treated group two days post blast (**p<0.01), one day post sub-6-OHDA injection (*p<0.05) which continually decreases even at fifteen days post surgery (*p<0.05). Error bars represent SEM. The 3-HPMA urine measurement results demonstrate that phenelzine can mitigate acrolein levels. Given that these data can be correlated with the behavior motor improvements as measured in the rotarod and open activity box, and the reduction of acrolein through phenelzine can mitigate these deficits, it suggests that acrolein post-mild TBI may have a key role in promoting the susceptibility of PD-like motor deficits.

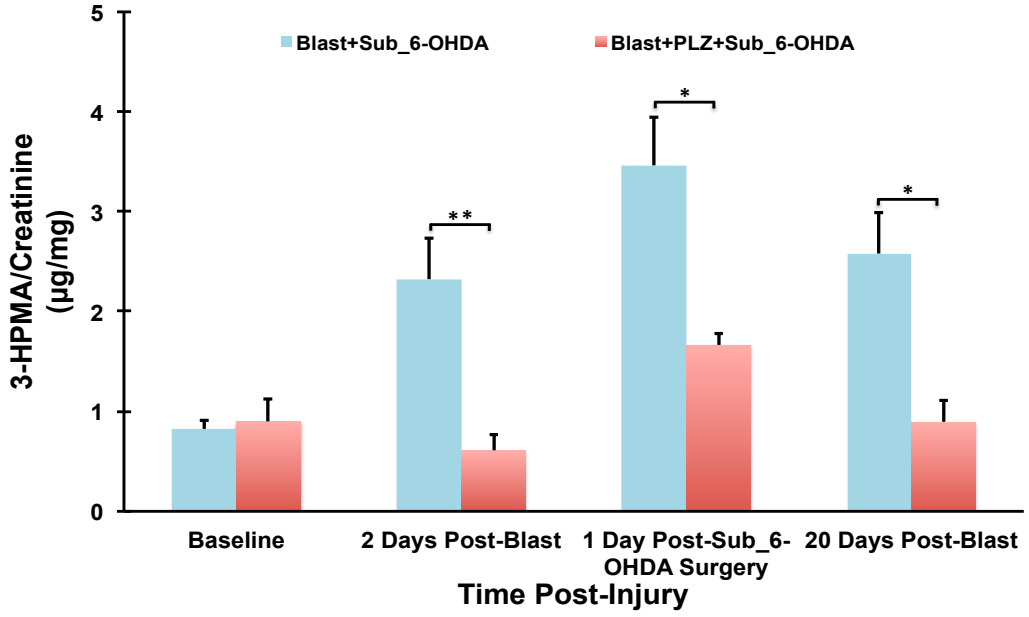

Figure 55: Treatment of phenelzine mild-bTBI injury reduces the levels of 3-HPMA, an acrolein metabolite, in the urine. Bar graphs are normalized levels of 3-HPMA to creatinine (µg/mg) in the urine 2 days post-mild bTBI, 1 day post sub_6-OHDA nigral injection and 20 days post-mild TBI; comparison between the phenelzine treated group (Blast/PLZ/6OH) and the non-treated group (Blast/6OH). Multivariate ANOVA indicates there is a significant overall effect of Blast/Injury [$F(1,7)=46.3, p<0.01$] and comparison between the Blast/Sub6OH and Blast/PLZ/Sub6OH using a two-sample t-test assuming equal variance show significant differences 2 days Post-Blast (**p<0.01), 1 Day Post Surgery (*p<0.05), and 20 days post-blast (*p<0.05). Error bars represent SEM.

5. CONCLUSIONS AND FUTURE DIRECTIONS

The lack of understanding of mild-blast TBI pathophysiological mechanisms as well as the limited number of effective PD therapies motivates us to find alternative avenues for therapeutic targets, particularly to treat in the window of time between post-blast and pre-PD symptoms. We hypothesize that oxidative stress, specifically acrolein, plays a critical role in linking blast-TBI and PD. Our results from this study demonstrate that acrolein scavenging may provide a more effective method for neuroprotection from such neuronal insults (Section 4). Because we are limited with the variability of these injuries in human studies and lack of animal models, a consistent and reliable model is essential to further understand the pathology of mild bTBI. Our model shows no motor deficits on our rotarod performance test, as relatively similar to those observed clinically (Fig. 4, 5). However, post-mortem tissue analysis shows extensive biochemical changes in the whole brain and nigrostriatal pathway (Section 1). From these results, we can speculate that secondary injuries such as acrolein are elevated post-mild TBI and can be a critical factor in regulating PD biomarkers such as TH and α-synuclein.

PD is a complex disease and the mechanisms of dopaminergic neuronal death are still largely uncharacterized. Senescence and genetic mutations are the most common factors for increased susceptibility, but other factors such as traumatic brain injury have been gaining attention [87]. As one of the most frequent injuries suffered from increased military conflicts, the main focus of this research is mild bTBI. Individuals that are deployed to war conflicts have a higher exposure to blast injuries and most of them suffer from long term consequences such as post-traumatic stress disorder, depression, and PD, our main research focus. Our biochemical results show that mild bTBI can modulate PD markers such as increased aberrant expression of α-synuclein, dysregulation TH activity and increased Tau neuropathy in the whole brain and nigrostriatal region hence supporting that mild bTBI increases susceptibility to PD.

Since acrolein has been identified as an essential mediator of secondary injury in spinal cord injury and its high reactivity to biomolecules [36, 44, 47, 185, 264], points toward the idea that the elevated acrolein levels post-blast are contributing in part to the dysregulation of PD biomarkers, particularly tyrosine hydroxylase and α-synuclein. Due to acrolein's longer half-life, on the order of hours to days [36], it provides a longer time period compared to the transient

free radicals (ROS), which can further impose injury to the CNS. Therefore, acrolein scavenging may provide a more effective method for neuroprotection from such neuronal insults.

However, further investigation is warranted to understand precisely how these PD markers are affected by acrolein. Specifically, future studies need to focus on how acrolein induces post-translational modifications of α-synuclein, particularly ubiquitination, since we observed a species of suspected to be ubiquitinated α-synuclein (25 kDa) post-blast. Future *in vitro* experiments are needed to test if acrolein directly induces ubiquitination. Measuring ubiquitinated α-synuclein in post-mortem tissue of blast-injured animals would potentially validate those results. In addition, we can further investigate on how ubiquitinated α-synuclein species can regulate the activity of TH at pSer 40 and also further investigate the other TH phosphorylation sites. Future experiments are warranted to investigate both the regulation of TH through PKA and PKCδ and how acrolein affects these kinases to further understand the observed post-mBINT decrease in TH activity. Thorough investigation of acrolein effects the molecules such as kinases and phosphatases which regulate the key players in PD pathology, specifically TH and α-synuclein, will help us understand the pathogenesis of mBINT and how it can potentiate the development of PD. This will further our knowledge on how to treat and find avenues for therapeutic intervention and/or potentially prevent the long-term consequences of mBINT, particularly PD.

To further resolve the relationship between mBINT and PD, we established a sub-threshold 6OHDA model, a lower dosage of 6-OHDA from the full 6OHDA PD model, which shows no motor deficits, and combine it with mBINT. Our results show that a combination of mBINT and a sub-threshold injection of 6-OHDA produce PD-like motor deficits, similar to the full 6-OHDA PD model (Rotarod and open box measurements. These locomotor and exploratory deficits can be correlated with acrolein measurements obtained by utilizing 3-HPMA detection in the urine and provide further evidence on the role of acrolein post-mBINT. We also show that treatment with phenelzine, an effective acrolein scavenger, can mitigate these motor deficits and that it also correlated with our acrolein measurements. These results support acrolein's role post-mBINT in potentiating may susceptibility to PD.

In summary, these studies support the hypothesis that acrolein post-mBINT contributes significantly to the secondary injury mechanisms similar to what is observed in SCI, and can promote development of PD pathology. Our results further demonstrate that acrolein plays a key

role in both mBINT and PD, providing additional evidence regarding cellular and biochemical mechanism of acrolein-mediated insults for both pathologies. These studies can serve to expand our knowledge of the role of acrolein in both mBINT and PD; in order to further investigate mechanisms to effectively attenuate oxidative stress and improve recovery after the injury, and collectively promote neuroprotection. Thus, acrolein scavenging may be a novel therapeutic avenue to attenuate oxidative stress following neuronal trauma and can prevent further long-term consequences such as PD.

Our future studies will further assess the ability of acrolein scavenging to mitigate the risk of PD in post-blast injured rats and also the effect of comorbidities such as smoking and alcohol to intensify the susceptibility of PD in post-mild TBI. Another desirable future study would be the investigation of multiple mild-bTBIs and how it can potentiate in the development of PD. Nonetheless, the results from our project will advance our understanding of the long-term consequences of blast and development of PD. Our findings show potential for therapeutic application to improve the lifestyle of our military personnel and patients with PD as well as to alleviate the emotional and financial costs associated with these diseases. Once established, acrolein-targeting therapeutics could be extended to diseases such as multiple sclerosis, Alzheimer's disease and even cancer.

Overall, this present study provides a comprehensive biochemical and behavioral understanding of a rodent mild blast injury model. This will contribute to our limited knowledge of the injury and its susceptibility to other diseases particularly, PD and the development for diagnostics of blast-induced traumatic brain injury. Furthermore, it will provide a basis for better therapeutic targets to mitigate the long-term consequences of bTBI.

REFERENCES

1. Chen, Y.C., D.H. Smith, and D.F. Meaney, *In-vitro approaches for studying blast-induced traumatic brain injury.* J Neurotrauma, 2009. **26**(6): p. 861-76.
2. DePalma, R.G., et al., *Blast injuries.* N Engl J Med, 2005. **352**(13): p. 1335-42.
3. Long, J.B., et al., *Blast overpressure in rats: recreating a battlefield injury in the laboratory.* J Neurotrauma, 2009. **26**(6): p. 827-40.
4. Bell, R.S., et al., *Military traumatic brain and spinal column injury: a 5-year study of the impact blast and other military grade weaponry on the central nervous system.* J Trauma, 2009. **66**(4 Suppl): p. S104-11.
5. Elder, G.A. and A. Cristian, *Blast-related mild traumatic brain injury: mechanisms of injury and impact on clinical care.* Mt Sinai J Med, 2009. **76**(2): p. 111-8.
6. Taber, K.H., D.L. Warden, and R.A. Hurley, *Blast-related traumatic brain injury: what is known?* J Neuropsychiatry Clin Neurosci, 2006. **18**(2): p. 141-5.
7. Coupland, R.M. and D.R. Meddings, *Mortality associated with use of weapons in armed conflicts, wartime atrocities, and civilian mass shootings: literature review.* BMJ, 1999. **319**(7207): p. 407-10.
8. Ling, G., et al., *Explosive blast neurotrauma.* J Neurotrauma, 2009. **26**(6): p. 815-25.
9. Moochhala, S.M., et al., *Neuroprotective role of aminoguanidine in behavioral changes after blast injury.* J Trauma, 2004. **56**(2): p. 393-403.
10. Defense, D.o., *2008 DoD Survey of Health Related Behaviors Among Active Duty Personnel*, 2009, Department of Defense: Washington DC.
11. Deforest, M.J., *Principles of Improvised Explosive Devices*. 1984, Boulder, CO: Paladin Press.
12. Sciences and Technology Division on Earth and Life Studies., N.R.C.U.S.C.o.D.I.E.D.B.R.t.i.t.I.D.C.N.R.C.U.S.B.o.C., *National Research Council (U.S.) Naval Studies Board Division on Engineering and Physical Sciences. Countering the threat of improvised explosive devices: Basic Research opportunities, abbreviated version*, 2007, National Academies Press: Washington, DC.
13. Turner, S., *Terrorist Explosive Sourcebook: Countering Terrorist use of improvised explosive devices*. 1994, Boulder, CO: Paladin Press.
14. Cernak, I., et al., *Blast injury from explosive munitions.* J Trauma, 1999. **47**(1): p. 96-103; discussion 103-4.
15. Kaur, C., et al., *The response of neurons and microglia to blast injury in the rat brain.* Neuropathol Appl Neurobiol, 1995. **21**(5): p. 369-77.
16. Kaur, C., et al., *Ultrastructural changes of macroglial cells in the rat brain following an exposure to a non-penetrative blast.* Ann Acad Med Singapore, 1997. **26**(1): p. 27-9.
17. Scott, S.G., et al., *Mechanism-of-injury approach to evaluating patients with blast-related polytrauma.* J Am Osteopath Assoc, 2006. **106**(5): p. 265-70.
18. Hoge, C.W., et al., *Mild traumatic brain injury in U.S. Soldiers returning from Iraq.* N Engl J Med, 2008. **358**(5): p. 453-63.
19. Terrio, H., et al., *Traumatic brain injury screening: preliminary findings in a US Army Brigade Combat Team.* J Head Trauma Rehabil, 2009. **24**(1): p. 14-23.
20. Bombardier, C.H., et al., *Rates of major depressive disorder and clinical outcomes following traumatic brain injury.* JAMA, 2010. **303**(19): p. 1938-45.

21. Spikman, J.M., et al., *Social cognition impairments in relation to general cognitive deficits, injury severity, and prefrontal lesions in traumatic brain injury patients.* J Neurotrauma, 2012. **29**(1): p. 101-11.
22. Veitch, D.P., K.E. Friedl, and M.W. Weiner, *Military risk factors for cognitive decline, dementia and Alzheimer's disease.* Curr Alzheimer Res, 2013. **10**(9): p. 907-30.
23. Weiner, M.W., et al., *Military risk factors for Alzheimer's disease.* Alzheimers Dement, 2013. **9**(4): p. 445-51.
24. Braak, H., et al., *Stanley Fahn Lecture 2005: The staging procedure for the inclusion body pathology associated with sporadic Parkinson's disease reconsidered.* Mov Disord, 2006. **21**(12): p. 2042-51.
25. Braak, H., et al., *Staging of the intracerebral inclusion body pathology associated with idiopathic Parkinson's disease (preclinical and clinical stages).* J Neurol, 2002. **249 Suppl 3**: p. III/1-5.
26. Goldman, S.M., et al., *Head injury and Parkinson's disease risk in twins.* Ann Neurol, 2006. **60**(1): p. 65-72.
27. Clemedson, C.J., *Blast injury.* Physiol Rev, 1956. **36**(3): p. 336-54.
28. Cernak, I., et al., *The pathobiology of blast injuries and blast-induced neurotrauma as identified using a new experimental model of injury in mice.* Neurobiol Dis, 2011. **41**(2): p. 538-51.
29. Hemphill, M.A., et al., *A possible role for integrin signaling in diffuse axonal injury.* PLoS One, 2011. **6**(7): p. e22899.
30. Park, E., et al., *A model of low-level primary blast brain trauma results in cytoskeletal proteolysis and chronic functional impairment in the absence of lung barotrauma.* J Neurotrauma, 2011. **28**(3): p. 343-57.
31. Ravin, R., et al., *Shear forces during blast, not abrupt changes in pressure alone, generate calcium activity in human brain cells.* PLoS One, 2012. **7**(6): p. e39421.
32. Cardona, S.M., J.A. Garcia, and A.E. Cardona, *The fine balance of chemokines during disease: trafficking, inflammation, and homeostasis.* Methods Mol Biol, 2013. **1013**: p. 1-16.
33. Werner, C. and K. Engelhard, *Pathophysiology of traumatic brain injury.* Br J Anaesth, 2007. **99**(1): p. 4-9.
34. Giulian, D., *Reactive glia as rivals in regulating neuronal survival.* Glia, 1993. **7**(1): p. 102-10.
35. Banik, N.L., *Pathogenesis of myelin breakdown in demyelinating diseases: role of proteolytic enzymes.* Crit Rev Neurobiol, 1992. **6**(4): p. 257-71.
36. Ghilarducci, D.P. and R.S. Tjeerdema, *Fate and effects of acrolein.* Rev Environ Contam Toxicol, 1995. **144**: p. 95-146.
37. Hamann, K. and R. Shi, *Acrolein scavenging: a potential novel mechanism of attenuating oxidative stress following spinal cord injury.* J Neurochem, 2009. **111**(6): p. 1348-56.
38. Park, E., J.D. Bell, and A.J. Baker, *Traumatic brain injury: can the consequences be stopped?* CMAJ, 2008. **178**(9): p. 1163-70.
39. Syburra, C. and S. Passi, *Oxidative stress in patients with multiple sclerosis.* Ukr Biokhim Zh, 1999. **71**(3): p. 112-5.
40. Yin, H., L. Xu, and N.A. Porter, *Free radical lipid peroxidation: mechanisms and analysis.* Chem Rev, 2011. **111**(10): p. 5944-72.

41. Butterfield, D.A., et al., *Evidence that amyloid beta-peptide-induced lipid peroxidation and its sequelae in Alzheimer's disease brain contribute to neuronal death.* Neurobiol Aging, 2002. **23**(5): p. 655-64.
42. Pugazhenthi, S., et al., *Differential regulation of c-jun and CREB by acrolein and 4-hydroxynonenal.* Free Radic Biol Med, 2006. **40**(1): p. 21-34.
43. Uchida, K., *4-Hydroxy-2-nonenal: a product and mediator of oxidative stress.* Prog Lipid Res, 2003. **42**(4): p. 318-43.
44. Esterbauer, H., R.J. Schaur, and H. Zollner, *Chemistry and biochemistry of 4-hydroxynonenal, malonaldehyde and related aldehydes.* Free Radic Biol Med, 1991. **11**(1): p. 81-128.
45. Lovell, M.A., C. Xie, and W.R. Markesbery, *Acrolein is increased in Alzheimer's disease brain and is toxic to primary hippocampal cultures.* Neurobiol Aging, 2001. **22**(2): p. 187-94.
46. Tanaka, N., et al., *Immunohistochemical detection of lipid peroxidation products, protein-bound acrolein and 4-hydroxynonenal protein adducts, in actinic elastosis of photodamaged skin.* Arch Dermatol Res, 2001. **293**(7): p. 363-7.
47. Uchida, K., et al., *Acrolein is a product of lipid peroxidation reaction. Formation of free acrolein and its conjugate with lysine residues in oxidized low density lipoproteins.* J Biol Chem, 1998. **273**(26): p. 16058-66.
48. Kruman, I., et al., *Evidence that 4-hydroxynonenal mediates oxidative stress-induced neuronal apoptosis.* J Neurosci, 1997. **17**(13): p. 5089-100.
49. Butterfield, D.A., et al., *Evidence of oxidative damage in Alzheimer's disease brain: central role for amyloid beta-peptide.* Trends Mol Med, 2001. **7**(12): p. 548-54.
50. Uchida, K., et al., *Protein-bound acrolein: potential markers for oxidative stress.* Proc Natl Acad Sci U S A, 1998. **95**(9): p. 4882-7.
51. Luo, J., K. Uchida, and R. Shi, *Accumulation of acrolein-protein adducts after traumatic spinal cord injury.* Neurochem Res, 2005. **30**(3): p. 291-5.
52. Hamann, K., et al., *Critical role of acrolein in secondary injury following ex vivo spinal cord trauma.* J Neurochem, 2008. **107**(3): p. 712-21.
53. Hamann, K., et al., *Hydralazine inhibits compression and acrolein-mediated injuries in ex vivo spinal cord.* J Neurochem, 2008. **104**(3): p. 708-18.
54. Luo, J. and R. Shi, *Acrolein induces axolemmal disruption, oxidative stress, and mitochondrial impairment in spinal cord tissue.* Neurochem Int, 2004. **44**(7): p. 475-86.
55. Shi, Y., et al., *Acrolein induces myelin damage in mammalian spinal cord.* J Neurochem, 2011. **117**(3): p. 554-64.
56. Leung, G., et al., *Anti-acrolein treatment improves behavioral outcome and alleviates myelin damage in experimental autoimmune encephalomyelitis mouse.* Neuroscience, 2011. **173**: p. 150-5.
57. Luo, J. and R. Shi, *Acrolein induces oxidative stress in brain mitochondria.* Neurochem Int, 2005. **46**(3): p. 243-52.
58. Burcham, P.C., et al., *Aldehyde-sequestering drugs: tools for studying protein damage by lipid peroxidation products.* Toxicology, 2002. **181-182**: p. 229-36.
59. Burcham, P.C., P.G. Kerr, and F. Fontaine, *The antihypertensive hydralazine is an efficient scavenger of acrolein.* Redox Rep, 2000. **5**(1): p. 47-9.

60. Kaminskas, L.M., S.M. Pyke, and P.C. Burcham, *Reactivity of hydrazinophthalazine drugs with the lipid peroxidation products acrolein and crotonaldehyde.* Org Biomol Chem, 2004. **2**(18): p. 2578-84.
61. Burcham, P.C., et al., *Protein adduct-trapping by hydrazinophthalazine drugs: mechanisms of cytoprotection against acrolein-mediated toxicity.* Mol Pharmacol, 2004. **65**(3): p. 655-64.
62. Burcham, P.C. and S.M. Pyke, *Hydralazine inhibits rapid acrolein-induced protein oligomerization: role of aldehyde scavenging and adduct trapping in cross-link blocking and cytoprotection.* Mol Pharmacol, 2006. **69**(3): p. 1056-65.
63. Kaminskas, L.M., S.M. Pyke, and P.C. Burcham, *Strong protein adduct trapping accompanies abolition of acrolein-mediated hepatotoxicity by hydralazine in mice.* J Pharmacol Exp Ther, 2004. **310**(3): p. 1003-10.
64. Liu-Snyder, P., R.B. Borgens, and R. Shi, *Hydralazine rescues PC12 cells from acrolein-mediated death.* J Neurosci Res, 2006. **84**(1): p. 219-27.
65. Liu-Snyder, P., et al., *Acrolein-mediated mechanisms of neuronal death.* J Neurosci Res, 2006. **84**(1): p. 209-18.
66. Reece, P.A., *Hydralazine and related compounds: chemistry, metabolism, and mode of action.* Med Res Rev, 1981. **1**(1): p. 73-96.
67. McGrath, P.J., et al., *Phenelzine treatment of melancholia.* J Clin Psychiatry, 1986. **47**(8): p. 420-2.
68. Paykel, E.S., et al., *Response to phenelzine and amitriptyline in subtypes of outpatient depression.* Arch Gen Psychiatry, 1982. **39**(9): p. 1041-9.
69. Paykel, E.S., et al., *Influence of acetylator phenotype on antidepressant effects of phenelzine.* Br J Psychiatry, 1982. **141**: p. 243-8.
70. Buigues, J. and J. Vallejo, *Therapeutic response to phenelzine in patients with panic disorder and agoraphobia with panic attacks.* J Clin Psychiatry, 1987. **48**(2): p. 55-9.
71. Sheehan, D.V., J. Ballenger, and G. Jacobsen, *Treatment of endogenous anxiety with phobic, hysterical, and hypochondriacal symptoms.* Arch Gen Psychiatry, 1980. **37**(1): p. 51-9.
72. Frank, J.B., et al., *A randomized clinical trial of phenelzine and imipramine for posttraumatic stress disorder.* Am J Psychiatry, 1988. **145**(10): p. 1289-91.
73. Liebowitz, M.R., et al., *Pharmacotherapy of social phobia: an interim report of a placebo-controlled comparison of phenelzine and atenolol.* J Clin Psychiatry, 1988. **49**(7): p. 252-7.
74. Mackenzie, J.E. and L.W. Frank, *Influence of pretreatment with a monoamine oxidase inhibitor (phenelzine) on the effects of buprenorphine and pethidine in the conscious rabbit.* Br J Anaesth, 1988. **60**(2): p. 216-21.
75. Wood, P.L., et al., *Aldehyde load in ischemia-reperfusion brain injury: neuroprotection by neutralization of reactive aldehydes with phenelzine.* Brain Res, 2006. **1122**(1): p. 184-90.
76. Khandhar, S.M. and W.J. Marks, *Epidemiology of Parkinson's disease.* Dis Mon, 2007. **53**(4): p. 200-5.
77. Starkstein, S.E., et al., *Anxiety Has Specific Syndromal Profiles in Parkinson Disease: A Data-Driven Approach.* Am J Geriatr Psychiatry, 2013.
78. Stefanis, L., *alpha-Synuclein in Parkinson's disease.* Cold Spring Harb Perspect Med, 2012. **2**(2): p. a009399.

79. Lo Bianco, C., et al., *alpha -Synucleinopathy and selective dopaminergic neuron loss in a rat lentiviral-based model of Parkinson's disease.* Proc Natl Acad Sci U S A, 2002. **99**(16): p. 10813-8.
80. Spillantini, M.G., et al., *Alpha-synuclein in Lewy bodies.* Nature, 1997. **388**(6645): p. 839-40.
81. Castellani, R., et al., *Glycoxidation and oxidative stress in Parkinson disease and diffuse Lewy body disease.* Brain Res, 1996. **737**(1-2): p. 195-200.
82. Owen, A.D., et al., *Indices of oxidative stress in Parkinson's disease, Alzheimer's disease and dementia with Lewy bodies.* J Neural Transm Suppl, 1997. **51**: p. 167-73.
83. Yan, M.H., X. Wang, and X. Zhu, *Mitochondrial defects and oxidative stress in Alzheimer disease and Parkinson disease.* Free Radic Biol Med, 2013. **62**: p. 90-101.
84. Shamoto-Nagai, M., et al., *In parkinsonian substantia nigra, alpha-synuclein is modified by acrolein, a lipid-peroxidation product, and accumulates in the dopamine neurons with inhibition of proteasome activity.* J Neural Transm, 2007. **114**(12): p. 1559-67.
85. Coyle, J.T. and P. Puttfarcken, *Oxidative stress, glutamate, and neurodegenerative disorders.* Science, 1993. **262**(5134): p. 689-95.
86. Xu, S., et al., *Oxidative stress induces nuclear translocation of C-terminus of alpha-synuclein in dopaminergic cells.* Biochem Biophys Res Commun, 2006. **342**(1): p. 330-5.
87. Chade, A.R., M. Kasten, and C.M. Tanner, *Nongenetic causes of Parkinson's disease.* J Neural Transm Suppl, 2006(70): p. 147-51.
88. Elsayed, N.M., et al., *Antioxidant depletion, lipid peroxidation, and impairment of calcium transport induced by air-blast overpressure in rat lungs.* Exp Lung Res, 1996. **22**(2): p. 179-200.
89. Saljo, A., et al., *Exposure to short-lasting impulse noise causes neuronal c-Jun expression and induction of apoptosis in the adult rat brain.* J Neurotrauma, 2002. **19**(8): p. 985-91.
90. Saljo, A., et al., *Expression of c-Fos and c-Myc and deposition of beta-APP in neurons in the adult rat brain as a result of exposure to short-lasting impulse noise.* J Neurotrauma, 2002. **19**(3): p. 379-85.
91. Shi, R., T. Rickett, and W. Sun, *Acrolein-mediated injury in nervous system trauma and diseases.* Mol Nutr Food Res, 2011. **55**(9): p. 1320-31.
92. Shi, R.Y., et al., *Calcium antagonists fail to protect mammalian spinal neurons after physical injury.* J Neurotrauma, 1989. **6**(4): p. 261-76; discussion 277-8.
93. Whalen, M.J., et al., *Acute plasmalemma permeability and protracted clearance of injured cells after controlled cortical impact in mice.* J Cereb Blood Flow Metab, 2008. **28**(3): p. 490-505.
94. Newell, K.L., et al., *Alpha-synuclein immunoreactivity is present in axonal swellings in neuroaxonal dystrophy and acute traumatic brain injury.* J Neuropathol Exp Neurol, 1999. **58**(12): p. 1263-8.
95. Schmidt, M.L., et al., *Tau isoform profile and phosphorylation state in dementia pugilistica recapitulate Alzheimer's disease.* Acta Neuropathol, 2001. **101**(5): p. 518-24.
96. Smith, D.H., et al., *Protein accumulation in traumatic brain injury.* Neuromolecular Med, 2003. **4**(1-2): p. 59-72.
97. Morganti-Kossmann, M.C., et al., *Modulation of immune response by head injury.* Injury, 2007. **38**(12): p. 1392-400.

98. Bhattacharjee, Y., *Neuroscience. Shell shock revisited: solving the puzzle of blast trauma.* Science, 2008. **319**(5862): p. 406-8.
99. Graham, D.G., *Oxidative pathways for catecholamines in the genesis of neuromelanin and cytotoxic quinones.* Mol Pharmacol, 1978. **14**(4): p. 633-43.
100. Jenner, P., *Oxidative stress in Parkinson's disease.* Ann Neurol, 2003. **53 Suppl 3**: p. S26-36; discussion S36-8.
101. Jenner, P. and C.W. Olanow, *Understanding cell death in Parkinson's disease.* Ann Neurol, 1998. **44**(3 Suppl 1): p. S72-84.
102. Jenner, P. and C.W. Olanow, *The pathogenesis of cell death in Parkinson's disease.* Neurology, 2006. **66**(10 Suppl 4): p. S24-36.
103. Connell, S., H. Ouyang, and R. Shi, *Modeling blast induced neurotrauma in isolated spinal cord white matter.* J Med Syst, 2011. **35**(5): p. 765-70.
104. Bryan, C.J., et al., *Loss of consciousness, depression, posttraumatic stress disorder, and suicide risk among deployed military personnel with mild traumatic brain injury.* J Head Trauma Rehabil, 2013. **28**(1): p. 13-20.
105. Andre, E., et al., *Cigarette smoke-induced neurogenic inflammation is mediated by alpha,beta-unsaturated aldehydes and the TRPA1 receptor in rodents.* J Clin Invest, 2008. **118**(7): p. 2574-82.
106. Facchinetti, F., et al., *Alpha,beta-unsaturated aldehydes in cigarette smoke release inflammatory mediators from human macrophages.* Am J Respir Cell Mol Biol, 2007. **37**(5): p. 617-23.
107. Sayer, N.A., et al., *Characteristics and rehabilitation outcomes among patients with blast and other injuries sustained during the Global War on Terror.* Archives of physical medicine and rehabilitation, 2008. **89**(1): p. 163-170.
108. Prevention, N.C.f.I., Control, and U.S.o. America, *Blast Injuries: Fact Sheets for Professionals.* 2013.
109. Koob, A.O., J. Cirillo, and C.F. Babbs, *A novel open field activity detector to determine spatial and temporal movement of laboratory animals after injury and disease.* J Neurosci Methods, 2006. **157**(2): p. 330-6.
110. Tate, C.M., et al., *Serum brain biomarker level, neurocognitive performance, and self-reported symptom changes in soldiers repeatedly exposed to low-level blast: a breacher pilot study.* J Neurotrauma, 2013. **30**(19): p. 1620-30.
111. Connell, S., et al. *Modeling traumatic brain injury using a compressed-gas blast chamber*. in *Biomedical Engineering and Informatics (BMEI), 2011 4th International Conference on*. 2011. IEEE.
112. Yeoh, S., E.D. Bell, and K.L. Monson, *Distribution of blood-brain barrier disruption in primary blast injury.* Ann Biomed Eng, 2013. **41**(10): p. 2206-14.
113. Cho, H.J., et al., *Blast induces oxidative stress, inflammation, neuronal loss and subsequent short-term memory impairment in rats.* Neuroscience, 2013. **253**: p. 9-20.
114. VandeVord, P.J., *Measuring Intracranial Pressure and Correlation with Severity of Blast Traumatic Brain Injury*, 2013, DTIC Document.
115. Vandevord, P.J., et al., *Mild neurotrauma indicates a range-specific pressure response to low level shock wave exposure.* Ann Biomed Eng, 2012. **40**(1): p. 227-36.
116. Skotak, M., et al., *Rat injury model under controlled field-relevant primary blast conditions: Acute response to a wide range of peak overpressures.* Journal of neurotrauma, 2013. **30**(13): p. 1147-1160.

117. Bower, J.H., et al., *Incidence and distribution of parkinsonism in Olmsted County, Minnesota, 1976-1990.* Neurology, 1999. **52**(6): p. 1214-20.
118. Goldman, S.M., et al., *Head injury, alpha-synuclein Rep1, and Parkinson's disease.* Ann Neurol, 2012. **71**(1): p. 40-8.
119. Acosta, S.A., et al., *Alpha-synuclein as a pathological link between chronic traumatic brain injury and Parkinson's disease.* J Cell Physiol, 2015. **230**(5): p. 1024-32.
120. Jafari, S., et al., *Head injury and risk of Parkinson disease: a systematic review and meta-analysis.* Mov Disord, 2013. **28**(9): p. 1222-9.
121. Johnson, V.E., W. Stewart, and D.H. Smith, *Axonal pathology in traumatic brain injury.* Exp Neurol, 2012.
122. Laino, C., *MILITARY DEPLOYMENT MAY RAISE RISK OF PARKINSON DISEASE.* Neurology Today, 2005. **5**(6): p. 48.
123. Lee, P.C., et al., *Traumatic brain injury, paraquat exposure, and their relationship to Parkinson disease.* Neurology, 2012. **79**(20): p. 2061-6.
124. Van Den Eeden, S.K., et al., *Incidence of Parkinson's disease: variation by age, gender, and race/ethnicity.* Am J Epidemiol, 2003. **157**(11): p. 1015-22.
125. Galarneau, M.R., et al., *Traumatic brain injury during Operation Iraqi Freedom: findings from the United States Navy-Marine Corps Combat Trauma Registry.* J Neurosurg, 2008. **108**(5): p. 950-7.
126. Arciniegas, D.B. and J.M. Silver, *Regarding the search for a unified definition of mild traumatic brain injury.* Brain Inj, 2001. **15**(7): p. 649-52.
127. Brenner, L.A., R.D. Vanderploeg, and H. Terrio, *Assessment and diagnosis of mild traumatic brain injury, posttraumatic stress disorder, and other polytrauma conditions: burden of adversity hypothesis.* Rehabil Psychol, 2009. **54**(3): p. 239-46.
128. Carlson, K.F., et al., *Prevalence, assessment, and treatment of mild traumatic brain injury and posttraumatic stress disorder: a systematic review of the evidence.* J Head Trauma Rehabil, 2011. **26**(2): p. 103-15.
129. Carlson, K.F., et al., *Psychiatric diagnoses among Iraq and Afghanistan war veterans screened for deployment-related traumatic brain injury.* J Trauma Stress, 2010. **23**(1): p. 17-24.
130. Ruff, R.M. and P. Jurica, *In search of a unified definition for mild traumatic brain injury.* Brain Inj, 1999. **13**(12): p. 943-52.
131. Shively, S.B. and D.P. Perl, *Traumatic brain injury, shell shock, and posttraumatic stress disorder in the military--past, present, and future.* J Head Trauma Rehabil, 2012. **27**(3): p. 234-9.
132. Glover, L.E., et al., *Immediate, but not delayed, microsurgical skull reconstruction exacerbates brain damage in experimental traumatic brain injury model.* PLoS One, 2012. **7**(3): p. e33646.
133. Yu, S., et al., *Severity of controlled cortical impact traumatic brain injury in rats and mice dictates degree of behavioral deficits.* Brain Res, 2009. **1287**: p. 157-63.
134. Desmoulin, G.T. and J.P. Dionne, *Blast-induced neurotrauma: surrogate use, loading mechanisms, and cellular responses.* J Trauma, 2009. **67**(5): p. 1113-22.
135. Miller, G., *Neuropathology. Blast injuries linked to neurodegeneration in veterans.* Science, 2012. **336**(6083): p. 790-1.
136. Rosenfeld, J.V., et al., *Blast-related traumatic brain injury.* Lancet Neurol, 2013. **12**(9): p. 882-93.

137. Walls, M.K., et al., *Structural and biochemical abnormalities in the absence of acute deficits in mild primary blast-induced head trauma.* J Neurosurg, 2016. **124**(3): p. 675-86.
138. Saing, T., et al., *Frontal cortex neuropathology in dementia pugilistica.* J Neurotrauma, 2012. **29**(6): p. 1054-70.
139. Xiong, Y., A. Mahmood, and M. Chopp, *Animal models of traumatic brain injury.* Nat Rev Neurosci, 2013. **14**(2): p. 128-42.
140. Lo Bianco, C., et al., *Lentiviral vector delivery of parkin prevents dopaminergic degeneration in an alpha-synuclein rat model of Parkinson's disease.* Proc Natl Acad Sci U S A, 2004. **101**(50): p. 17510-5.
141. Mogi, M., et al., *Homospecific activity (activity per enzyme protein) of tyrosine hydroxylase increases in parkinsonian brain.* J Neural Transm, 1988. **72**(1): p. 77-82.
142. Nakashima, A., et al., *A possible pathophysiological role of tyrosine hydroxylase in Parkinson's disease suggested by postmortem brain biochemistry: a contribution for the special 70th birthday symposium in honor of Prof. Peter Riederer.* J Neural Transm (Vienna), 2013. **120**(1): p. 49-54.
143. Bernheimer, H., et al., *Brain dopamine and the syndromes of Parkinson and Huntington. Clinical, morphological and neurochemical correlations.* J Neurol Sci, 1973. **20**(4): p. 415-55.
144. Kish, S.J., K. Shannak, and O. Hornykiewicz, *Uneven pattern of dopamine loss in the striatum of patients with idiopathic Parkinson's disease. Pathophysiologic and clinical implications.* N Engl J Med, 1988. **318**(14): p. 876-80.
145. Morrish, P.K., G.V. Sawle, and D.J. Brooks, *Clinical and [18F] dopa PET findings in early Parkinson's disease.* J Neurol Neurosurg Psychiatry, 1995. **59**(6): p. 597-600.
146. Shamoto-Nagai, M., et al., *In parkinsonian substantia nigra, a-synuclein is modified by acrolein, a lipid-peroxidation product, and accumulates in the dopamine neurons with inhibition of proteasome activity.* Journal of Neural Transmission, 2007.
147. Ando, Y., et al., *Histochemical detection of 4-hydroxynonenal protein in Alzheimer amyloid.* J Neurol Sci, 1998. **156**(2): p. 172-6.
148. Calingasan, N.Y., K. Uchida, and G.E. Gibson, *Protein-bound acrolein: a novel marker of oxidative stress in Alzheimer's disease.* J Neurochem, 1999. **72**(2): p. 751-6.
149. Chen, J., et al., *Formation of malondialdehyde adducts in livers of rats exposed to ethanol: role in ethanol-mediated inhibition of cytochrome c oxidase.* Alcohol Clin Exp Res, 2000. **24**(4): p. 544-52.
150. Comporti, M., *Lipid peroxidation and biogenic aldehydes: from the identification of 4-hydroxynonenal to further achievements in biopathology.* Free Radic Res, 1998. **28**(6): p. 623-35.
151. Uchida, K., *Role of reactive aldehyde in cardiovascular diseases.* Free Radic Biol Med, 2000. **28**(12): p. 1685-96.
152. Perbellini, L., N. Veronese, and A. Princivalle, *Mercapturic acids in the biological monitoring of occupational exposure to chemicals.* J Chromatogr B Analyt Technol Biomed Life Sci, 2002. **781**(1-2): p. 269-90.
153. Schettgen, T., A. Musiol, and T. Kraus, *Simultaneous determination of mercapturic acids derived from ethylene oxide (HEMA), propylene oxide (2-HPMA), acrolein (3-HPMA), acrylamide (AAMA) and N,N-dimethylformamide (AMCC) in human urine using liquid*

chromatography/tandem mass spectrometry. Rapid Commun Mass Spectrom, 2008. **22**(17): p. 2629-38.
154. Parent, R.A., et al., *Metabolism and distribution of [2,3-14C]acrolein in Sprague-Dawley rats. II. Identification of urinary and fecal metabolites.* Toxicol Sci, 1998. **43**(2): p. 110-20.
155. Stevens, J.F. and C.S. Maier, *Acrolein: sources, metabolism, and biomolecular interactions relevant to human health and disease.* Mol Nutr Food Res, 2008. **52**(1): p. 7-25.
156. Zheng, L., et al., *Determination of Urine 3-HPMA, a Stable Acrolein Metabolite in a Rat Model of Spinal Cord Injury.* J Neurotrauma, 2013. **30**(15): p. 1334-41.
157. Galvin, J.E., V.M. Lee, and J.Q. Trojanowski, *Synucleinopathies: clinical and pathological implications.* Arch Neurol, 2001. **58**(2): p. 186-90.
158. Kim, T.D., et al., *Structural changes in alpha-synuclein affect its chaperone-like activity in vitro.* Protein Sci, 2000. **9**(12): p. 2489-96.
159. Souza, J.M., et al., *Chaperone-like activity of synucleins.* FEBS Lett, 2000. **474**(1): p. 116-9.
160. Takeda, A., et al., *Abnormal distribution of the non-Abeta component of Alzheimer's disease amyloid precursor/alpha-synuclein in Lewy body disease as revealed by proteinase K and formic acid pretreatment.* Lab Invest, 1998. **78**(9): p. 1169-77.
161. Dang, T.N., et al., *Potential role of acrolein in neurodegeneration and in Alzheimer's disease.* Curr Mol Pharmacol, 2010. **3**(2): p. 66-78.
162. Drubin, D. and M. Kirschner, *Purification of tau protein from brain.* Methods Enzymol, 1986. **134**: p. 156-60.
163. Drubin, D., S. Kobayashi, and M. Kirschner, *Association of tau protein with microtubules in living cells.* Ann N Y Acad Sci, 1986. **466**: p. 257-68.
164. Drubin, D.G. and M.W. Kirschner, *Tau protein function in living cells.* J Cell Biol, 1986. **103**(6 Pt 2): p. 2739-46.
165. Montine, T.J., et al., *F2-isoprostanes in Alzheimer and other neurodegenerative diseases.* Antioxid Redox Signal, 2005. **7**(1-2): p. 269-75.
166. Aarsland, D., J. Zaccai, and C. Brayne, *A systematic review of prevalence studies of dementia in Parkinson's disease.* Mov Disord, 2005. **20**(10): p. 1255-63.
167. Bancher, C., et al., *Neuropathological staging of Alzheimer lesions and intellectual status in Alzheimer's and Parkinson's disease patients.* Neurosci Lett, 1993. **162**(1-2): p. 179-82.
168. Leverenz, J.B., et al., *Cognitive impairment and dementia in patients with Parkinson disease.* Curr Top Med Chem, 2009. **9**(10): p. 903-12.
169. Moussaud, S., et al., *Alpha-synuclein and tau: teammates in neurodegeneration?* Mol Neurodegener, 2014. **9**: p. 43.
170. Schneider, J.A., et al., *Substantia nigra tangles are related to gait impairment in older persons.* Ann Neurol, 2006. **59**(1): p. 166-73.
171. Bower, J.H., et al., *Head trauma preceding PD: a case-control study.* Neurology, 2003. **60**(10): p. 1610-5.
172. Shahaduzzaman, M., et al., *alpha-Synuclein is a pathological link and therapeutic target for Parkinson's disease and traumatic brain injury.* Med Hypotheses, 2013. **81**(4): p. 675-80.

173. Surgucheva, I., et al., *Role of synucleins in traumatic brain injury - an experimental in vitro and in vivo study in mice.* Mol Cell Neurosci, 2014. **63**: p. 114-23.
174. Uryu, K., et al., *Multiple proteins implicated in neurodegenerative diseases accumulate in axons after brain trauma in humans.* Exp Neurol, 2007. **208**(2): p. 185-92.
175. Yan, H.Q., et al., *Delayed increase of tyrosine hydroxylase expression in rat nigrostriatal system after traumatic brain injury.* Brain Res, 2007. **1134**(1): p. 171-9.
176. Butterfield, D.A. and T.T. Reed, *Lipid peroxidation and tyrosine nitration in traumatic brain injury: Insights into secondary injury from redox proteomics.* Proteomics Clin Appl, 2016. **10**(12): p. 1191-1204.
177. Lorente, L., et al., *Association between serum malondialdehyde levels and mortality in patients with severe brain trauma injury.* J Neurotrauma, 2015. **32**(1): p. 1-6.
178. Santos, A., et al., *Catalase activity and thiobarbituric acid reactive substances (TBARS) production in a rat model of diffuse axonal injury. Effect of gadolinium and amiloride.* Neurochem Res, 2005. **30**(5): p. 625-31.
179. Shao, C., et al., *Oxidative stress in head trauma in aging.* Free Radic Biol Med, 2006. **41**(1): p. 77-85.
180. Wu, A., Z. Ying, and F. Gomez-Pinilla, *Dietary strategy to repair plasma membrane after brain trauma: implications for plasticity and cognition.* Neurorehabil Neural Repair, 2014. **28**(1): p. 75-84.
181. Lovell, M.A., C. Xie, and W.R. Markesbery, *Acrolein is increased in Alzheimer's disease brain and is toxic to primary hippocampal cultures.* Neurobiology of Aging, 2001. **22**(2): p. 187-94.
182. Abraham, K., et al., *Toxicology and risk assessment of acrolein in food.* Mol Nutr Food Res, 2011. **55**(9): p. 1277-90.
183. Osorio, V.M. and Z. de Lourdes Cardeal, *Determination of acrolein in french fries by solid-phase microextraction gas chromatography and mass spectrometry.* J Chromatogr A, 2011. **1218**(21): p. 3332-6.
184. Adams, J.D., Jr. and L.K. Klaidman, *Acrolein-induced oxygen radical formation.* Free Radic Biol Med, 1993. **15**(2): p. 187-93.
185. Kehrer, J.P. and S.S. Biswal, *The molecular effects of acrolein.* Toxicol Sci, 2000. **57**(1): p. 6-15.
186. Esterbauer, H., R.J. Schaur, and H. Zollner, *Chemistry and biochemistry of 4-hydroxynonenal, malonaldehyde and related aldehydes.* Free Radical Biology & Medicine, 1991. **11**(1): p. 81-128.
187. Uchida, K., et al., *Protein-bound acrolein: potential markers for oxidative stress.* Proceedings of the National Academy of Sciences of the United States of America, 1998. **95**(9): p. 4882-7.
188. Guingab-Cagmat, J.D., et al., *Integration of proteomics, bioinformatics, and systems biology in traumatic brain injury biomarker discovery.* Front Neurol, 2013. **4**: p. 61.
189. Kobeissy, F.H., et al., *Novel differential neuroproteomics analysis of traumatic brain injury in rats.* Mol Cell Proteomics, 2006. **5**(10): p. 1887-98.
190. Lazarus, R.C., et al., *Protein carbonylation after traumatic brain injury: cell specificity, regional susceptibility, and gender differences.* Free Radic Biol Med, 2015. **78**: p. 89-100.
191. Khan, W., et al., *A brief overview of tyrosine hydroxylase and alpha-synuclein in the Parkinsonian brain.* CNS Neurol Disord Drug Targets, 2012. **11**(4): p. 456-62.

192. Maroteaux, L., J.T. Campanelli, and R.H. Scheller, *Synuclein: a neuron-specific protein localized to the nucleus and presynaptic nerve terminal.* J Neurosci, 1988. **8**(8): p. 2804-15.
193. Rokad, D., et al., *Role of neurotoxicants and traumatic brain injury in alpha-synuclein protein misfolding and aggregation.* Brain Res Bull, 2016.
194. Uryu, K., et al., *Age-dependent synuclein pathology following traumatic brain injury in mice.* Exp Neurol, 2003. **184**(1): p. 214-24.
195. Pivato, M., et al., *Covalent alpha-synuclein dimers: chemico-physical and aggregation properties.* PLoS One, 2012. **7**(12): p. e50027.
196. Ulmer, T.S. and A. Bax, *Comparison of structure and dynamics of micelle-bound human alpha-synuclein and Parkinson disease variants.* J Biol Chem, 2005. **280**(52): p. 43179-87.
197. Ulmer, T.S., et al., *Structure and dynamics of micelle-bound human alpha-synuclein.* J Biol Chem, 2005. **280**(10): p. 9595-603.
198. Chung, K.K., et al., *Parkin ubiquitinates the alpha-synuclein-interacting protein, synphilin-1: implications for Lewy-body formation in Parkinson disease.* Nat Med, 2001. **7**(10): p. 1144-50.
199. Winner, B., et al., *In vivo demonstration that alpha-synuclein oligomers are toxic.* Proc Natl Acad Sci U S A, 2011. **108**(10): p. 4194-9.
200. Wang, Y.T., et al., *Acrolein acts as a neurotoxin in the nigrostriatal dopaminergic system of rat: involvement of alpha-synuclein aggregation and programmed cell death.* Sci Rep, 2017. **7**: p. 45741.
201. Nagatsu, T., M. Levitt, and S. Udenfriend, *Tyrosine Hydroxylase. The Initial Step in Norepinephrine Biosynthesis.* J Biol Chem, 1964. **239**: p. 2910-7.
202. Zhu, Y., J. Zhang, and Y. Zeng, *Overview of tyrosine hydroxylase in Parkinson's disease.* CNS Neurol Disord Drug Targets, 2012. **11**(4): p. 350-8.
203. Bademci, G., et al., *A rare novel deletion of the tyrosine hydroxylase gene in Parkinson disease.* Hum Mutat, 2010. **31**(10): p. E1767-71.
204. Maxwell, S.L. and M. Li, *Midbrain dopaminergic development in vivo and in vitro from embryonic stem cells.* J Anat, 2005. **207**(3): p. 209-18.
205. Lindgren, N., et al., *Regulation of tyrosine hydroxylase activity and phosphorylation at Ser(19) and Ser(40) via activation of glutamate NMDA receptors in rat striatum.* J Neurochem, 2000. **74**(6): p. 2470-7.
206. Shin, S.S., et al., *Traumatic brain injury reduces striatal tyrosine hydroxylase activity and potassium-evoked dopamine release in rats.* Brain Res, 2011. **1369**: p. 208-15.
207. Keller, C.M., et al., *Biphasic dopamine regulation in mesoaccumbens pathway in response to non-contingent binge and escalating methamphetamine regimens in the Wistar rat.* Psychopharmacology (Berl), 2011. **215**(3): p. 513-26.
208. Salvatore, M.F., E.S. Calipari, and S.R. Jones, *Regulation of Tyrosine Hydroxylase Expression and Phosphorylation in Dopamine Transporter-Deficient Mice.* ACS Chem Neurosci, 2016. **7**(7): p. 941-51.
209. Burns, R.S., et al., *A primate model of parkinsonism: selective destruction of dopaminergic neurons in the pars compacta of the substantia nigra by N-methyl-4-phenyl-1,2,3,6-tetrahydropyridine.* Proc Natl Acad Sci U S A, 1983. **80**(14): p. 4546-50.

210. Hung, H.C. and E.H. Lee, *MPTP produces differential oxidative stress and antioxidative responses in the nigrostriatal and mesolimbic dopaminergic pathways.* Free Radic Biol Med, 1998. **24**(1): p. 76-84.
211. McCormack, A.L., et al., *Role of oxidative stress in paraquat-induced dopaminergic cell degeneration.* J Neurochem, 2005. **93**(4): p. 1030-7.
212. Wang, X. and E.K. Michaelis, *Selective neuronal vulnerability to oxidative stress in the brain.* Front Aging Neurosci, 2010. **2**: p. 12.
213. Beal, M.F., *Mitochondria, oxidative damage, and inflammation in Parkinson's disease.* Ann N Y Acad Sci, 2003. **991**: p. 120-31.
214. Zhang, Y., et al., *Intravenous nonviral gene therapy causes normalization of striatal tyrosine hydroxylase and reversal of motor impairment in experimental parkinsonism.* Hum Gene Ther, 2003. **14**(1): p. 1-12.
215. Daadi, M.M., et al., *Distribution of AAV2-hAADC-transduced cells after 3 years in Parkinsonian monkeys.* Neuroreport, 2006. **17**(2): p. 201-4.
216. Fujita, M., et al., *Chaperone and anti-chaperone: two-faced synuclein as stimulator of synaptic evolution.* Neuropathology, 2006. **26**(5): p. 383-92.
217. Kim, T.D., S.R. Paik, and C.H. Yang, *Structural and functional implications of C-terminal regions of alpha-synuclein.* Biochemistry, 2002. **41**(46): p. 13782-90.
218. Ostrerova, N., et al., *alpha-Synuclein shares physical and functional homology with 14-3-3 proteins.* J Neurosci, 1999. **19**(14): p. 5782-91.
219. Itagaki, C., et al., *Stimulus-coupled interaction of tyrosine hydroxylase with 14-3-3 proteins.* Biochemistry, 1999. **38**(47): p. 15673-80.
220. Tofaris, G.K., et al., *Ubiquitination of alpha-synuclein in Lewy bodies is a pathological event not associated with impairment of proteasome function.* J Biol Chem, 2003. **278**(45): p. 44405-11.
221. Toska, K., et al., *Regulation of tyrosine hydroxylase by stress-activated protein kinases.* J Neurochem, 2002. **83**(4): p. 775-83.
222. Sutherland, C., et al., *Phosphorylation and activation of human tyrosine hydroxylase in vitro by mitogen-activated protein (MAP) kinase and MAP-kinase-activated kinases 1 and 2.* Eur J Biochem, 1993. **217**(2): p. 715-22.
223. Thomas, G., J. Haavik, and P. Cohen, *Participation of a stress-activated protein kinase cascade in the activation of tyrosine hydroxylase in chromaffin cells.* Eur J Biochem, 1997. **247**(3): p. 1180-9.
224. Polanski, W., H. Reichmann, and G. Gille, *Stimulation, protection and regeneration of dopaminergic neurons by 9-methyl-beta-carboline: a new anti-Parkinson drug?* Expert Rev Neurother, 2011. **11**(6): p. 845-60.
225. Ranganna, K., et al., *Acrolein activates mitogen-activated protein kinase signal transduction pathways in rat vascular smooth muscle cells.* Mol Cell Biochem, 2002. **240**(1-2): p. 83-98.
226. Tanel, A. and D.A. Averill-Bates, *P38 and ERK mitogen-activated protein kinases mediate acrolein-induced apoptosis in Chinese hamster ovary cells.* Cell Signal, 2007. **19**(5): p. 968-77.
227. Randall, M.J., et al., *Acrolein-induced activation of mitogen-activated protein kinase signaling is mediated by alkylation of thioredoxin reductase and thioredoxin 1.* Redox Biol, 2013. **1**: p. 265-75.

228. Svetlov, S.I., et al., *Biomarkers of blast-induced neurotrauma: profiling molecular and cellular mechanisms of blast brain injury.* J Neurotrauma, 2009. **26**(6): p. 913-21.
229. Cernak, I., *Penetrating and Blast Injury.* Restor. Neurol. Neurosci, 2005. **23**: p. 5.
230. Walls, M.K., et al., *Structural and biochemical abnormalities in the absence of acute deficits in mild primary blast-induced head trauma.* J Neurosurg, 2015: p. 1-12.
231. Zheng, L., et al., *Determination of urine 3-HPMA, a stable acrolein metabolite in rat model of spinal cord injury.* Journal of Neurotrauma, 2013(ja).
232. Ciechanover, A., *Linking ubiquitin, parkin and synphilin-1.* Nat Med, 2001. **7**(10): p. 1108-9.
233. Recchia, A., et al., *Alpha-synuclein and Parkinson's disease.* FASEB J, 2004. **18**(6): p. 617-26.
234. McNaught, K.S., et al., *Altered proteasomal function in sporadic Parkinson's disease.* Exp Neurol, 2003. **179**(1): p. 38-46.
235. McNaught, K.S. and C.W. Olanow, *Proteolytic stress: a unifying concept for the etiopathogenesis of Parkinson's disease.* Ann Neurol, 2003. **53 Suppl 3**: p. S73-84; discussion S84-6.
236. Sato, H., et al., *Authentically phosphorylated alpha-synuclein at Ser129 accelerates neurodegeneration in a rat model of familial Parkinson's disease.* J Neurosci, 2011. **31**(46): p. 16884-94.
237. Baptista, M.J., et al., *Co-ordinate transcriptional regulation of dopamine synthesis genes by alpha-synuclein in human neuroblastoma cell lines.* J Neurochem, 2003. **85**(4): p. 957-68.
238. Gao, N., et al., *Effect of alpha-synuclein on the promoter activity of tyrosine hydroxylase gene.* Neurosci Bull, 2007. **23**(1): p. 53-7.
239. Yoritaka, A., et al., *Immunohistochemical detection of 4-hydroxynonenal protein adducts in Parkinson disease.* Proc Natl Acad Sci U S A, 1996. **93**(7): p. 2696-701.
240. Salvatore, M.F., et al., *Stoichiometry of tyrosine hydroxylase phosphorylation in the nigrostriatal and mesolimbic systems in vivo: effects of acute haloperidol and related compounds.* J Neurochem, 2000. **75**(1): p. 225-32.
241. Lou, H., et al., *Serine 129 phosphorylation reduces the ability of alpha-synuclein to regulate tyrosine hydroxylase and protein phosphatase 2A in vitro and in vivo.* J Biol Chem, 2010. **285**(23): p. 17648-61.
242. Nakashima, A., et al., *A possible pathophysiological role of tyrosine hydroxylase in Parkinson's disease suggested by postmortem brain biochemistry: a contribution for the special 70th birthday symposium in honor of Prof. Peter Riederer.* J Neural Transm, 2013. **120**(1): p. 49-54.
243. Shi, X. and B.A. Habecker, *gp130 cytokines stimulate proteasomal degradation of tyrosine hydroxylase via extracellular signal regulated kinases 1 and 2.* J Neurochem, 2012. **120**(2): p. 239-47.
244. Bergstrom, B.P., et al., *Partial, graded losses of dopamine terminals in the rat caudate-putamen: an animal model for the study of compensatory adaptation in preclinical parkinsonism.* J Neurosci Methods, 2001. **106**(1): p. 15-28.
245. Costall, B., R.J. Naylor, and C. Pycock, *Non-specific supersensitivity of striatal dopamine receptors after 6-hydroxydopamine lesion of the nigrostriatal pathway.* Eur J Pharmacol, 1976. **35**(2): p. 276-83.

246. Maneuf, Y.P., et al., *On the role of enkephalin cotransmission in the GABAergic striatal efferents to the globus pallidus.* Exp Neurol, 1994. **125**(1): p. 65-71.
247. Robertson, G.S., et al., *L-dopa activates c-fos in the striatum ipsilateral to a 6-hydroxydopamine lesion of the substantia nigra.* Eur J Pharmacol, 1989. **159**(1): p. 99-100.
248. Robertson, G.S. and H.A. Robertson, *Evidence that L-dopa-induced rotational behavior is dependent on both striatal and nigral mechanisms.* J Neurosci, 1989. **9**(9): p. 3326-31.
249. Thiele, S.L., R. Warre, and J.E. Nash, *Development of a unilaterally-lesioned 6-OHDA mouse model of Parkinson's disease.* J Vis Exp, 2012(60).
250. Ungerstedt, U. and G.W. Arbuthnott, *Quantitative recording of rotational behavior in rats after 6-hydroxy-dopamine lesions of the nigrostriatal dopamine system.* Brain Res, 1970. **24**(3): p. 485-93.
251. Cornell-Bell, A.H., et al., *Glutamate induces calcium waves in cultured astrocytes: long-range glial signaling.* Science, 1990. **247**(4941): p. 470-3.
252. Chauhan, N.B., *Chronic neurodegenerative consequences of traumatic brain injury.* Restor Neurol Neurosci, 2014. **32**(2): p. 337-65.
253. Cole, J.H., et al., *Prediction of brain age suggests accelerated atrophy after traumatic brain injury.* Ann Neurol, 2015. **77**(4): p. 571-81.
254. Corps, K.N., T.L. Roth, and D.B. McGavern, *Inflammation and neuroprotection in traumatic brain injury.* JAMA Neurol, 2015. **72**(3): p. 355-62.
255. Gavett, B.E., et al., *Mild traumatic brain injury: a risk factor for neurodegeneration.* Alzheimers Res Ther, 2010. **2**(3): p. 18.
256. McConeghy, K.W., et al., *A review of neuroprotection pharmacology and therapies in patients with acute traumatic brain injury.* CNS Drugs, 2012. **26**(7): p. 613-36.
257. Pottker, B., et al., *Traumatic brain injury causes long-term behavioral changes related to region-specific increases of cerebral blood flow.* Brain Struct Funct, 2017.
258. Bolkvadze, T. and A. Pitkanen, *Development of post-traumatic epilepsy after controlled cortical impact and lateral fluid-percussion-induced brain injury in the mouse.* J Neurotrauma, 2012. **29**(5): p. 789-812.
259. Gold, E.M., et al., *Functional assessment of long-term deficits in rodent models of traumatic brain injury.* Regen Med, 2013. **8**(4): p. 483-516.
260. Lindner, M.D., et al., *Dissociable long-term cognitive deficits after frontal versus sensorimotor cortical contusions.* J Neurotrauma, 1998. **15**(3): p. 199-216.
261. Osier, N.D., et al., *Chronic Histopathological and Behavioral Outcomes of Experimental Traumatic Brain Injury in Adult Male Animals.* J Neurotrauma, 2015. **32**(23): p. 1861-82.
262. Peterson, T.C., et al., *A behavioral and histological comparison of fluid percussion injury and controlled cortical impact injury to the rat sensorimotor cortex.* Behav Brain Res, 2015. **294**: p. 254-63.
263. Marklund, N. and L. Hillered, *Animal modelling of traumatic brain injury in preclinical drug development: where do we go from here?* Br J Pharmacol, 2011. **164**(4): p. 1207-29.
264. Witz, G., *Biological interactions of alpha,beta-unsaturated aldehydes.* Free Radic Biol Med, 1989. **7**(3): p. 333-49.

PUBLICATIONS

Published

1. B. Butler, **G. Acosta**, R. Shi (2017). Exogenous acrolein intensifies sensory hypersensitivity after spinal cord injury in rat. *Journal of the Neurological Sciences,* 379: 29-35.
2. M. Haces[*], J. Tang[*], **G. Acosta**[*], J. Fernandez, R. Shi (2017). Pathological correlations between traumatic brain injury and chronic neurodegenerative diseases. *Translational Neurodegeneration*, 6:20. [*]Equal Cont.
3. Z. Chen, J. Park, B. Muratori, **G. Acosta**, S. Alvarez, L. Zheng, P. Cao, R. Shi (2016). Mitigation of sensory and motor deficits by acrolein scavenger phenelzine in a rat model of spinal cord contusive injury. *Journal of Neurochemistry*, 10.1111/jnc.13639.
4. J. Park, L. Zheng, **G. Acosta**, S. Alvarez, Z. Chen, B. Muratori, P. Cao, R. Shi (2015). Acrolein contributes to TRPA1 up-regulation in peripheral and central sensory hypersensitivity following spinal cord injury. *Journal of Neurochemistry*, 135(5): 987-97.
5. M. Walls, N. Race, L. Zheng, S. Alvarez, **G. Acosta**, J. Park, R. Shi (2015). Structural and biochemical abnormalities in the absence of acute deficits in mild primary blast-induced head trauma. *Journal of Neurosurgery*, 21: 1-12.
6. M. Tully, L. Zheng, **G. Acosta**, R. Tian, R. Shi (2014). Acute systemic accumulation of acrolein in mice by inhalation at a concentration similar to that in cigarette smoke. *Neuroscience Bulletin*, 6:1017-24.
7. D. Kumar,V. Arun, N. Kumar, **G. Acosta**, B. Noel, K. Shah (2012). A Facile Synthesis of Novel bis-(indolyl)-1,3,4-oxadiazoles as Potent Cytotoxic Agents. *ChemMedChem***,** 7: 1915-1920.
8. **G. Acosta**, D.P. Friedman, K. Grant, S.E. Hemby (2011). Alternative Splicing of AMPA Subunits in Prefrontal Cortical Fields of Cynomolgus Monkeys following Chronic Ethanol Self-Administration. *Frontiers in Psychiatry***,** 2:72.
9. **G. Acosta**, W. Hasenkamp, J.B. Daunais, D.P. Friedman, K.A. Grant, S.E. Hemby (2010). Ethanol Self-Administration in Prefrontal Cortical Fields. *Brain Research,* 1318:144-154.
10. A. Abdolahi, F. Breslin, **G. Acosta**, S.E. Hemby, W. Lynch. (2010) Incubation of Nicotine Seeking is Associated with Enhanced Protein Kinase A-Regulated Signaling of Dopamine- and cAMP-Regulated Phosphoprotein of 32 kDa in the Insular Cortex. *European Journal of Neuroscience***,** 31:733-741.
11. W. Lynch , K. Piehl, **G. Acosta**, A.B. Peterson, S.E. Hemby, (2010). Aerobic Exercise Attenuates Reinstatement of Cocaine-Seeking Behavior and Associated Neuroadaptations in the Prefrontal Cortex. *Biological Psychiatry***,** 68: 774-777.
12. S.E. Hemby, J. O'Connor, **G. Acosta**, D. Floyd, N. Anderson, B.A. McCool, D. Friedman, K.A. Grant (2006). Ethanol-Induced Regulation of GABA-A Subunit mRNAs. *Experimental Research*, 30:1978-1985.

Manuscripts in Preparation

1. **G. Acosta**, N. Race, J. Fernandez R. Shi. Acrolein involvement in the aberrant presentation of α-synuclein post-mildTBI. (Submitted: Journal of Neurochemistry).
2. M. Tully, L. Zheng, **G. Acosta**, R. Tian, L. Hayward, J. Tang, N. Race, D. Mattson, R. Shi. Systemic acrolein elevations in mice with experimental autoimmune encephalomyelitis and patients with multiple sclerosis. (Submitted: Journal of Translational Medicine).
3. D. Garcia-Gonzalez, N. Race, N. Voets, D. Jenkins, S. Sotiropoulos, **G. Acosta**, M. Haces, J. Tang, R. Shi, A. Jerusalem. Cognition based bTBI mechanistic criteria in the rat; a tool for preventive and therapeutic interventions. (Submitted to: Nature Biomedical Engineering).
4. A. Ambaw, S. Hubers, F. Liu, A. Pond, C. Rochet, L. Zheng, M. Tambe, E. Walls, **G. Acosta**, A. Truong, R. Shi. Acrolein-mediated neuronal death and alpha-synuclein aggregation: implications for Parkinson's disease. (Submitted: Molecular and Cellular Neuroscience).
5. N. Race*, E. Lungwitz*, S. Vega Alvarez*, **G. Acosta**, T. Warner, K. Andrews, J. Cao, K. Lu, Z. Liu, A. Shekhar, W. Truitt, R. Shi. Psychosocial dysfunction after combat-related TBI: toward neurobiological basis.
6. **G. Acosta**, E. Rogaev, Y. Jiang, S. Akbarian and S.E. Hemby. Antipsychotic regulated BDNF/trkB mRNA and protein expression in the dorsolateral prefrontal cortex of rhesus monkeys following chronic administration.